

ISSN 1913-1844 (Print)
ISSN 1913-1852 (Online)

MODERN APPLIED SCIENCE

**Vol. 4, No. 7
July 2010**



Canadian Center of Science and Education®

Editorial Board

Abdel Salhi	University of Essex, UK
Abdul Talib Bon	Universiti Tun Hussein Onn Malaysia, Malaysia
Ahmad Mujahid Ahmad Zaidi	Universiti Tun Hussein Onn Malaysia, Malaysia
Alessandra Crosato	Delft University of Technology, the Netherlands
Armen Bagdasaryan	Russian Academy of Sciences, Russia
Bahattin TANYOLAC	Ege University, Turkey
Cheng Y. Lin	Old Dominion University, United States
Cristian Lussana	ARPA Lombardia – weather service, Italy
Guy L Plourde	University of Northern British Columbia, Canada
Hatem M. Gaber	National Organization for Drug Control and Research (NODCAR), Egypt
J S Prakash	Sri Bhagawan Mahaveer Jain College of Engineering, India
Jiantao Guo	The Scripps Research Institute, United States
Jin Zhang	University of California, United States
Junjie Lu	Florida State University, United States
Justin Madigan	Intel, United States
Lim Hwee San	Universiti Sains Malaysia, Malaysia
Mirza Hasanuzzaman	Sher-e-Bangla Agricultural University, Bangladesh
Musa Mailah	Universiti Teknologi Malaysia, Malaysia
Panagiotis Vlamos	Ionian University, Greece
Peter Kusch	Bonn-Rhein-Sieg University of Applied Sciences, Germany
Prabir sarker	Curtin University of Technology, Australia
Rajiv Pandey	Indian Council of Forestry Research and Education, India
Roger	Curtin University of Technology, Australia
Sarhan Musa	Prairie View A&M University, United States
Skrynyk Oleg	Ukrainian Research Hydrometeorological Institute, Ukraine
Srikanth Pilla	Stanford University, United States
Stefanos Dailianis	University of Patras, Greece
Suchada Chanprateep	Chulalongkorn University, Thailand
Sujatha. C.H	Cochin University of Science and Technology, India
Supakit Wongwiwatthananutit	University of Hawaii at Hilo, United States
Susan Sun	Canadian Center of Science and Education, Canada
Sutopo Hadi	University of Lampung, Indonesia
Tao Zhang	The Research Institute for Children, United States
Thomas Schwengler	Qwest Communications and University of Colorado, United States
Veeranun Pongsapakdee	Silpakorn University, Thailand
Wichian Sittiprapaporn	Mahidol University, Thailand
Wimonrat Trakarnpruk	Chulalongkorn University, Thailand
Xin Fei	Lawrence Berkeley National Laboratory & University of Utah, United States
Yijun Liu	Clemson University, United States

Contents

Physical and Mechanical Assessments of Fire Retardant-Treated <i>Shorea macrophylla</i> and <i>Acacia mangium</i> Particleboards <i>Izran Kamal, Khairul Maseat, Koh Mok Poh, Tan Yu Eng, Saimin Basir, Nordin Puteh, Rosly Mat Joha & Naziffuad Noran</i>	3
Methods and Problems of Drilling Implantation in Rural Water Supply in the Fractured Basement Area in Chad: Case of Ouaddaï Geographic <i>Massing Oursingbé, Zhonghua Tang & Yonoudjoum M. Médard</i>	9
A Distributed Dynamic Bandwidth Allocation Algorithm in EPON <i>Feng Cao, Deming Liu, Minming Zhang, Kang Yang & Yinbo Qian</i>	20
Determination of Soil Organic Carbon Variability of Rainfed Crop Land in Semi-arid Region (Neural Network Approach) <i>Yahya Parvizi, Manochehr Gorji, Mahmoud Omid, Mohammad Hossain Mahdian & Manochehr Amini</i>	25
Comparison of Some Chromatic, Mechanical and Chemical Properties of Banana Fruit at Different Stages of Ripeness <i>Mahmoud Soltani, Reza Alimardani & Mahmoud Omid</i>	34
The Drawbacks and Superiorities of Using IR-Microwave System in Cake and Bread Baking: A Review <i>K.A. Abbas, S. M. Abdulkarim, M. Ebrahimian & N. Suleiman</i>	42
Study of Two-level P2P Model on Self-adaptive Dynamic Network <i>Feixue Huang & Zhijie Li</i>	59
Mass Transfer Coefficient Studies in Bubble Column Reactor <i>D.Devakumar, Dr.K.Saravanan, Dr.T.Kannadasan & B.Meenakshipriya</i>	65
Land Suitability Evaluation Using Fuzzy Continuous Classification (A Case Study: Ziaran Region) <i>Ali Keshavarzi, Fereydoon Sarmadian, Ahmad Heidari & Mahmoud Omid</i>	72
Strongly Multiplicative Labeling for Some Cycle Related Graphs <i>S K Vaidya & K K Kanani</i>	82
Equivalent Resistance of $5 \times n$ -laddered Network <i>Xingpeng Yang, Xingcheng Dong, Zhongyong Chen, Yingkai Liu & Zhang Xiong</i>	89
Analysis on Essence, Types and Characteristics of Leisure Sports <i>Jie Min & Houzhong Jin</i>	99
Adaptive Vibration Condition Monitoring Techniques for Local Tooth Damage in Gearbox <i>Kobra Heidarbeigi, Hojat Ahmadi & M.Omid</i>	104
Disadvantages of Control Chart in Printing Quality Control over Solder Paste and Strategies for Improvement <i>Chen Peng, Kenny Liu & Xiaohui Gu</i>	111
Comparison Study on Oil Palm Trunk and Oil Palm Fruit Bunch Fibre Reinforced Laterite Bricks <i>Noorsaidi Mahat, Zaiton Yaacob, Nadia Fatihah Mastan, Ahmad Faiz Abd Rashid, Zainab Zainordin, Mohamad Rohaidzat Mohamed Rashid, Husrul Nizam Husin, Natasha Khalil, Mohamat Najib Mat Noor, Wan Faizal Iskandar Wan Abdullah, Nurul Asra Abd Rahman & Suryani Ahmad</i>	119

Contents

Design and Analysis of Automobiles Manufacturing System Based on Simulation Model <i>Razman Bin Mat Tahar & Ali Asghar J.Adham</i>	130
Moisture-Dependent Physical Properties of Sunflower Seed (<i>SHF8190</i>) <i>Mohammad Reza Seifi & Reza Alimardani</i>	135
Solid Wood and Veneer Study of 12-Year Old Sesenduk Clone <i>Khairul Maseat, Mohd. Noor Mahat, Mohamad Omar Mohamad Khaidzir, Abdul Hamid Salleh, Mohd. Hafiz Musa, Khairul Awang & Izran Kamal</i>	144
Ontology Based Fuzzy Document Clustering Scheme <i>Thangamani.M & Dr. Thangaraj.P</i>	148
Sum and Difference Squeeze Properties of Entangle Coherent States <i>Yongxin Zhan</i>	157
Treatment Induced Germination Improvement in Medicinal Species of <i>Foeniculum vulgare Miller</i> and <i>Cuscuta epithimum(L.) L</i> <i>Tavili, Ali, Asghar Farajollahi, Hossein Pouzesh & Eisa Bandak</i>	163
The Weak Stable Sets for Fuzzy Cooperative Games <i>Shuli Wang & Ning Jiang</i>	170
Strength Behavior Study of Apples (cv. <i>Shafi Abadi & Golab Kohanz</i>) under Compression Loading <i>Abbas Gorji Chakespari, Ali Rajabipour & Hossein Mobli</i>	173
Strategies to Prohibit Intruders Eluding the Detection of Snort through SSH <i>Siqing Gao, Pan Qi & Dihua Liu</i>	183
Application of Constriction Factor Particle Swarm Optimization to Optimum Load Shedding in Power System <i>Ahmad Reza Malekpour & Ali Reza Seifi</i>	188
An Integrated Inventory Model for Vendor and Buyer <i>Zhiguang Zhang</i>	197
Network Security Policy <i>Lihua Han</i>	201

Physical and Mechanical Assessments of Fire Retardant-Treated *Shorea macrophylla* and *Acacia mangium* Particleboards

Izran Kamal (Corresponding author), Khairul Maseat, Koh Mok Poh, Tan Yu Eng

Saimin Basir, Nordin Puteh, Rosly Mat Joha & Naziffuad Noran

Forest Research Institute Malaysia (FRIM), 52109, Kepong, Malaysia

Tel: 60-3-6279-7285 E-mail: izran_kamal@yahoo.com

The research is financed by FRIM-ITTO 50300304008

Abstract

Physical and mechanical properties of fire retardant-treated engkabang (*Shorea macrophylla*) and *Acacia mangium* particleboards were assessed. Tests selected for the assessments were water absorption, thickness swelling, modulus of rupture (MOR), modulus of elasticity (MOE) and internal bond (IB). The engkabang and *Acacia mangium* particles were mixed with 10% w/w of two different fire retardants namely zinc borate ($4ZnO \cdot 6B_2O_3 \cdot 7H_2O$)-simplified as ZBr and monoammonium phosphate ($(NH_4)H_2PO_4$) during the mixing stage of the particleboard manufacturing processes. The properties of the particleboards were tested using British European 1993 standard. An analysis of variance was carried out to study the effects of fire retardant types on the boards of both species. The study showed that MAP-treated particleboards were superior to ZBr-treated particleboards for both mechanical and physical performances except for modulus of elasticity (MOE). Overall, the fire retardants reduced the physical and mechanical properties of the engkabang and *Acacia mangium* particleboards. However, all treated and untreated particleboards complied with the standard requirement values and these findings are expected to increase the promotion of both species to be used in producing fire-retardant particleboards.

Keywords: Fire retardants, Internal bond, Modulus of rupture, Modulus of elasticity, Zinc borate and monoammonium phosphate

1. Introduction

Engkabang jantung (*Shorea macrophylla*) and *Acacia mangium* are two of the most popular wood species that frequently used as inputs for interior decoration such as cabinets, furnitures, and turnery. The plants are also used for particleboard, plywood, veneer, pulp, fence, firewood and charcoal (Sanchez, 2006, Anon, 2009). Mohamad Azani *et al.*, (2001) studied that engkabang jantung can grow very fast and form wide spreading crowns, even though it is planted under shades of the higher trees. Engkabang is a protected species and can be found scattering throughout Sarawak, usually on clay alluvial soil of riparian forest and lower slopes of clay hill sides below 600m above sea level (Anon, 2009 and Anon 2009a). The information about this species is still limited compared to *Acacia mangium*. Engkabang is popular due to its nut known as False Illipe Nut, which has moisturising properties that are similar to cocoa butter for skincare and haircare products (Fleckenstein, 2009). Like engkabang jantung, *Acacia mangium* is a fast growing species too. *Acacia mangium* can be found on many different types of sites such as primary and secondary forests, forest margin, savannah, grassland, savanna woodland, mangrove forest and abandoned shifting cultivation sites (Sanchez, 2006). This species can achieve 15m height within 3 years, even when it is planted on mining degraded sites (Velez Torres and Valle Del, 2007), giving it a short rotation. It is also relatively free from disease. Tropical forest is disappearing at the rate of 15-20 million ha/year. The rate might increase if the usage upon the forest resources is not controlled. Due to that, the wood-based product manufacturers would like to find new raw materials that can reduce the pressure bears by the forest elimination rate (Xavier, 2009). *Acacia mangium* and engkabang are two crops with high potential for that purpose. Thereby, this research is to promote these two species as raw materials for fire retardant-treated particleboard. The specific aim of this study is evaluate the physical and mechanical properties of the fire retardant-treated particleboards made of engkabang and *Acacia mangium*.

2. Materials and Method

2.1 Materials

Engkabang (*Shorea macrophylla*) and *Acacia mangium* were used in this research. The logs of engkabang were

brought from Sarawak Forest Department and the *Acacia mangium* logs were supplied by Asia Prima, Mentakab and Aramijaya Ulu Selidi, Johore. The logs of both species were grinded separately and then were flaked using Knife Ring Flaker at Wood Composite Workshop, Forest Research Institute (FRIM). The flakes were screened and only particles with size 1-2mm were taken and were spread on the oven trays for drying. The particles were dried at $105\pm 2^\circ\text{C}$ to reduce the moisture content to 5% before they were mixed with adhesive. Adhesive used in this study was urea formaldehyde (UF) supplied by Malaysian Adhesive Company Sdn. Bhd., Shah Alam. Two fire retardants were selected to be scattered onto the particles-adhesive mixtures i.e monoammonium phosphate (MAP) and zinc borate ($4\text{ZnO}\cdot 6\text{B}_2\text{O}_3\cdot 7\text{H}_2\text{O}$) during the mixing stage.

2.2 Manufacture of *Acacia mangium* and engkabang boards

The targeted board density was 700 kg/m^3 . About 897.29g dried particles, 182g UF resin, 27.31g hardener and 14.2g wax were needed to fabricate a particleboard with that targeted density as exhibited in Table 1. The dried particles with the 5%MC were placed into the particleboard mixer. Adhesive-wax-hardener combination was sprayed to the particles in the mixer by using airless spray gun which was attached on top of the mixer. Once the particles were mixed evenly with the adhesive, the particleboard mixer was turned off and 10% w/w fire retardant was placed on the furnish (Figure 1). The amount of fire retardant for the targeted density is determined by following the previous study done by (Izran *et al.*,2009). That amount of fire retardant was found effective to increase the fire resistance of the particleboards. The particleboard mixer with the mixture of particles-fire retardant-adhesive in it was re-operated for the next 5 min to make sure that the fire retardant was evenly scattered. The moisture content of the furnish was 12%MC. The MC was determined using Moisture Content Calculator. The furnish was then placed in a former, cold-pressed and subsequently pressed in a hot press at 165°C (Figure 2). The temperature of the hot press was increased to that temperature in intention to dismiss excessive water of the furnish, which was being absorbed from the surrounding during the mixing and cold pressing stages. The pressing time for each treatment varied from 6 to 9 minutes. Variations in pressing time for different fire retardant types were occupied based on the effect of fire retardant to the gelation time of the adhesive. Effects of phosphorous and boric-based fire retardants to the gelation time of UF adhesive was reported by (Izran *et al.*,2010 and Izran *et al.*,2009a). The MAP-mixed furnish was pressed for 6 min, slightly shorter than the control which was pressed for 7 min. Zinc borate-mixed furnish was pressed for 9 min due to the alkalinity of the fire retardant that was expected to delay the curing of the UF resin. The particleboards were exposed to the surrounding before they were brought to the conditioning room and conditioned at $20\pm 2^\circ\text{C}$ and $65\pm 2\%$ relative humidity until equilibrium, i.e 12% for 1 week. Total of three boards for each treatment were trimmed according to the standard requirement size and were distributed for the strength tests.

2.3 Physical and mechanical evaluations

The tests were conducted in accordance with British Standard EN. The physical and mechanical testing conducted were static bending (BS EN 310:1993), thickness swelling and water absorption (BS EN 317:1993), internal bond (BS EN 319:1993) and density (BS EN 323:1993). Ten blocks were distributed for each test. The blocks were randomly cut from each of the untreated and treated boards and conditioned in the conditioning room until they reached constant weights. The particleboard were cut to two sizes of blocks: 1) $50 \times 50 \times 12\text{ mm}$ for internal bond and thickness swelling, 2) $240 \times 50 \times 12\text{ mm}$ for modulus of rupture (MOR) and modulus of elasticity (MOE). The mean values of the samples obtained from the tests were analyzed using ANOVA, to study the relationship between the fire retardant types and the strength of the engkabang and *Acacia mangium* particleboards.

3. Results and Discussions

The data are summarised and presented in Table 2. For modulus of rupture (MOR) and modulus of elasticity (MOE) values, the negative signs indicate a reduction in the value of properties, while for thickness swelling and water absorption, the negative sign reflects an improvement in dimensional stability. The treated samples were compared with the untreated samples in order to investigate the effects of the fire retardants to the physical and mechanical performances.

3.1 Physical properties

Thickness swelling is to measure the dimensional stability of the particleboards. Lower thickness swelling value indicates a more stable board. There were two different thickness swelling tests conducted i.e 2h immersion in cold water and 24h immersion in cold water. The results show the fire-retardant treatments reduced the dimensional stability and increase the water absorption of the particleboards for both species. The longer the immersion the greater the thickness swelling and the amount of water absorbed. The differences between the treated engkabang and *Acacia mangium* to the untreated, when they were immersed for 2h were -0.77, 2.63, 1.34

and 3.63% respectively. As for water absorption test, the differences were -0.38, 2.7, 1.1 and 4.68% respectively. Similar result patterns were recorded for samples immersed for 24h but greater than 2h: -4.68, 4.68, 11.28, 17.25% for thickness swelling and -9.7, 18.82, 15.24 and 27.99% for water absorption. The differences indicate that the MAP-treated engkabang was more stable than the untreated. The ZBr-treated engkabang and *Acacia mangium* were less dimensionally stable than their treated counterparts with MAP. Naturally, fire retardants are hygroscopic and they are able to increase the water absorption of the treated particleboards. This claim has been investigated in depth (Izran *et al.*, 2009 and Izran *et al.*, 2009a), where it was found that kenaf core particleboard treated with phosphorous-based fire retardants (MAP, BP®, and diammonium phosphate) presented increase of thickness swelling from 10.11 to 35.91% and water absorption from -3.79 up to 35.91% respectively. It was also recorded that the TS and WA can become worse if the amount or concentration of fire retardants is increased (Abdul Rashid *et al.*, 1990, Muehl *et al.*, 1999 and Winandy *et al.*, 2008)

3.2 Mechanical Properties

The treated particleboards tended to have lower mechanical properties compared with the untreated, but generally, the treated particleboards complied with the standard requirements. Results in Table 2 show that ZBr caused greater reduction of most mechanical strength properties for both species than MAP. The MOR values for particleboards treated with ZBr for *Acacia mangium* and engkabang were 13.23 and 14.08 respectively, which were significantly lower compared to untreated particleboards i.e 21.17 and 20.38 N/mm² and those treated with MAP i.e 14.42 and 17.42 N/mm². Similar results can be seen for MOE except for the treated *Acacia mangium* particleboards. For engkabang, once again, ZBr-treated possessed the lowest MOE value i.e 3155 N/mm² compared with the untreated and MAP-treated, which the MOE values were 3924 and 3337 N/mm². For *Acacia mangium*, the MAP-treated particleboards were significantly lower than that of ZBr. The ZBr-treated MOE value was 2940 and the MAP-treated was 2818 N/mm². However, the values were still lower than the original stiffness of the untreated i.e 3483 N/mm². There were no significant differences of internal bond (IB) between the untreated and treated particleboards for engkabang and *Acacia mangium*. However, the result pattern was similar with that of MOR, where the ZBr-treated, still presented lower values compared with the untreated and MAP-treated. The different UF adhesive curing rate as it was mixed with fire retardants, which brought to the longer and shorter hot pressing time was expected to be a factor that influencing the MOR, MOE and IB of the treated particle boards (Izran *et al.*, 2008, 2009 2009a and 2009b). The ZBr-treated furnish was exposed to the heat longer as it required longer pressing time than other furnishes and these could cause slight decreases in internal bond. The effect of the hot pressing time on the strength of the particleboard has been investigated by Zhiyong *et al.* (2006), who fabricated medium density fibreboard with five different pressing schedules. They found that as the press platen was closing from 90 to 160% the MOE value decreased from 110 to 70%. It was also suspected that strength loss occurred during chemical treatment and subsequent redrying of the panel (White and Sweet, 1992). Thus, modifications on the hot pressing time and temperature are required to fully cure the resin and at the same time preserving the strength of the particles.

4. Conclusions

The findings from this study revealed that flame retardant treatments significantly affect the physical and mechanical properties of the engkabang and *Acacia mangium* particleboards. The fire retardants were found to affect the curing of the resin and modification on the hot pressing time was occupied to be sure that the resin is fully cured and compact particleboards could be produced. The reductions of the mechanical properties maybe the result of the hot pressing temperature, time and subsequent re-drying of the particleboards. Between species, engkabang appears to possess better physical and mechanical performances compared to *Acacia mangium*, for both fire retardant types. However for both species, treated and untreated, generally complied with the standard requirements. As a whole, the treatment system used in this study may be suitable for the manufacturing of fire retardant-treated particleboard from engkabang and *Acacia mangium*. It appears possible increase in resistivity against thermal degradation may further expand the usage of the panels and will be discussed in future papers.

Acknowledgements

A special thank to FRIM-ITTO for the securing grant for this project and to members of FRIM for their supervision and commitment in this research work

References

- Abdul Rashid, A.M., and Chew, L.T. (1990). Fire retardant treated chipboards, In. Pre-proceedings of a Conference on Forestry and Forest Product Resource. CFFPR-90, Malaysia, pp.37
- Anonymous. (2009). Dipterocarpaceae-Shorea macrophylla-engkabang jantung, *Species Information*, Sarawak

Forestry Department

Anonymous. (2009a). Second Schedule Part II on Protected Plants from the Wildlife Protection Ordinance, Sarawak Forestry Department

Flackenstein, R. (2009). Which is better for hair, Illipe butter or Shea Butter?, Organic Skincare, Available online: <http://organicskincare001.blogspot.com/2009/03/which-is-better-for-hair-illipe-or-shea.html>

Izran, K., Koh, M.P., Tan, Y.E and Faezah, M. (2010). Buffering Capacity of Fast-Growing Species and Curing Time of UF Resin Modified with Zinc Borate and Monoammonium Phosphate, *Unpublished report of FRIM-ITTO Project 2009*.

Izran, K., Zaidon, A., Abdul Rashid, A.M, F., Abood, Mohamad Jani, S., Zaihan, J. and Faezah, M. (2009a). A preliminary study in Determining the Curing Time of Urea Formaldehyde resin mixed with different concentrations of fire retardants and assessments of its properties, In. Proceedings of National Postgraduate Conference on Engineering, Science and Technology, Malaysia, pp.89

Izran, K., Zaidon, A., Abdul Rashid, A.M. and Abood, F. (2009b). Fire Performance and Properties of Particleboard Made From Kenaf Core Treated with Fire Retardants, MSc. thesis, Universiti Putra Malaysia.

Izran, K., Zaidon, A., Abdul Rashid, A.M., Abood, F., Mohd. Nor, M.Y., and Maseat, K. (2009). Physical and Mechanical Properties of Flame-Retardant Treated Hibiscus cannabinus Particleboard, *Journal of Modern Applied Science* 3(8):2-8

Mohamad Azani, A., Nik Muhammad Majid, and Meguro, S. (2001). Rehabilitation of Tropical Rainforests Based on Indigenous Species for Degraded Areas in Sarawak, Malaysia, In. Workshop Proceedings of Rehabilitation of Degraded Tropical Forest Ecosystems, 2-4 November 1999, Bogor, Indonesia, Center for International Forestry Research, Bogor, Indonesia, pp.226

Muehl, H.J., Kryzysik, M.A., Youngquist, A.J., Chow, P., & Bao, Z. (1999). Performance of hardboard made from kenaf, In. Terry Sellers, J.R., Nancy A. Reichert, Eugene P. Columbus. Marty J. Fuller, and Karen Williams (Eds.), *Kenaf properties: processing and products*. Mississippi State University

Sanchez, R.L. (2006). Acacia mangium, Finca Leola Costa Rica Reforestation, available online : <http://www.fincaleola.com/acacia.html>

Velez Torres, D.A and Valle Del, J.I. (2007). Growth and Yield Modelling of Acacia mangium in Colombia, *Journal of New Forests* 34(3):293-305

White, H.R. and Sweet, M.S. (1992). Flame Retardancy of Wood: Present Status, Recent Problems, And Future Fields In. Recent Advances in Flame Retardancy of Polymeric Materials: Proceedings of 3rd annual BCC Conference. on Flame Retardance, Stamford CT. Norwalk, CT: Business Communications Company, Inc, pp. 250-257

Winandy, J. And Wang, Q., and White, R.H. (2008). Fire Retardant-Treated Strandboard: Properties and Fire Performance, *Journal of Wood Fibre and Science*, 40(1):62-71

Xavier, V.P. (2009). Using Acacia mangium as a single material in producing particleboard, presented to Jayakuik Sdn Bhd by a staff of Universiti Malaysia Sabah, Available online: www.jayakuik.com.my/event/victorviva.pps

Zhiyong, C., Muehl, H.J and Winandy, J.E. (2006). Effect of pressing schedule on formation of vertical density profile for MDF boards, In Proceedings of 40th International Wood Composites Symposium, 11-12 April 2006, Seattle, Washington D.C.

Table 1. Parameters for producing a particleboard

Raw Material	Engkabang and <i>Acacia mangium</i> (1-2 mm particle size)
Targeted board density	700 kg/m ³
Targeted board MC	12%
Board Size	(350 x 350 x 12) mm ³
Adhesive	
UF resin	12% (w/w of dried particles)
Hardener (NH ₄ Cl)	3% (based on resin)
Wax	1% (based on dried particles)
Fire retardants	
1. monoammonium phosphate (MAP)	10% (w/w of dried particles)
2. zinc borate (4Zn0.6B ₂ O ₃ .7H ₂ O)	

Table 2. Physical and mechanical performances of fire retardant-treated engkabang and *Acacia mangium* particleboards.

Performance	Standard requirements	Control -Eng±S.D	Fire retardant-treated samples				
			MAP-Eng ± S.D	ZBr-Eng ±S.D	Cont-AM ±S.D	MAP-AM ±S.D	ZBr-AM ±S.D
1TS (%)	NA	5.46 ^a ±0.8	4.69 ^a ±0.7 (-0.77)	8.09 ^a ±1.6 (2.63)	3.30 ^a ±0.6	4.64 ^a ±0.2 (1.34)	6.93 ^a ±0.9 (3.63)
2TS (%)	≤ 16 %	20.57 ^a ±5.9	16.34 ^b ±1.7 (-4.68)	36.47 ^c ±3.8 (4.68)	8.82 ^a ±0.8	20.10 ^b ±9.4 (11.28)	26.07 ^c ±1.2 (17.25)
1WA (%)	NA	13.42 ^a ±2.1	10.34 ^b ±1.1 (-0.38)	16.12 ^c ±3.0 (2.7)	8.09 ^a ±1.6	9.19 ^a ±4.0 (1.1)	12.77 ^a ±1.5 (4.68)
2WA (%)	NA	45.69 ^a ±9.5	35.99 ^b ±1.8 (-9.7)	64.51 ^c ±8.4 (18.82)	20.38 ^a ±1.2	35.62 ^a ±14.0 (15.24)	48.37 ^a ±5.2 (27.99)
MOR (N/mm ²)	≥14N/mm ²	21.17 ^a ±4.0	17.42 ^b ±5.0 (-17.71)	14.08 ^c ±3.5 (-33.49)	20.64 ^a ±3.6	14.42 ^b ±4.0 (-30.13)	13.23 ^c ±2.1 (-35.9)
MOE(N/mm ²)	≥1800N/mm ²	3924 ^a ±447	3337 ^b ±337 (-14.96)	3155 ^c ±532 (-19.59)	3483 ^a ±702	2818 ^b ±499 (-19.09)	2940 ^c ±404 (-15.59)
IB (N/mm ²)	≥0.4N/mm ²	0.6 ^a ±0.06	0.57 ^a ±0.05 (-5.0)	0.43 ^a ±0.09 (-28.33)	0.90 ^a ±0.12	0.68 ^a ±0.23 (-24.44)	0.36 ^a ±0.1 (-60.0)

¹Means within a row followed by the same alphabets under each species are not significantly different at p≤0.05, ²Values in parentheses are percent change over untreated, ³1TS=Thickness swelling and water absorption of samples immersed in cold water for 2h, 2TS and 2WA= thickness swelling and water absorption of samples immersed in cold water for 24h, MOR=modulus of rupture, MOE=modulus of elasticity, IB= internal bond



Figure 1. Scattering the fire retardant on the particle-adhesive mixture



Figure 2. Hot pressing

Methods and Problems of Drilling Implantation in Rural Water Supply in the Fractured Basement Area in Chad: Case of Ouaddaï Geographic

Massing Oursingbé (Corresponding author) & Zhonghua Tang

Department of Hydrogeology and Water Resources, School of Environment Studies

China University of Geosciences, 430074-Wuhan, Lumo Road 388, Hubei, China

Tel: 86-27-5972-3504 E-mail: massing.2@hotmail.com

Yonoudjoum M. Médard

Ministry of Water, Direction of Water Resources and Meteorology, 429 Ndjamen, Republic of Chad

Tel: 23-5-6620-7704 E-mail: monodjomi1977@yahoo.fr

Abstract

This study focuses on the Ouaddaï Geographic Region, located on the eastern edge of the Chad basin, along the Sudanese border of Darfur where fracturing is well developed. It aims to highlight the factors affecting the productivity of hydraulic structures by the characterization of fracture networks in crystalline and metamorphic rocks using stereotyped results from the interpretation of satellite images Landsat-7 ETM + and exogenous data collected in Directorate of the Hydraulics Field Knowledge of Ministry of Water. All techniques resulted in the enhancement of structural and linear elements content in the raw images, enabling better geological cartography. The lineaments map obtained after treatment is very dense and consists of lineaments (discontinuities images) in various sizes. The analysis of these fracture networks has enabled us to highlight the presence of certain tectonic directions N40 to 60° E and N110 to 130° E potentially more favorable. The appearance tectonics is a fundamental criterion for the establishment of hydraulic work. However, satellite images study in comparison with aerial photography makes it possible to know what scale is imperative to make study for a project of rural water supply. The statistic of the various data shows a high flow rate of dry borehole (approximately 60%) and nearly 20% of works have a flow rate ranging between 0.5-1.5 m³/s. For this propose, many dry boreholes are mostly localized on anomalies associated with fault zones very wide and very marked and conductive. These zones often correspond to shearing zones. On this kind of anomaly, the drillings should be established on geophysical gradients, but not in the center of anomaly which could be systematically plugged. It may also include the cemented areas which the electrical tomography in pole dipole directs and inverse can refine the establishment. In all this analysis, we have made from some recommendations in order to allow raising some ambiguities relating to borehole establishment in fractured basement: carry out the drilling in the border of the large and conductive geophysical anomalies. Indeed; carry out the borehole just in the inselbergs border to verify certain hydrogeological assumptions which consist in saying that border of these massive outcrops is aquifer; and carry out the drilling in hydraulic border upstream of dyke, acid, basic and quartz vein. All these considerations are essential to increase significantly the success rate of the drillings establishment in the basement areas.

Keywords: Fractured basement, Ouaddaï geography, Statistics, Productivity, Rural water supply

1. Introduction

Water, essential for life and for any economic development, becomes a major strategic challenge in many parts of the globe. But it can also be the vector of epidemic and contribute to human exposure to toxic substances or undesirable. However, the quality of the resource depends in large part to anthropogenic pressure, planning and activities that support the watershed or environment.

However access to safe drinking water is one of the major objectives of development projects around the world. In Chad, many efforts have been made in recent years by the Government under the assistance of Breton Wood Institutions (World Bank) to improve the supply of drinking water to people in general and particularly to rural communities. Thus, several projects on rural water supply have been initiated in Chad.

The concept of rural water supply is to provide drinking water to population isolated starting from drillings generally equipped with hand pumps. The productivity target is modest and drillings are generally declared positives and equipped from obtaining a flow rate greater than 0.5m³/h at the end of drilling. The term

"productivity" here indicates the ability of aquifer to provide, through a catchment, a minimum flow rate that can be exploited.

For budgetary reasons, the depths of investigation are contractually limited, usually to 60m. When borehole does not reach this flow whith that depth, it is declared negative and abandoned, and then the building site moves on another site. Despite of more or less rigorous screening by photo interpretation and geophysical investigation, all the survey sites do not have the same chance of success.

Unfortunately, access to groundwater remains random in some territories parts where the aquifers have a certain complexity. Indeed, the research of groundwater in medium of fractured or fissured bedrock is mainly based on the identification of fractures which are witnesses of the tectonic deformation. Thus, drilling which doesn't cross any fracture can not produce water. Therefore, failures are generally many during the drilling campaigns when the establishment is not conducted under optimal conditions.

The region of geographical Ouaddaï, area of our study registered in this hydrogeological context, and of which it poses the problem of rational choice for the sites establishment of the works of catchment area. Despite the technical of prospecting carried out, the failure of drilling can exceed 50% in the discontinuous bedrock aquifers, which covers nearly 62% of Central and East Africa [Gombert P., 1997].

Thus, it is to cope with these difficulties which this study was initiated with a new prospecting approach of groundwater exploration by integrating the maximum information. It is a contribution to a better knowledge of the geometry of fracture networks. It makes it possible to highlight the critical factors that influence the productivity of the hydraulic works (drillings & wells). These lead to determine, in the term, the probable sites for establishment of drilling in order to improve the drillings success at the time of rural water supply campaigns in the study area. Indeed, if the groundwater is increasingly occupying an important place in daily activities (domestic, industrial and agricultural) of geographical Ouaddaï, the accurate information's are essential on the factors which influence the productivity, accessibility as well as the exploitability of aquifers and water drillings.

2. Characterization of bedrock aquifers

The aquifers are composed of crystalline rocks of plutonic origin (granite) and metamorphic (gneiss, schist, mica, etc...). From the hydrogeological point of view, it is hard rock which presents a mechanical behavior and hydraulic properties of all relatively homogeneous and which is characterized mainly by a permeability of fissure and fractures. These aquifers are considered as "discontinuous" because of the large spatial variability of their hydrodynamic properties [L. Patrick, Robert W., 2005]. These basement rocks (plutonic and metamorphic rocks) are aquifers only within their superficial fringe on the first 100 meters approximately under the ground surface[R. Taylor, K. Howard., 2000], which has been subjected to processes of supergene deterioration. The deterioration profile type includes, from top to bottom, the following horizons, which have specific hydrodynamic properties.

The otherness covers the "healthy" rock on a variable thickness (from 0, where the horizon is eroded to several tens of meters). This compartment is characterized by a significant porosity of interstice (within granite porphyritic, the effective porosity can exceed 5%) and by a relatively low permeability. When it is saturated with water, this compartment provides a function of capacitive storage of groundwater in the aquifer [JC Maréchal et al., 2003].

The fissured horizon consists of hard rock, affected, on several tens meters of thickness, by the presence of fissure, decreasing frequency with the depth. These cracks, whose origin was associated a long time with "superficial decompression", resulting also from the deterioration processes [R. Wyns et al., 1999]. Their genesis is mainly due to alteration of phyllitic minerals (especially biotite), which swelling causes this fissure [JC Maréchal et al., 2003]. Within textured isotropic rocks (granites, for example), the fissure is expressed preferentially along sub horizontal plans, perpendicular to minimal constraint. Therefore, these plans are generally parallel to the morphology of contemporary deterioration. Within not folded anisotropic rocks (foliated granites, gneiss), the cracking remains planar, but its direction and intensity are determined by the angle between the foliation and topographic surface. Within intensely folded rocks (Schist, mica schist), cracking has a generally random orientation, even at the scale of the outcrop. At the top of the fissured horizon, the frequency of micro cracks becomes close to the grain size of the rock (about one millimeter), marking the transition with otherness's overlying [JC Maréchal et al., 2003]. An important consequence of these methods of genesis is that the fissured horizon of granite is parallel to the paleo-surfaces of deterioration. This horizon ensures transmissive function of the aquifer and is collected by most drillings carried out in the base area.

The importance of couple fracturing- alteration is undeniable in the crystalline rocks because groundwater is limited to the secondary structures where voids were produced by combined action of tectonics and alteration.

The massive parts of rock can contain water only if the secondary openings side are present, because matrix porosity and primary permeability induced of the most crystalline rocks are extremely low [Issiaka S., John B., 1999].

3. Physical context of study

Located between 11° and 16° of northern latitude and 20° at 23° longitude East, Ouaddaï geographic is limited to north by the massive of Ennedi, in the west by the depression of Mochta, east by the Republic of Sudan and in the South by the Central African Republic. Ouaddaï geographic is located almost entirely in the Sahelian zone and extends of about 150 000km² along Chad's eastern border, thus including the two prefectures of Biltine and Ouaddai. It is characterized by three climatic zones from south to north [G. Joseph, 1980]: the Sahelian-Sudanian zone, the Sahelian zone and the Sahel-Saharan zone. (i) The Sahelian-Sudanian zone is bounded by isohyets 750 and 600mm. The duration of the rainy season is about five months per year and is distributed from May to September with a peak in July-August [H. Plote, 1970]. The vegetation is characterized by sparse savannah not very dense and gradually sparse northward. (ii) The Sahelian zone is bounded by isohyets 600 and 300mm/year. It has an average duration of rainy season of five months (May to September) with maximum rainfall in August. Evaporation is estimated at 4500mm/year (about 10mm/day). The trees are rare and they are replaced by shrubs among which there are thorny. Under these shrubs installed an herbaceous carpet of pseudo-steppe type. (iii) At the Sahelo-Saharan zone, the rainfall is less than 200mm/year. The differences between the minimum and maximum temperatures are high (in the order of 40°C). It is the most arid of Ouaddaï. The months most rainy are July and August. The vegetation is characterized by rare grasses. However, inside the same zone, the vegetation varies with soil type on which it is installed.

The hydrographic network is constituted of the ouadis (local terminology to designate the intermittent rivers of Ouaddaï) flowing towards tornado. About them, Texier (1960) writes: "we are far from Classic River whose flow rate grows by successive tributaries". The ouadis occur at the crest lines and flowing generally towards the west on the Chadian basin (itself divided into NW and SW side) and towards the east on the Sudanese side along the slopes. On the Chadian basin, they are thrown either in a lake (Batha is thrown into Lake Fitri), or they disappear beneath the dunes forming downstream of them the vast marshes: the "Nagas". The flow direction is generally E-W or NE-SW, rarely N-S except for Batha tributaries.

Geologically, the region belongs to large batholithic of granite calco-alkaline of Precambrian, called "regional granite" [Plotte, 1970], crossed by many intrusions: granitites acids (alkaline granite) have basic (grano diorites), pegmatite and quartz. The basement is everywhere outcrops or sub-outcrops beneath a thin cover of Quaternary sandy silt deposit from the surrounding reliefs. By places a layer of otherness's granular develops, thin given the low efficiency of the current climate. Two tectonic phases have affected the Ouaddaï [J. Sonet., 1963]. One, of folding and previous to the Paleozoic sandstone has affected the basement and allowed the installation of wrinkles. The other, brittle, is at the origin of the installation of veins and faults. It was held at the Paleozoic and Tertiary. Probably during this phase that the Ouaddaï has been shaped in tiers, one of which is the piedmont.

From the hydrogeological view point, we come cross in Ouaddaï geographic the classic superposition of the superficial porous tank (alluvium and otherness's) and a discontinuous aquifer hosted by fractures of the basement [Cefigre, 1990]. These aquifers are located in zone of basement outcrops and where this one is sub-outcrops, including under several meters of covering thickness (otherness's and Quaternary deposits and Tertiary), configuration which we found on the whole Ouaddaï geographical [Mr. Steenhoutdt., 1993]. The geometry of aquifers tanks include: (i) covering formation likely, under certain conditions, to contain a resource of sub-surface circumscribed within space limits of the shop rock. (ii) The bedrock formations, under their various lithology and the stages of evolution and deterioration, with capacitive function provided by otherness's clayey and sandy-clay saturated and, possibly by granular arena preceding transition zone with boulders and cracking's dense marking the forehead of deterioration and breakdown of bedrock; a transmissibility function provided by surface of discontinuities of bedrock (fissures, fractures, lithological contacts) to selective spatial distribution, possibly homogenized by the presence of transition zone and / or granular saturated arenas developed [M. Steenhoutdt., 1993]. The low and irregularity precipitation coupled with the importance of evaporation and transpiration, allows only low infiltration estimated at 40mm per year [Moussie., 1986]. These conditions do not make it possible to maintain saturation the superficial aquifer [Engalenc et al., 1981] and the static level is established within the fractured bedrock. This discontinuous aquifer is a reflection of the fractal distribution of fractures in reservoir rock. In Chad, where the clay orientation is poorly developed, the location of fracture aquifers is not at all sensitive to conventional geophysical prospecting, including geo-electric [Gombert, 1997 & Ouedraogo, 1988].

4. Methodology

The cartographic database used in this study include: the structural map of the Ouaddaï, as modified by Gachet A in 2004 and 2005, and Ragot J, M.2005 [Marc-André Bünzli. Yves Haerberlin., 2005]. The suture line separates a metamorphic filed in the south from a basement with granitic prevalence in north. Map background with topographic relief SRTM shaded in 45° (NASA.SRTM); the watersheds map of Chad eastern whose the quotient km per km² of river makes it possible to evaluate the type of flow regime and the potential of basement recharge; the hydrogeological and geological maps extracted respectively from the explanatory leaflet of the hydrogeological map of the east [Marc-André Bünzli. Yves Haerberlin., 2005] and of the hydrogeological synthesis of data relating to the western and southern piedmont of the massif of Ouaddaï [Djoret Daira., 1992]; the stereotypes resulting from the interpretation of satellite images LANDSAT 7 ETM + in panchromatic mode realized by UNHCR in 2005 were also of paramount importance in this study. In addition to these maps and images, the Directorate of the Hydraulics Field Knowledge (DHFD) of the Ministry of Water has placed at our disposal a database of hydraulic structures made by the various projects that have succeeded in this area and those carried out by NGOs. Thus, we identified 1758 hydraulic structures of any kind (boreholes, wells) and whose 717 were retained our attention for having details information's. This information's are summarized as hydrogeological parameters, the nature of the crossing structures and the types of hydraulic structures made, such as wells, boreholes and piezometers.

MapInfo7.8 software was a key tool determining for the cartography of the maps. Thus, from the structural map we had taken over the lineaments and structural anomalies under MapInfo7.8 after having to proceed to the calibration of the latter with 25 points for a maximum error of pixels equal to 5 (Figure 1). Then, the geographical coordinates of the 717 hydraulics work in Degree Minute Second (DMS) identified in X, Y and converted into Decimal Degree (DD). Those were plotted (Figure 2) on the maps carried out of the UNHCR/RTF [Marc-André Bünzli. Yves Haerberlin., 2005], in order to allot to each work its geological parameters, its watershed and its attributes, its location compared to a dyke, a fault. The juxtaposition of different tables, that is to say, the works table on the lineaments table gives us a simplified structure map of establishment of positive and negative works. This map allows us to highlight the productivity of these works according to their location. That is to say, the rate of positive and negative works obtained despite the resources mobilized and the methods of exploration and exploitation of water used in the Ouaddaï geographic area. The satellite images LANDSAT 7 ETM +, multispectral in panchromatic mode, whose interpretation was made by the UNHCR show innumerable structural formations with some precision. Thus, we carried out the systematic cartography of the dykes and faults through MapInfo7.8 software. The inventory of their orientation from their route on the map made it possible to highlight the main directions of the extension and compression movements which have affected the study area. The cartography of these various structures (dikes and faults) also allowed us to understand the hydrogeological context in order to locate sites suitable for the establishment of hydraulic works in the basement of Ouaddaï geographic.

5. Results and discussion

The extraction of lineaments has led to the establishment of the map of the structural frame of the study area. On the one hand, the juxtaposition of the hydraulic works and the main structural allowed us to obtain structural map and establishment of hydraulic works; and on the other hand, the compilation of different catchment area with principal structural formations gave catchment area map and structural formations of Ouaddaï Geographic.

The parameter study on the productivity of drilling is maximum exploitation flow rate, parameter generally available on the projects of Hydraulic villager and most representative of power draining fractures among known parameters for these drillings. It is available for all drilling inventoried in the area. This flow rate is given to be calculated on the basis of pumping test results by applying standard method defined by CIEH (1988). The flow rate of drilling that has not been tested, that is to say the least productive wells, is recorded like null.

In our study area, structural analysis allowed identification of several lineaments, usually corresponding to fractures, faults, veins or dikes. These rosettes of directions resulting from statistics carried out from cartography of HCR give regional directions, associated with opening of Atlantic rift and the Red Sea more recently. We note the directions N70°E to N50°E and N110°E to 160°E in the northern part and N50°E to 70°E and N110°E to 120°E in the southern part [Marc-André Bünzli. Yves Haerberlin. 2005]. However, for the dykes, one note the directions N5°E and 120°E for the quartz veins, especially present in the southern zone, N60°E for the basic dykes and N60°E to 70°E acids dykes. In comparison, the rosettes established from lineaments of aerial photographs, for positive and negative drilling are provide in the Figure 3. The rosettes show the regional direction namely N60 and 110-130°E. At these regional directions, added the N40°E direction, which is not

highlight by UNHCR study, but which is present on all types of drilling. The distribution of drillings shows that the directions N60°E and 90°E give more positive drilling, whereas those N20, 80, 110 and 130°E are often the most negative.

In considering direction of extension N60°E for the opening of the Red Sea (the most recent direction), then the parallel fracturing theoretically have tendency to open or reopen whereas the perpendicular directions are closed. In this case, the associated shear fractures are around 45° (N10°E and 100°E approximately). In complement, the influences of the Atlantic rift are situate towards N130°E in opening, closing at N40 and N85°E and shearing at 175°E. These considerations have values only if the influence of the Mediterranean plates does not create compressive constraint in the area and if there is no major accident redistributing locally the constraint field. There is general indication which will be able to guide partially hydrogeologists during aerial photographs study. These regional considerations are in phase with previously established rosettes.

It should be noted also that the result of the analysis of our data shows that most productive hydraulic works are located in basin with density hydrographic coefficients higher and middle basins and especially in groundwater flow direction. The distribution of the hydraulic works according to the organizations, quantity and ratio productivity are determined as follows (Table 1).

It appears that about 60% of hydraulic works are dry and nearly 20% have a flow rate raging between 0.5-1.5 m³/s. These results raise pertinent questions about methods of exploration and establishment of drilling in the basement areas. For this propose, many dry boreholes are mostly localized on anomalies associated with fault zones very wide and very marked and conductive. These zones often correspond to shearing zones. On this kind of anomaly, the drillings should be established on geophysical gradients, but not in the center of anomaly which could be systematically plugged. Thus, the areas moderately resistant above the fault which are superimposed on the anomalies of deeper fractures can correspond to the less fractured levels and limiting the buffer reservoirs. It may also include the cemented areas which the electrical tomography in pole dipole directs and inverse can refine the establishment.

The approach combining inventory of the lineaments on satellite image, exogenous data and field work led establishment of fractures and understanding geological structures [Berard et al, 1990]. Thus, the detailed map of lineaments (Figure 4) was achieved through an interpretation of images derived from different processing techniques. This map shows an important density of lineaments of varying sizes, up to several hundred meters. This study of lineaments highlighted the various nodes of fractures which, constituted by the intersections of fractures have a significant water potential. They can help to direct the recognition campaigns by defining the areas potentially favorable and to select the specific sites for drilling establishment.

Several studies conducted in different contexts have shown interest and importance to the analysis of lineaments on satellite images for hydrogeological exploration. Dutartre *et al.* (1990), in a study carried out in Burkina Faso, have been set from SPOT imagery the repetitive interpretation rulers in three complementary fields: research of fracture zones, the seepage areas delimitation and areas identification having an agronomic potential. Berard *et al.* (1990), in a study for the water supply of an industrial complex (gold mine) in Sudan, have shown the contribution of Landsat images combined with previous studies to establish drilling and highlight the existence of new aquifers. In a study of lineaments in the region of Marahoué (Ivory Coast) on Landsat images, Biémi *et al.* (1991) have established a diagram making it possible to define drillings in fissured basement in order to control future drilling establishment and to ensure their management.

From the general point, the studies by satellite photos are very important for general knowledge of the perimeter study. On the order hand, it is clear that the scale of cartography only helps very rarely for specific establishment on the field. The correlations to the faults, dykes, watex zones, geology, watershed etc ... are interesting, even fundamental if there has a margin of establishment of several kilometers.

In all this analysis, we have made from the hydrogeological divisions carried out, given the general recommendations in order to allow raising some ambiguities. They are: (i) carry out drilling in the border of the large and conductive geophysical anomalies. Indeed, it is possible that these anomalies correspond to an important shearing. Thus, hydraulic gradient upstream can be aquifer in this case. (ii) Carry out drilling just in the inselbergs border to verify certain hydrogeological assumptions which consist in saying that border of these massive outcrops is aquifer. (iii) Carry out drilling in hydraulic border upstream of dyke, acid, basic and quartz vein, to check any aspect of the hydraulic barrier and / or drain of these structures. All these considerations are essential to increase significantly the success rate of the drillings in the basement areas.

6. Conclusion

Using the approach combining interpretation of satellite imagery, the exogenous data and the field work, has allowed the cartography and the analysis of fractures and the profile deterioration associated with them. This makes it possible to guide the drilling establishment able to provide a large flow rate. Castaing *et al.* (1989) have shown the necessity of using aerial photography or the satellite imagery to cartography the traces of these fractures on the ground. Indeed, the hydraulic works carried out in of these fractures mapped, or better still to the place where two or more fractures intersect provide generally a great groundwater flow rate. However, the principal criteria were the presence of at least two lineaments of kilometeric extension crossing a node of fault; the proximity of ouadi to support the recharge; certain tectonic directions potentially more favorable as knowing N40 to 60°E and N110 to 130°E; the possible presence of dyke to form watertight barriers or the drains; the possible presence of coarse-grained lithology etc..... These brittle accidents have hydrogeological role. Indeed, to ensure an optimum flow rate for the drilling, the research for fractures or fracture intersections is advised. Thus for this study we have identified several fractures that present the interest sure for the future campaigns of rural water supply.

Acknowledgement

This research was supported by China Scholarship Council and China University of Geosciences (Wuhan), School of Environmental Studies. We wish to thank the China Scholarship Council, the Hydrogeology and Water Resources Department of Environment Studies School, China University of Geosciences in Wuhan and Water Ministry of Chad Republic for their support.

References

- CEFIGRE. (1990). Summary of knowledge on the hydrogeology of West Africa. *Crystalline and metamorphic basement*. Old Sedimentary, collection Maitrise de l'Eau, 47p., Ministry of Cooperation and Development, Paris.
- Berard, P., Castaing, C. & Scanvic, J. Y. (1990). Water supply of the Gold mine in Hassi (Sudan): Impact of remote sensing study. *Hydrogeology* 2, 101-111
- Biémi, J., Deslandes, S., Gwyn, Q. H. J. & Jourda, P. (1991). Geology and networks of regional lineaments of the catchment area of upper Marahoué (Ivory Coast): cartography using Landsat TM data and total magnetic field. In: *Remote Sensing and Management Resource*, Vol. VII, 135-145. Association Québécoise de Télédétection.
- Djoret Daira. (1992). Synthesis of the hydrogeological data on the western and southern piedmont of the Massif of Ouaddai. PhD Thesis.
- Dutartre, P., King, C., Motti, E. & Pointet, T. (1990). Use of SPOT imagery in hydrogeological prospection in Burkina Faso. *Hydrogeology* 2, 146-154.
- Engalenc M., Grillot J.C., Lachaud J.C. (1981). Method of study and research of groundwater in crystalline rocks of West Africa. *Geo-hydro-LCHF*, House-Alfort, France
- Gombert P. (1997). Variabilité spatiale de la productivité aquifère du socle sahélien en hydraulique rurale. In: *Hard Rock Hydro-systems*, POINTET T. ed IAHS Publ. no 241, 113-122
- Issiaka S., Jean B. (1999). Remote sensing and GIS for the study of crystalline basement aquifers of Odienné (North-West of Cote d'Ivoire). *OPA (Overseas Publisher Association)*, vol.1, p.47-64
- J-C Maréchal *et al.* (2003). Vertical anisotropy of the permeability of the fissured horizon of the basement aquifers: correlation with the geological structure of the deterioration profile.
- Joseph G. (1980). *The hydrogeology of Ouaddai (eastern Chad) in the geological context and hydro-climate of the Republic of Chad*. University of Nice, 182 p.
- Lamine. Y. Kosso. (1997). Report on the ending of short drilling on the crystalline basement areas north and center of the project, November 97 page 5.
- Marc-André Bunzli., Yves Haeberlin. (2005). *Hydrogeological Map of Eastern Chad: Explanatory Notes*.
- M. Steenhoutdt. (1993). Program of hydraulic villager and Pastoral in the Salamat, Ouaddai and Biltine. Technical and financial feasibility Study. BRGM
- Moussie B. (1986). Map of potential groundwater resources of the West and Central Africa at 1/5 000 000. BRGM, Orléans, France, Report 86 AFO 178 EAU, 82 p.

Ouedraogo B. (1988). Drilling Productivity on crystalline and metamorphic basement in sub-Saharan region. Th. Doct., Univ. Le Mans, France 252 P

Patrick L., Robert W. (2005). Basement aquifer: New concepts. Application to the prospecting and water resources management. *Geosciences* No. 2.

Plote H. (1970). Quadrennial program of hydraulic development of Ouaddaï: hydrology of Ouaddai. *Synthesis Report*. Vol.1 and 2. BRGM Paris., 448 p

R. Taylor., K. Howard. (2000). A tectono-geomorphic model of the hydrogeology of deeply weathered crystalline rock: evidence from Uganda, *Hydrogeol. J.* 8 (3) 279–294.

R. Wyls., JC. Gourry., J.-M. Baltassat., F. Lebert. (1999). Multi-parameter characterization of the horizons of sub-surface (0-100 m) in the context of altered bedrock, in: 2nd Symposium GEOFCAN, BRGM, IRD, UPMC, pp. 105-110.

Sonet. J. (1963). Geological map at 1/500 000 and explanatory, Niéré Sheet.

Texier. J. (1960). Hydrological research in the areas of Batha, Guéra and Ouaddaï (data bases for the development of water points on the surface or at a shallow depth). ORSTOM., CRT, *hydrology section*. 71 p.

Table 1. Distribution of works according to the organizations depending on their productivity

Organizations	Number of works carried out	ratio Productivity of the work carried out					Negative
		Positive					
		0.5 -1.5 m ³ /s	1.5 -5 m ³ /s	5 -10.1 m ³ /s	10.1-20 m ³ /s	>20 m ³ /s	
PHVOB, GTZ, SECADEV, Almy Bahaïm....	660	18.94%	13.18 %	04.40 %	01.97%	01.66%	59.85%
TOTALS	100%	40.15%					59.85%

PHVOB, Hydraulic Villager Project in Ouaddai and Biltine ; **SECADEV** : Catholic Relief Development ; **GTZ**: Deutsche Gesellschaft Für Technische Zusammenarbeit GmbH (German Society for Technical cooperation); **Almy Bahaïm** : water for livestock

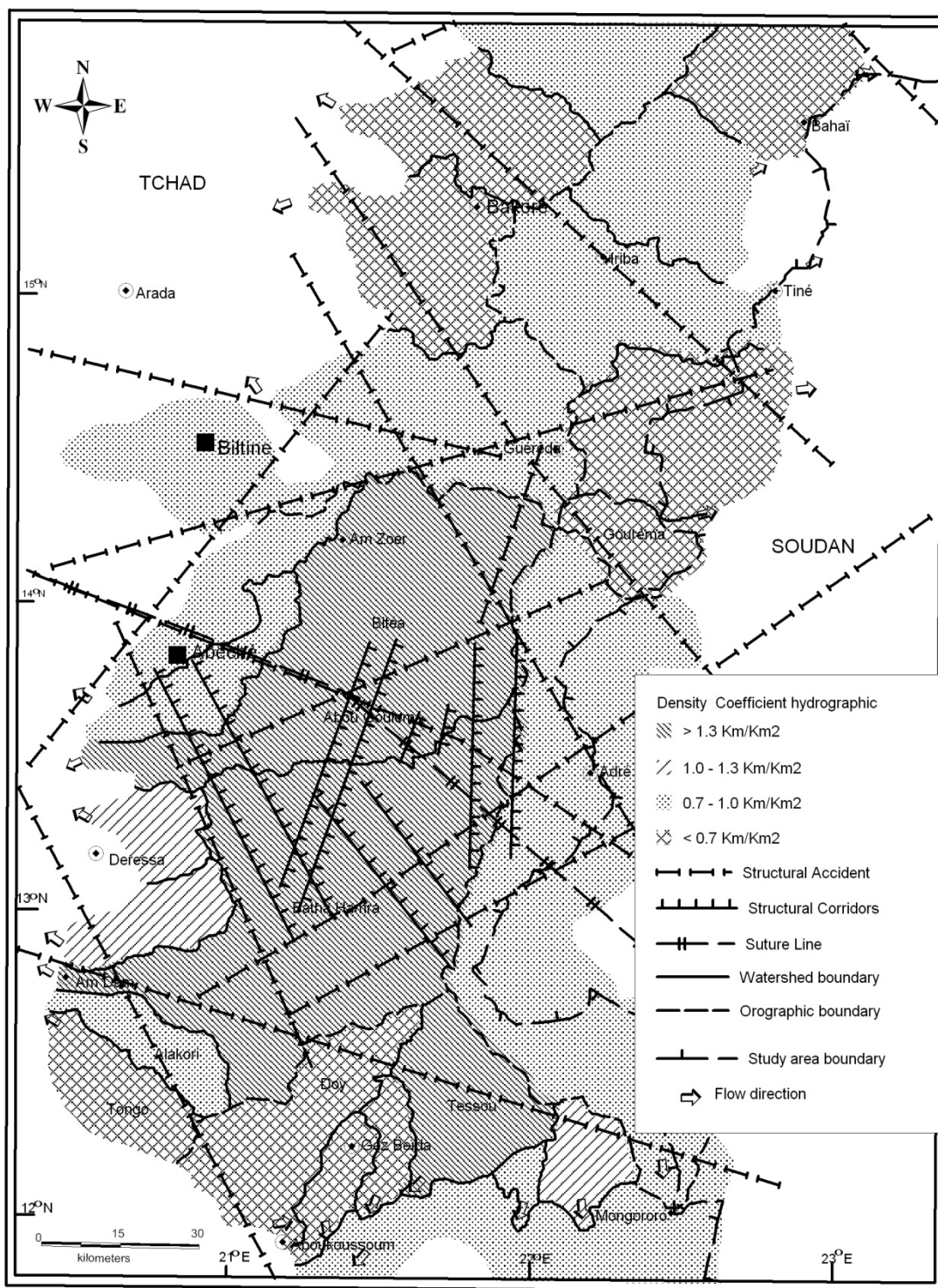


Figure 1. Map of simplified structural formation and watersheds division of Ouaddaï Geographic

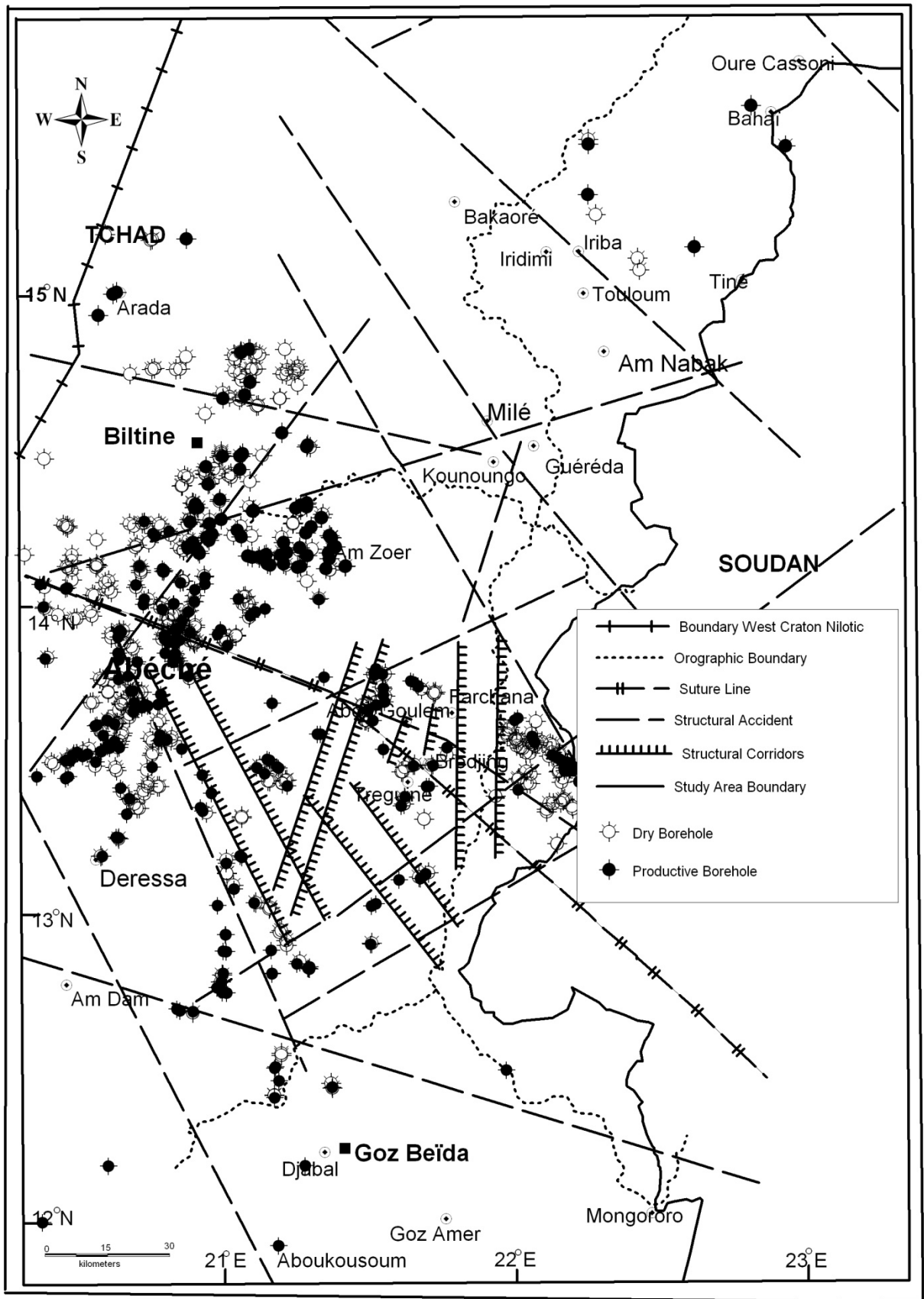


Figure 2. Simplified structural map and of distribution of borehole in Geographical Ouaddai

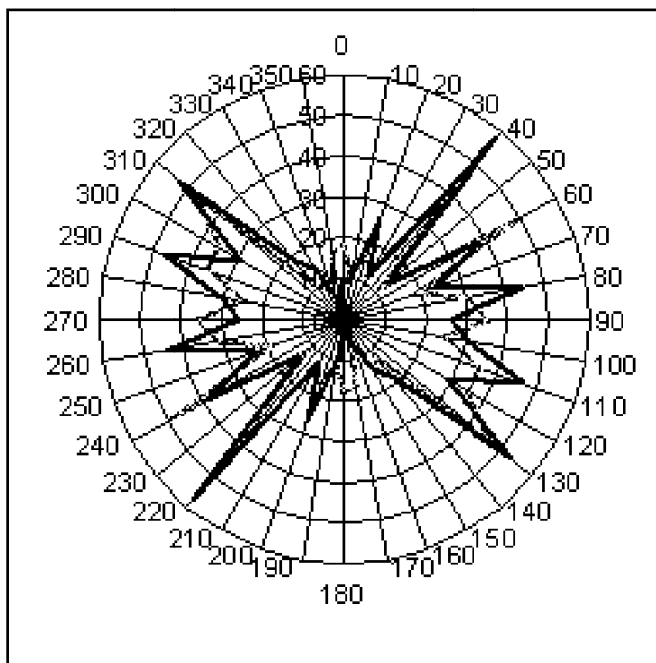


Figure 3. Rosette of the fracturing drilling directions of PHVOB (modified by Ragot JM 2005); Comparison positive drilling / negative drilling



Figure 4. Detailed structural map

A Distributed Dynamic Bandwidth Allocation Algorithm in EPON

Feng Cao, Deming Liu, Minming Zhang, Kang Yang & Yinbo Qian

School of Optoelectronic Science and Engineering

Huazhong University of Science and Technology, Wuhan 430074, China

National Engineering Laboratory for Next Generation Internet Access System, Wuhan 430074, China

Wuhan National Laboratory for Optoelectronics, Wuhan 430074, China

E-mail:hellocanfeng@gmail.com

Abstract

EPON (Ethernet Passive Optical Network) is a rising bandwidth access technology, and it could realize the comprehensive operation access including data, video, and voice, with good economic characters. IEEE 802.3ah is the industrial standard of EPON, but it doesn't concretely regulate the uplink bandwidth allocation algorithm of EPON. Therefore, aiming at the uplink channel access of EPON, people have put forward various dynamic bandwidth allocation algorithms, but most of them belong to intensive algorithm, i.e. the distributed bandwidth allocation (DBA) algorithm runs in OLT which is the interceder to allocate the uplink transmission time slot for ONU. A new distributed dynamic bandwidth allocation algorithm (DDBA) is proposed in this article, in which ONU decides the size of transmission window based on the assistant information transmitted by OLT and self queue length. The simulation result indicates that comparing with IPACT (Interleaved Poling with Adaptive Cycle Time) (G. Kramer, 2002, P.89-107), under the high network load, DDBA could obviously improve the average end-to-end time delay and the average queue length.

Keywords: EPON, DBA, Distributed scheduling, Access network (AN)

1. Introduction

With the occurrence of VOIP (voice of internet phone), video conference, and continually increasing data operation, new requirements occur for the bandwidth of network. But the bottleneck of the existing network bandwidth is in the access network, because the mainstream bandwidth access mode is the technology of DSL. The DSL technology developed based on the original phone network, and it doesn't fit for the transmission of data operation. PON is thought as one of the most hopeful technical projects to solve this bandwidth access bottleneck, and EPON adopting the Ethernet protocol has larger competitive advantage, and it begins to be produced in the market. EPON could realize the comprehensive operation access of data, voice, and video, with good economic character. Insiders generally think that FTTH is the final solution of the bandwidth access, but EPON will be a mainstream bandwidth access technology. Because of the characters of EPON network structure, the special advantage of bandwidth access, and the natural organic combination with the computer network, all experts in the whole world think that EPON is the optimal transmission medium to realize "three networks in one" and solve the "final one kilometer" of the info-highway.

EPON adopts the point-to-point network frame. The direction from OLT to ONU is the downlink direction, and OLT broadcasts, and ONU selectively accept the information according to the intention address of frame. The direction from ONU to OLT is the uplink direction, and there is only one uplink channel, and the data transmitted by different ONUs will conflict. To void that the frames sent by various ONUs conflict, a mechanism needs to harmonize the conflict induced by various ONUs transmit data to OLT. IEEE 802.3ah standard defines multi-point control protocol (MPCP), and it defines five control frames for the login, the bandwidth request, and the bandwidth authorization of ONU. Where, REPORT frame is the bandwidth request frame that ONU transmits to OLT, and it is used to report the length of the ONU buffer queue. GATE frame is the bandwidth authorization frame that OLT transmits to ONU, and it is used to report when ONU transmits data. But the standard didn't concretely define which scheduling algorithm will exceed the standard range when it is used to allocate the uplink channel bandwidth. The uplink bandwidth allocation algorithm of EPON could be divided into the FBA and DBA. Because FBA allocate ONU for fixed size bandwidth (time slot) each time, so the statistical reuse could not be used among ONUs, and it could not accord with the abruptness of the network operation, and the bandwidth use rate is low. But DBA has not these disadvantages, and it could not only fairly allocate the uplink bandwidth, but provide better QoS support. At present, most research works emphasize particularly on the intensive DBA algorithm, i.e. OLT accepts the bandwidth request of ONU, and compute DBA, and allocate the uplink transmission window for ONU. Many articles only improved this intensive DBA algorithm, and emphasize the improvement of the bandwidth use rate, the time delay, and QoS. In this article, a

new distributed scheduling algorithm is proposed, and it could fairly and effectively allocate the bandwidth. In this algorithm, the access control of the uplink channel is intensive, because it still could be run in OLT, but for all ONUs distributed in PON in the scheduling process, ONUs would decide the size of the uplink transmission window themselves.

2. Distributed DBA algorithm

2.1 Basic principle

The common character of the existing distributed DBA algorithms is that the computation of the uplink transmission time slot is accomplished by ONU, not by OLT, so ONU must know the transmission window information of other ONU. Therefore, the distributed DBA algorithm proposed before modified the frame of EPON. For example, in E. Wong's article (E. Wong, 2005, P.3) the network frame is simulated in LAN and all ONUs are conneted with one star coupler by two fibers, and ONUs could accept the frames transmitted by other ONUs. SR. Sherif (SR. Sherif, 2004, P.2483-2497) changes the light branch in EPON by a star coupler, so part of signal lights come from ONU could be reflected, and other ONUs will detect them. The DDBA algorithm proposed in this article needs not modify the existing EPON frame, and only transfer the window information transmitted by other ONUs to certain one ONU by the agency of OLT, and it completely accords with the MPCP protocol regulated by IEEE 802.3ah standard, and only needs add some new fields in the REPORT frame and the GATE frame.

In the algorithm of DDBA, ONU decides the size of tile slot, and transmits the REPORT frame to OLT, and after OLT receives the REPORT frame, it transmits it to the GATE frame at one, and the authorization length is the time slot requested by ONU. Of course, OLT adds some extra information in the GATE frame, so ONU could compute the size of the uplink transmission window. Extra information includes a weight vector (θ), i.e. the weight factors of all ONUs. These weight factors are defined as the proportion of the total using bandwidth allocated to the bandwidth of ONU and one polling cycle. ONU could know the size of other ONUs' transmission windows in last polling cycle by the weight information. When ONU transmits the REPORT frame, it will re-compute the weight factor according to the request bandwidth, and fill in relative field of the REPORT frame, and the weight information from OLT will be updated continually. When the scheduling begins, a fixed weight will be allocated to each ONU according to the information of SLA.

The polling mode generally includes the interleaved polling and the interleaved polling with pause. In the intensive DBA algorithm, if the interleaved polling mode is adopted, OLT will implement the DBA operation according to the REPORT algorithm of each single one ONU, and if the interleaved polling mode with pause is adopted, OLT will allocate the bandwidth after receiving the REPORT frames of all ONUs. Therefore, the former mode makes against that OLT makes fair and reasonable authorization, but the latter mode could ensure the justice of the bandwidth allocation under certain condition, i.e. the bandwidth use rate will be reduced, because the time slot will occur in two times of polling, and in this period, the uplink channel could not be utilized. For DDBA, because ONU could acquire the window information transmitted by other ONUs, and OLT needs not wait the arrival of all REPORT frames, so the interleaved polling mode is adopted (seen in Figure 1).

2.2 Bandwidth allocation

Here, W_{MAX} is the maximum bandwidth (time slot) which could be allocated in one polling cycle. One cycle is the time expensed by OLT when it polls all ONUs, i.e. the sum of N time slots and the protection time slots among them. From the formula (1), when the sum of all ONU's weight factors is 1, the bandwidth of the i'th ONU is $\theta_i W_{MAX}$.

The concrete approach of the DDBA algorithm could be described as follows.

(1) OLT maintains one weight vector table (seen in Table 1), where $\theta_i(n)$ denotes the weight factor of the i'th ONU in the n'th cycle. When OLT receives the REPORT frame of the i'th ONU, it will compare the new weight factor and the factors in the weight vector table, and if the new weight factor is bigger, it will be used to update the value in the weight vector table. Then, OLT transmits the GATE frame to ONU, and allocates the authorization bandwidth in next cycle, and the value of bandwidth is the size of the REPORT frame requested by ONU. If the EPON system supports QoS, the GATE will carry the follow parameter matrix.

$$\theta(n) = \begin{bmatrix} \theta_{11}(n) & \theta_{1M}(n) \\ \theta_{N1}(n) & \theta_{NM}(n) \end{bmatrix}$$

Where, N denotes the amount of ONU, and M denotes the amount of QoS sort. In the description of algorithm,

the value of M is 1. But the REPORT frame only carry the weight of single ONU and the information of QoS.

(2) When ONU receives the GATE frame, it will transmit the data with the length of $R_i(n)$ to OLT after the authorization time begins. Where, $R_i(n)$ denotes the bandwidth requested by ONU in the i 'th cycle. Then ONU will compute the maximum transmission window in $n+1$ cycles according to the extra information in the GATE frame, and the computation formula is

$$W_i(n+1) = \frac{\theta_i}{\sum_{j=1}^N \theta_j(n)} W_{MAX}$$

Hereby, the size of the bandwidth requested by ONU in $n+1$ cycles, i.e. $R_i(n+1) = \text{MIN}(W_i(n+1), Q_i)$, where, Q_i denotes the queue length of the i 'th ONU. Finally, ONU transmits the REPORT frame at the end of the authorization time slot, and informs OLT its queue length and new weight factor. These weight factors could be obtained by the following formula.

$$\theta_i(n+1) = \frac{R_i(n+1) \sum_{j=1}^N \theta_j(n)}{W_{MAX}}$$

Thus, the authorization to the i 'th ONU is accomplished, and other ONUs could be authorized according to above process. The beginning of the authorization time is still controlled by OLT, because only OLT know the size of the window transmitted by each ONU.

3. Simulation and analysis

The IPACT proposed by G. Kramer et al is an intensive interleaved polling algorithm, and its disadvantages have been described as follows. But the DDBA algorithm is a distributed interleaved polling algorithm, it could not only ensure the bandwidth use rate theoretically, but guarantee the justice of the bandwidth allocation. Here, these two algorithms will be simulated and compared. The IPACT algorithm adopts the limitation service mode to confirm the size of the transmission window, i.e. if the size of the bandwidth requested by ONU doesn't exceed the pre-established maximum transmission window, the size of the authorized time slot is the bandwidth requested by ONU, or else, the authorized length is this pre-established value.

By adopting the OPNET network simulation tool to model the EPON system, the network-level model is seen in Figure 2. The model adopts the tree network topology with one OLT and 16 ONUs. The distance from OLT to the light branch is 5km, and the distance from ONU to the branch is in 0-15km, so RTT will be distributed in 50us to 200us evenly. Each ONU node meets with one user node which will produce the network operation, and transmit it to ONU.

To acquire real network performance, the operation model with self-similarity and correlation is adopted (M. Crovella, 1996). The Hurst parameter with the self-similarity source is 0.8. According to the definition of Ethernet frame format, the lengths of the data package are in 512 bits to 12144 bits and obey the even distribution.

These concrete simulation parameters include that the speed from the user to ONU is 100Mbps, and the uplink and downlink channel speed is 1Gbps, and one buffer queue is set at the place of ONU, and the maximum length is 1Mbyte, and the protection time slot is 2ms. To simulate the performance of the simulation algorithms in different referring loads, ONU will share the total loads evenly. For example, if the total referring load is 1Gbps, the load referred by each ONU will be 62.5Mbps, and the operation production speed is 9383 packets/s.

The statistical quantities collected by the simulation include the average end-to-end time delay, the average queue length, the uplink bandwidth use rate, and the downlink bandwidth use rate. The average end-to-end time delay includes three aspects, (1) the polling time delay, i.e. the time interval from time when the packet arrives at ONU to the time that ONU transmits the REPORT frame, (2) the authorization time delay, i.e. the time interval from the time that ONU transmits the request to the time that ONU receives the authorization, (3) the queue time delay, i.e. the awaiting time of the data package in the transmitter queue. The average queue length denotes the lengths of all data package in the ONU buffer queue, and the unit is bit. The downlink bandwidth use rate denotes the ratio of the bandwidth consumed by the control frame and the total bandwidth.

Under different referring loads, the performance data (seen in Figure 3) of IPACT and DDBA could be obtained after 3 seconds simulation. The abscissa denotes the referring loads which are standardized by the uplink channel speed 1Gbps. When the abscissa is 0.7, it denotes that the whole network referring load is 700Mbps. From the

Figure 3(a), when the total referring load is less than 0.75, the average end-to-end time delays of two algorithms are almost same, but when the total referring load exceeds 0.8, the average end-to-end time delay of the DDBA algorithm is a little less than the time delay of the IPACT algorithm. Especially when the load is 1, the time delay of the IPACT algorithm is more 11ms than the time delay of the DDBA algorithm. At the location of ONU, the change curve of the average queue length is consistent with the change curve of time delay (seen in Figure 3 (b)), and after the load exceeds 0.8, the queue lengths of two algorithms will increase quickly, but the increase of the queue length of the DDBA algorithm is slower. From the Figure 3 (c), when the load exceeds 0.9, the use rate of the DDS algorithm to the uplink bandwidth will be kept above 90%, but the IPACT algorithm only has about 88% bandwidth use rate. That could indicate the cause that the average end-to-end time delay and the average queue length under high load will increase abruptly, and the use of the uplink bandwidth will achieve the saturation. For the use rate of the downlink bandwidth, two algorithms could obtain almost same result, and only when the load exceeds 0.9, the downlink bandwidth consumed by the DDBA algorithm will be less.

4. Conclusions

Aiming at the uplink channel access of the EPON system, a new distributed dynamic bandwidth allocation algorithm is proposed in this article. By the extra information transmitted by OLT, various ONU could decide the size of the uplink transmission windows based on its buffer queue length and other ONU bandwidth request information. The operation process of DBA is distributed in various ONUs, and OLT only assists it. The simulation result shows that under high network load, comparing with the IPACT algorithm, this algorithm could acquire lower end-to-end time delay and smaller average queue length.

References

E. Wong, and C. Chang-Joon. (2005). Efficient dynamic bandwidth allocation based on upstream broadcast in Ethernet passive optical networks. *Optical Fiber Communication Conference*. No.6. P.3.

G. Kramer, B. Mukherjee and G. Pesavento. (2002). Interleaved Polling Distribution Scheme in an Optical Access Network. *Journal Photonic Network Communications*. No.4(1). P.89-107.

M. Crovella and A. Bestavros. (1996). Self-similarity in World Wide Web traffic: Evidence and possible causes. *In Proceedings of ACM SIGMETRICS International Conference on Measurement and Modeling of Computer Systems*. Philadelphia PA, May 1996.

SR. Sherif, A. Hadjiantonis, G. Ellinas, et al. (2004). A novel decentralized Ethernet-based PON access architecture for provisioning differentiated QoS. *Journal of Lightwave Technology*. No.22. P.2483-2497.

Table 1. Weight vector table

ONU_1	ONU_2	ONU_3	...	ONU_N
$\theta_1(n)$	$\theta_2(n)$	$\theta_3(n)$...	$\theta_N(n)$

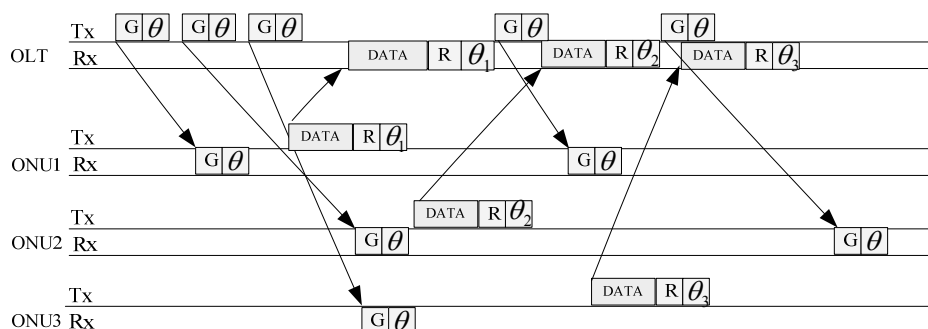


Figure 1. Interleaved Polling Mechanism of DDBA

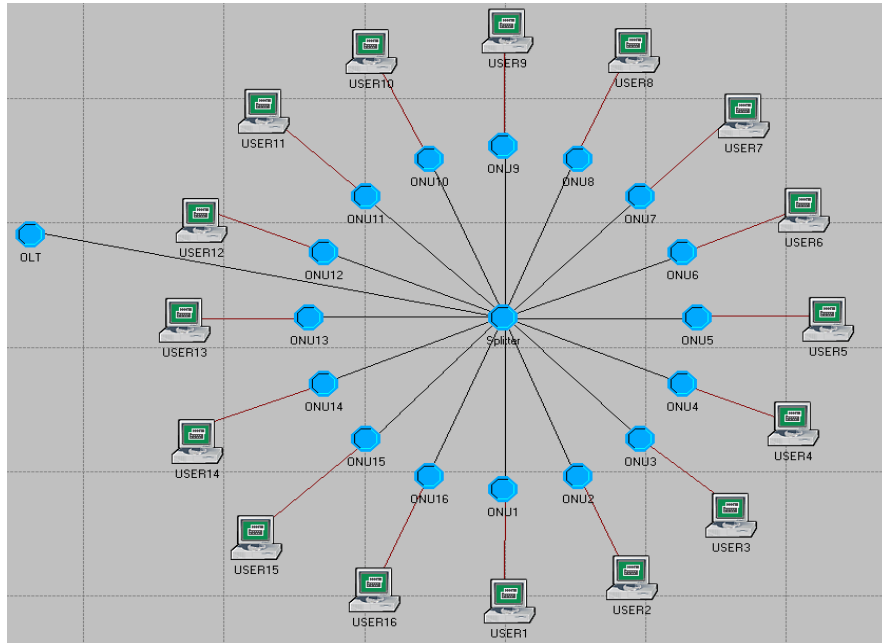


Figure 2. Network Model of EPON

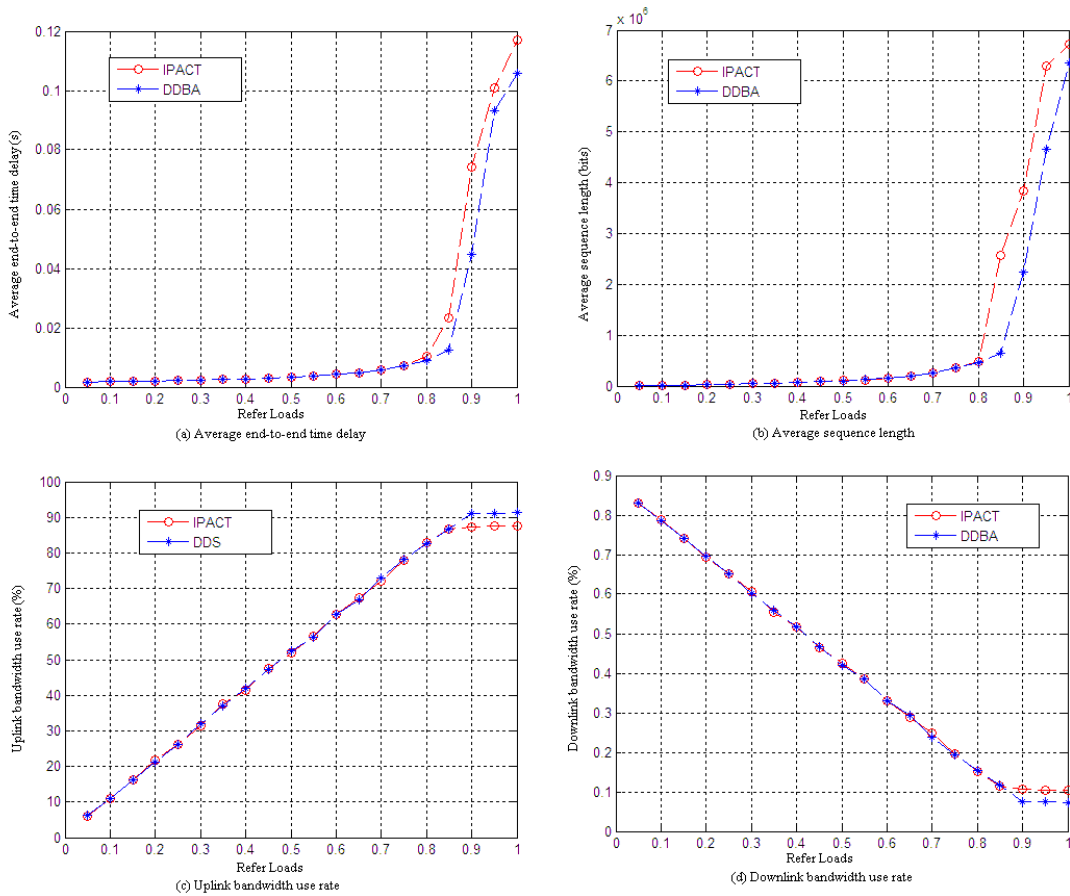


Figure 3. Performance Comparison of DDBA and IPACT

Determination of Soil Organic Carbon Variability of Rainfed Crop Land in Semi-arid Region (Neural Network Approach)

Yahya Parvizi (Corresponding author) & Manochehr Gorji

Soil Science engineering Department, University of Tehran, Karaj, Iran

Tel: 98-261-271-3431 E-mail: yparvizi@ut.ac.ir

Mahmoud Omid

Department of Agricultural Machinery, University of Tehran, Karaj, Iran

Mohammad Hossain Mahdian

Agricultural Research, Education and Extension Organization, Iran

Manochehr Amini

Swiss Federal Institute of Aquatic Science and Technology (EAWAG), Duebendorf Switzerland

Abstract

Soil organic carbon (SOC) is a very important component of soil that supports the sustainability and quality in all ecosystems, especially in semi-arid region. This study was conducted to evaluate the effects of 15 different climatic, soil, and geometric factors on the SOC contents in different land use patterns and to determine relative importance of these desired variables for SOC estimation in one of the semi arid watershed zones in the western part of Iran. Feed forward back propagation artificial neural networks (ANN), was used to model and predict SOC. The performance of the model was evaluated using R^2 and MBE values of tested data set. Results showed that 31-2-1 neural networks have highest predictive ability that explains %76 of SOC variability. Neural network models slightly overestimated SOC content, and had higher ability to detect management variables effects on SOC variability. In all ANN structure, management system dominantly controlled SOC variability in rainfed crop land of semi arid condition.

Keywords: CART, Modeling, Neural networks, Soil organic Carbon

1. Introduction

Soil is an important resource that is vital for the sustainability of life in ecosystems, and acts as a buffer to global climatic change (Sparling et al 2006). The soil organic carbon (SOC) is an important component, since it plays a key role in soil fertility and hydrology, contaminants control, and acts as a sink or source of terrestrial C, which affects the concentration of atmospheric CO₂. Atmospheric carbon is increased exponentially at a rate of 1.5% per year. Soil is regarded as an important sink and source for carbon sequestration and modifier of climate change. This can be done by proper land use selection and management practices (Tan and Lal, 2005).

Application of statistical methods include multiple linear regressions and partial least square regression, in SOC estimation, was limited, because of oversimplification, ignorance of complex nonlinear interactions. Another approach in dealing with nonlinear systems is to use non-linear and nonparametric regression methods included regression and nonparametric regression such as artificial intelligence (AI) modeling paradigms such as artificial neural network (ANN). ANN has been successfully used in classification, prediction and recognition problems (McCullagh, 2005, Zhang, 2004). The potential benefits of these methods include greater prediction reliability, cost-efficient estimation and solving complex problems involving nonlinearity and uncertainty. They have been successfully applied in various soil studies (Spencer et al., 2004). These applications include predictions of soil structure, hydraulic properties, pedotransfer functions (Amini et al., 2005, Sarmadian et al., 2009), pedometric use in soil survey (McBratney et al. 2002), environmental correlation of soil spatial variability (Park and Vlek, 2002)

This study was conducted to predict SOC variability at watershed scale across rainfed land use type in a semi-arid condition of Iran by using artificial neural networks (ANNs). Desired variables to predict SOC were consisted of climatic, soil, and topographic factors as physical variables, and tillage, rotation, crop residue

management, ownership, and soil degradation factors, as management parameters. Since the estimation model was data based, selection of appropriate input and output variables was important. Thus, sensitivity analysis on exploratory variables was carried out to select the best input combinations for modeling and estimating SOC.

2. Materials and Methods

2.1 Site description

Merek sub basin, from Karkheh river watershed, with area about 24000 ha, as an experimental site was selected for this study. The elevation of this site ranged from 1450 to 1850 m with annual average precipitation about 500 mm. This area consists of agricultural rainfed lands with area about 14500 ha, dominantly under Wheat and Pea rotation. Climate is semi-arid and cold. Soil temperature and moisture regimes are mesic and xeric. In this site, soil texture is ranged from clay to silt. Soils, in mountains and hill lands were covered by about 25-60% fine and coarse gravel. The pH varied between 7.3 and 7.9, EC ranged from 0.4 to 0.8 (dS/m), and lime content in topsoil was 4-60%.

2.2 Sampling and dataset

A sampling design based on randomized systematic method was performed with considering land use, soil, slope, and aspect maps. In each sampling site, soil samples were taken from topsoil (0–0.3 m depth). Figure 1 shows a general scheme of sampling and sample points. Totally, 245 different soil samples were collected. Soil samples were air dried and then sieved by 2 and 0.5 mm sieve. Soil organic carbon of these samples was determined. Some soil physio-chemical properties included; TNV, sand, silt, and clay percentages and SP percentages were determined.

In addition to soil variables that described above, climatic variables included mean annual temperature (MAT), mean annual rainfall (MAR), potential evapotranspiration (ETP) were recorded and climate types (C_{type}) determined using the Amberger method. Topographic variables (included elevation (Elev), slope (P), and aspect of the terrain of the sampling site) were also measured. Geometric factors such as curvature (Curv), and terrain parameter were derived from DEM that prepared based on digitized contour line map with 20 meter vertical lag apart. The transformed aspect (TA), which aligns the index along a SW-NE axis, for the sites was calculated according to Beers et al. (1966) using the following equation:

$$TA = \cos(45 - aspect) \quad (1)$$

TAP parameter was calculated by multiplying TA by sinus value of slope angle. This parameter was used to incorporate the effects of slope on direct-beam radiation.

To investigate management system effects, 13 raw quantified and three combined scenario indices, as management variables were defined by using collected data from field study. Primary 13 variables included: farm area and ownership, in ha (O_h), as ownership index, manuring (Mn), legegum (L.F) and cereal (C.F.) frequency in rotation period, winter fallow existence (W_f), crop residual pasture, straw harvest (S_h), straw burning, domestic density (D_d), machinery energy consumption (E) ($Mjha^{-1}year^{-1}$), tillage index (T_{index}) (Ferrara and Gersa, 2007) tillage direction index (P_{dir}), and accelerated soil degradation class (Er). Crop residual related variables were selected to define related variable as crop residue management scenario (S_{sen}) by classifying them with K-means clustering. Tillage management scenario index (T_{sen}) was defined by combine tillage related variables. Third management scenario variable was made by combining rotation related variables with K-means clustering. This variable, defined as rotation system (R_{sen}) variable.

2.3 Data selection and preprocessing

Selection of input data was based on theoretical contribution of physical and management variable, expert experiences and accessibility. Inputs were selected from climatic factors, soil physical properties, geometric factors and management system factors. The data set was split into a training set and a testing set. Before simulation, all data sets were standardized by using a linear algorithm software. Range normalization to transform the original data was used from $[x_{min}, x_{max}]$ so that each data point falls in the range $[-0.95, 0.95]$. The scaling formula is:

$$x^* = 1.9 \times \frac{(x - x_{min})}{(x_{max} - x_{min})} - 0.95 \quad (2)$$

Where: x_{min} and x_{max} are the minimum and maximum values that make up the series of data. Data is transformed so that 95% of the data points making up x fall between -0.95 and 0.95 . With this technique, data outliers who will fall above 97.5% or below 2.5% of the average value will not affect the normalization process.

2.4 Development of ANNs

A typical ANN consists of interconnected processing elements included an input layer, one or more hidden layers and an output layer (which provides the answer to the presented pattern). Between input and output layers, there could be several other hidden layers (see Figure 2). The input layer contains the input variables for the network, while output layer contains the desired output system, and the hidden layer often consists of a series of neurons associated with transfer functions.

The total error at the output layer is distributed back to the ANN and the connection weights are adjusted. This process of feed-forward mechanism and back propagation (BP) of errors and weight adjustment is repeated iteratively until convergence in terms of an acceptable level of error is achieved. Several methods for speeding up BP have been used including adding a momentum term or using a variable learning rate. In this paper, gradient descent with momentum (GDM) algorithm was used.

2.5 Sensitivity analysis

Since the SOC estimation model was data based, selection of appropriate input and output variables was important. A sensitivity analysis was performed on the chosen ANN's so that a better understanding of the relative importance of each input on the output could be examined. Thus, sensitivity analysis was carried out to investigate the dynamic behavior of input variables. This was done by imposing steps changes to various inputs and observing their effects on the network output. These responses were used as guides to select appropriate input and output variables that are suitable for model development.

2.6 Performance criteria

For the purpose of evaluation the accuracy of the prediction models, The performance of the models was evaluated by a set of test data using mean square error (MSE), coefficient of determination (R^2) on testing set, between the predicted values and the target (or experimental) values as follows (Omid et al., 2009). Additionally, two different measures including the mean bias error (MBE) and the correlation coefficient (ρ) were used. The MBE is a measure of bias and reveals the overestimation or underestimation. For ANN's evaluation, the testing sets were used to evaluate the effectiveness of techniques for predicting organic carbon.

2.7 Software

To design various neural networks, a commercial software package, NeuroSolutions (version 5.02), was used. The expression used to calculate the MSE is given by NeuroSolutions for Excel (2005). Statistical analysis was done by SPSS 16 and XLSTAT pro-7.5 package.

3. Results and Discussion

Descriptive statistic and variations of the SOC are given in Table 1. The SOC content varied from 0.34 for dry lands with abundant erosion, to 3.72% in low lands and manure applied soils. The correlation coefficients (ρ) between variables are given in Table 2. The correlation between SOC and T_{sen} was positive and with T_{index} and S_{sen} was negative, significantly ($\alpha = 0.050$). Significant correlation between climatic variables and SOC amounts was predictable, theoretically. But, there is insignificant correlation between geometric variables and SOC. On the other hand, comparing to physical variables, correlation coefficient of majority of management variables and SOC were significantly high. This result indicated that management measures eclipsed physical condition effects on SOC variability in rainfed condition of the semi arid regions in study area. TNV content of soils significantly lowered SOC contents, because of biological activity restriction in lime abundant.

3.1 ANN's structure optimization

Finding the optimum number of hidden neurons in the hidden layer is an important step in developing MLP networks. In neural network design, too many hidden units cause over-fitting, while too few hidden units cause under fitting. A summary of findings and best networks architecture is shown in Table 5. Among the different configurations examined, the N-2-1 configuration, exhibited highest accuracy and least error on cross validation data set (MSE = 0.0768). This optimum feature has N variables as input vector, 2 neurons in its hidden layer and 1 neuron as output vector. The performance of this network is shown in figure 3. After evaluating the optimized configuration with the test set, the MSE were obtained 0.107, 0.113 and 0.120, for all inputs, management, and physical, variables, respectively. The corresponding ρ -value was 0.88, 0.83 and 0.63. The MSE values for the ANN's, with different k = number of nodes in hidden layers values and epoch's, presented that when $k=2$ in calibration and validation data sets, the model was not over trained and optimum epochs in validation set equal to 46, 358, and 376, in all, management, and physical input vector models (Table 3). To find the optimum

number of hidden units, the MSE of the network with different inputs combination was plotted against the number of hidden units. Figure 4 presents this plot for ANN with all variables in input layer.

The scatter plot of the measured against predicted SOC, with different combinations and types of exploratory variables, in the test data set is given, respectively, in figure 5 for the ANN models, which was identified as being the best models for predicting SOC.

3.2 Sensitivity analysis

In order to test the hypothesis that not all of the inputs used were required to train the model networks effectively, it was necessary to measure the influence of each input variable on the output. This was done by measuring the mean rate of change of output when a single input was changed by some relatively small amount (0.001). The mean rate of change was determined by testing the model network 594 times using randomly selected input values. Sensitivities, defined as the MSE rate of output changes divided by rate of change of a given input. Sensitivity analysis results are shown in Figure 4. Results indicated that SOC variation was more sensitive to management condition change than physical variables. Changing in range of all management variables, especially tillage related variables, caused significant SOC variation. But among physical variables only aspect related variables (TA and TAP) and climate type affected SOC changes.

3.3 Comparison of ANNs

The test data set was used to evaluate the performance of the different network models for predicting SOC. The results of the research are given in Tables 3, 4, and 5, shows that the ANNs models can predict SOC contents more efficiently by all variables combination. But Spencer et al (2005) showed that ANNs with physical variables had better SOC estimation. On the other hand, ANNs showed higher ability to simulate management effects on SOC variability. This ability is in contract with Somaratne et al (2005) findings. The ANN models could contribute 45% of SOC variability to physical variables. The MBE values indicated that the network models slightly overestimated the SOC. This overestimation was however so small, especially for the network with physical input. The largest RMSE was produced by the neural network with physical predictors.

It seems that there are differences among the ANN models to distinguish kind of predictor variables effects on SOC. The similarity of the different procedures suggests that the relationship between SOC and predictor variables is essentially nonlinear. Significant differences in R^2 and evaluation indices of ANN models executed by different type of exploratory variables indicated that MLP-ANN algorithm can precisely detect interaction effects between physical and management variables.(Wang et al , 2008).

4. Conclusions

The newly developed, artificial neural network, can detect management effects on SOC variability. Management factors especially tillage scenario parameters (included kind of instruments (T_{index}), and tillage frequency), crop residue scenario parameters and also rotation parameters (especially legeum and cereal frequency in rotation period) dominantly determine SOC variability in semi arid conditions of study area. The models tested in this study, using physically based variables included: TAP, TNV, gravel, SP, MAT and AR could account for only up to 40-45% of the variation in SOC in the semi arid conditions of Iran. Analysis of sensitivity accuracy showed that adding more physical variables slightly improved variability prediction and did not significantly improve the modeling results. It seems that for improving prediction power of used methods, management practices, especially tillage, rotation, straw, and grazing management, are essential to be considered.

5. Acknowledgments

The financial support provided by the University of Tehran and Agriculture and Natural Resources Research Centre of Kermanshah Province is gratefully acknowledged.

References

- Amini M., Abbaspour, K.C., Khademi, H., Fathianpour, N., Afyuni, M., & Schulin, R. (2005). Neural network models to predict cation exchange capacity in arid regions of Iran. *European Journal of Soil Science*, 56,551–559.
- Beers, T.W., Dress, P.E., & Wensel, L.C. (1966). Aspect transformation in site productivity research. *Journal of Forestry*, 64,691–692.
- Liu, D., Wang, Z., Zhang, B., Song, K., Li, X., Li, J., Li, F., & Duan, H. (2006). Spatial distribution of soil organic carbon and analysis of related factors in croplands of the black soil region, Northeast China. *Agriculture, Ecosystems and Environment*, 113,73–81.

- McBratney, A.B., Minasny, B., Cattle, S.R., & Vervoot, R.W. (2002). From pedotransfer function to soil inference system. *Geoderma*, 109,41–73.
- McCullagh, J. (2005). A modular neural network architecture for rainfall estimation, *Artificial Intelligence and Applications*, Innsbruck, Austria, 767–772.
- McVay, K., & Rice, C. (2002). Soil organic carbon and the global carbon cycle, Technical Report MF-2548, Kansas State University.
- Omid M, Baharlooei A., & Ahmadi, H. (2009). Modeling drying kinetics of pistachio nuts with multilayer feed-forward neural network. *Drying Technology*, 27(10),1–9.
- Park, S.J. & Vlek, P.L.G. (2002). Environmental correlation of three dimension soil spatial variability: A comparison of three adaptive. *Geoderma*, 109,117–140..
- Sarmadian F., Taghizadeh Mehrjardi, R., & Akbarzadeh, A. (2009). Modeling of some soil properties using artificial neural network and multivariate regression in Gorgan province, north of Iran. *Australian Journal of Basic and Applied Science*, 3(1), 323-329.
- Somaratne S., Seneviratne, G., & Coomaraswamy, U. (2005). Prediction of Soil Organic Carbon across Different Land-use Patterns:A Neural Network Approach. *Soil Science Society Of American Journal*, 69,1580–1589
- Sparling, G.P., Wheeler, D., Wesely, E.T., & Schipper, L.A. (2006). What is soil organic matter worth?. *Journal of Environment Quality*, 35,548–557.
- Spencer M.J., Whitfort T., & McCullagh, J. (2006). Dynamic ensemble approach for estimating organic carbon using computational intelligence. Proceedings of the 2nd IASTED international conference on Advances in computer science and technology. Puerto Vallarta, Mexico
- Tan, Z. & Lal, R. (2005). Carbon sequestration potential estimates with changes in land use and tillage practice in Ohio, USA. *Agriculture, Ecosystems and Environment*, 126:113-121.
- Tan, Z., Lal, R., Smeck, N., & Calhoun, F. (2004). Relationships between surface soil organic carbon pool and site variables. *Geoderma*,121:187–195.
- Wang, L. & Mao, Y. (2008). A novel approach of multiple submodel integration based on decision forest construction. *Modern Applied Science*. 2(2):9-11.
- Zhang, G. (2004). *Neural networks in business forecasting*, IRM Press, Hershey, PA.

Table 1. Descriptive statistics of SOC variable

Descriptive Statistics	Minimum	Maximum	Mean	Variance	Standard deviation	Skewness	Kurtosis	C.V
SOC	0.34	3.67	1.52	0.51	0.71	1.19	1.15	0.47

Table 2. Pearson correlation coefficients (ρ) between SOC and physical and management variables

Physical variables	ρ	Management variables	ρ
Elev.	0.18	Er.	-0.12
P	0.07	O _h	-0.23
TA	-0.03	Mn.	0.35
TAP	-0.14	L.F	0.28
Curv.	-0.14	C.F	0.09
T.N.V	-0.23	W _f	0.05
S.P	0.24	Rsen.	0.25
Gravel	0.14	Pasture	0.34
clay	0.05	S _h	0.17
silt	-0.12	Burn.	0.45
sand	0.03	D _{den}	0.07
M.A.T	-0.19	Ssen.	-0.46
A.R	0.20	E	-0.51
ET	-0.15	T _{index}	-0.52
C.Type	-0.19*	P _{dir}	-0.09
---	---	Tsen.	0.46

*: In bolds, the correlation is significant at $\alpha = 0.05$

Table 3. ANNs performance with best architecture

Inputs		Train	CV	Test	Best Networks	Train	CV
All variables	MSE	0.001	0.118	0.107	Hidden 1 PEs	9	2
					Epoch #	1000	46
	ρ	0.860	0.862	0.883	Final MSE	0.001	0.043
Management variables	MSE	0.094	0.077	0.113	Hidden 1 PEs	10	2
					Epoch #	5000	358
	ρ	0.808	0.814	0.831	Final MSE	0.0018	0.0737
Physical variables	MSE	0.121	0.083	0.120	Hidden 1 PEs	9	2
					Epoch #	594	376
	ρ	0.651	0.376	0.631	Final MSE	0.0123	0.0413

Table 4. Mean Bias Error (MBE) of ANNs results with different input variables

Input variables	MBE		
	All variables	Management variables	Physical variables
	0.025	0.010	0.003

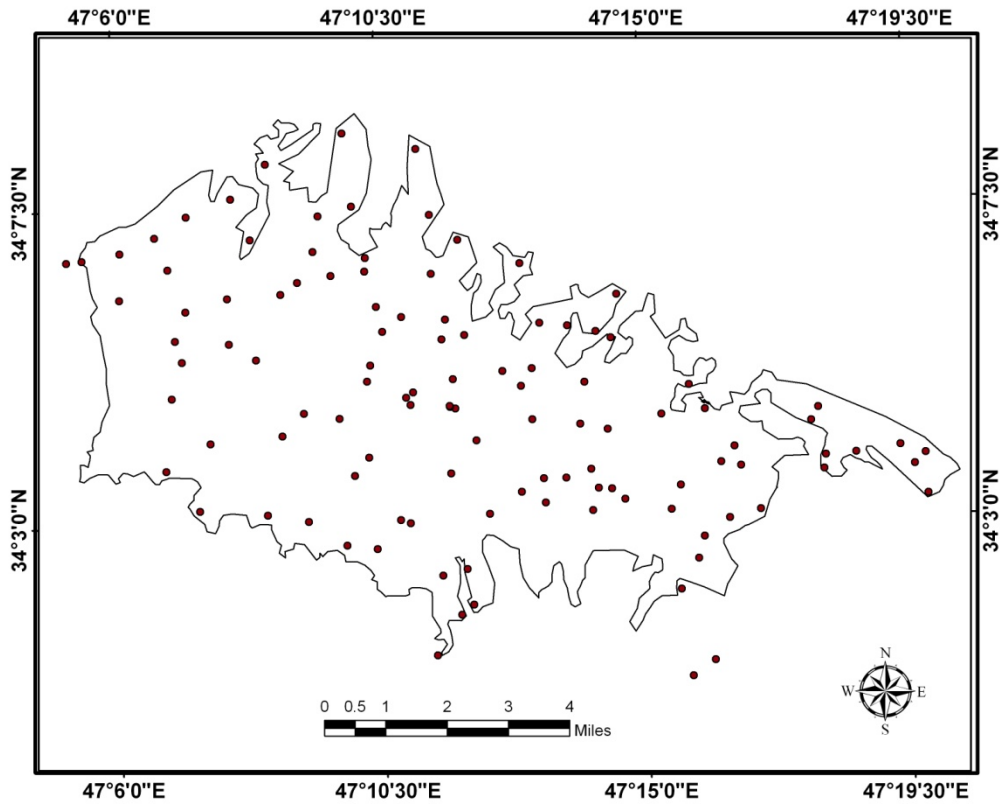


Figure 1. Rainfed land of Merek watershed and sampling point distribution

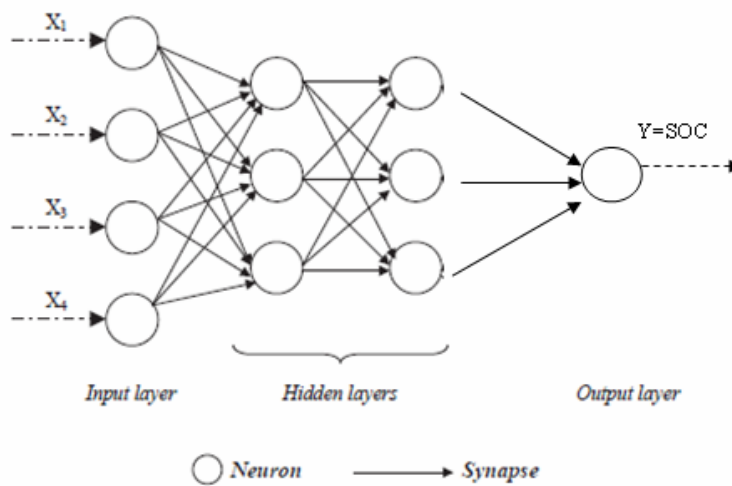


Figure 2. The structure of multi layer feed forward neural network

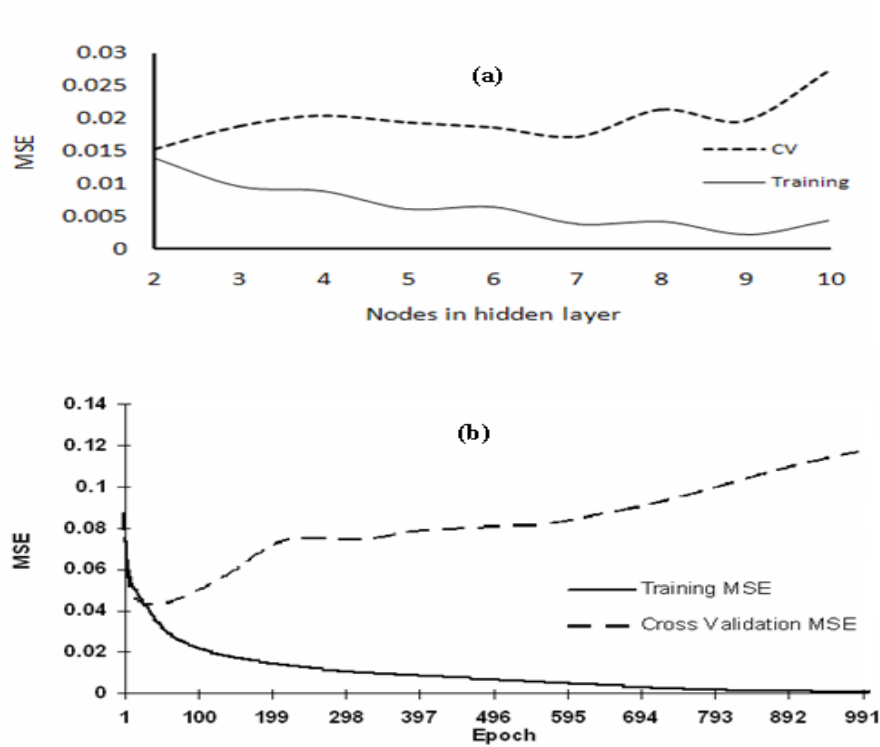


Figure 3. MSE of networks with all variables as inputs versus number of nodes (a) and epochs (b)

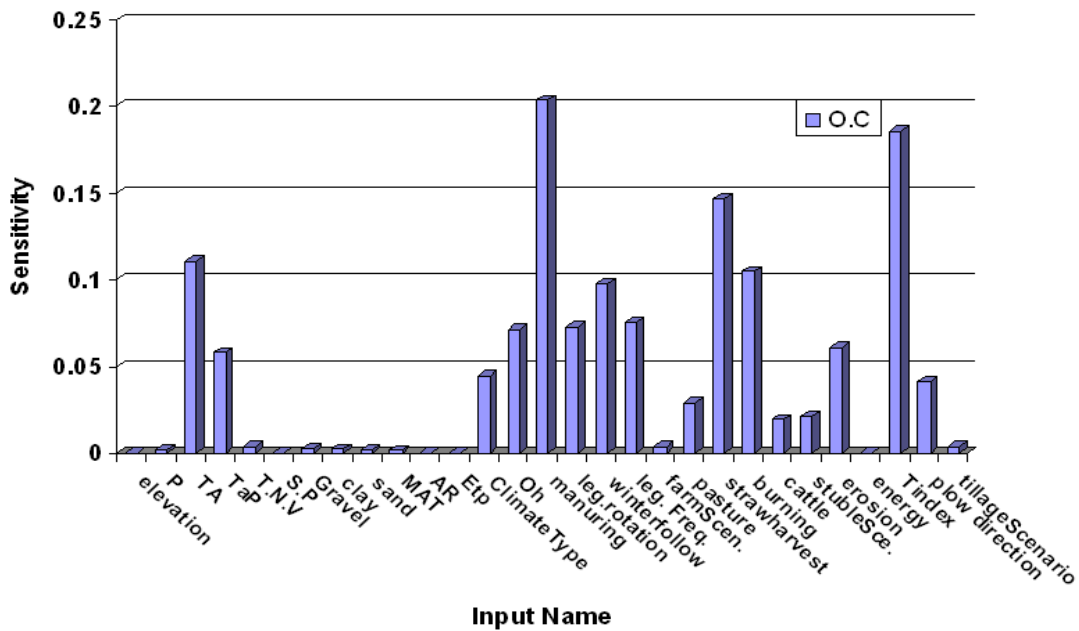


Figure 4. The result of sensitivity analysis about mean of input data for ANN with all variables

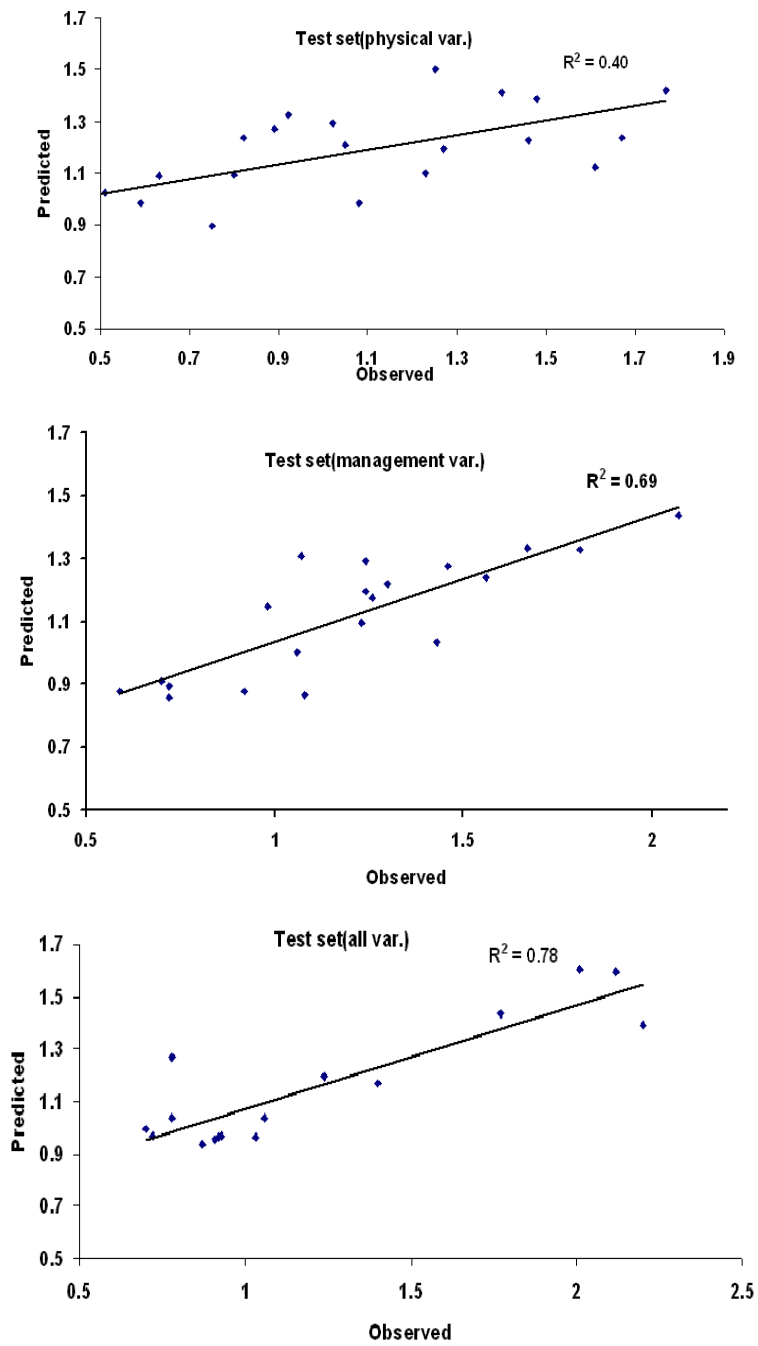


Figure 5. The scatter plot of the measured vs. predicted SOC using the ANNs with different inputs

Comparison of Some Chromatic, Mechanical and Chemical Properties of Banana Fruit at Different Stages of Ripeness

Mahmoud Soltani (Corresponding author)

Department of Agricultural Machinery Engineering
Faculty of Agricultural Engineering & Technology, University of Tehran
P.O. Box 4111, Karaj 31587-77871, Iran
Tel: 98-919-165-7116 E-mail: mahmoodsoltani39@yahoo.com

Reza Alimardani

Associate Professor, Department of Agricultural Machinery Engineering
Faculty of Agricultural Engineering & Technology, University of Tehran
P.O. Box 4111, Karaj 31587-77871, Iran

Mahmoud Omid

Associate Professor, Department of Agricultural Machinery Engineering
Faculty of Agricultural Engineering & Technology, University of Tehran
P.O. Box 4111, Karaj 31587-77871, Iran

Abstract

The physical, mechanical and chemical properties of banana fruits at different level of ripeness were determined. Relation between stages of banana ripeness and these properties were investigated and correlation coefficients were calculated. A significant difference at 5% level was found between the degree of ripeness and properties of banana fruit. Duncan multiple range test were conducted and results were reported. Comparisons indicated that ultimate strength and a^* appropriated the highest correlation coefficient, but mechanical experiments destroyed banana fruits thus were not suitable for ripening process.

Keywords: Banana fruit, Ripeness, Physical properties, Comparison

1. Introduction

Banana is one of the popular fruits in the world. Banana fruit is grown in many countries in sub-tropical areas and the big exporters are located in South East Asia, South America and the Caribbean. The Cavendish variety is widely produced by these countries. Banana is subsumed third place in the world fruits volume production after citrus fruit and grapes (FAO, 2000). Green-mature banana fruits are transported to consumer countries and ripened in controlled conditions. Imported banana fruits are transported to airtight warehouses with ethylene gas control system and are ripened. During ripening process, many changes are occurred in physical, mechanical and chemical properties of banana fruits. Skin color changes during ripening from green to yellow, firmness is decreased, banana is softened and starch is converted into sugar (Marriott *et al.*, 1981). Investigation of these changes was the subjects of many researches.

Finney *et al.* (1967) evaluated changes in firmness of banana fruit during ripening using sonic technique. Charles *et al.* (1973) studied on physical, rheological and chemical properties of bananas during ripening. Fernandes *et al.* (1978) studied changes of some physical properties of silver bananas (*M. Paradisiaca*) during ripening period. The results of their study showed the average of skin thickness was reduced from almost 4.0 mm to 1.5 mm. The results were correlated to the most important chemical changes in the fruit, such as total acidity, starch reducing and no reducing sugars and soluble solids. Kachru *et al.* (1995) investigated physical and mechanical characteristics of two varieties of green-mature banana fruit. Kajuna *et al.* (1997) investigated the textural changes of banana and plantain pulp during ripening. They found that untreated fruits of both varieties had a good correlation between pH and hardness, while treated fruits did not show any correlation between the two properties. Perera *et al.* (1998) studied physicochemical properties of some local banana cultivars. Saeed Ahmad *et al.* (2002) conciliated the temperature effect of ripening treatment on properties of banana fruit. Also investigation on reciprocal effect of storage humidity, temperature and fruit length on characteristics of banana fruit were done (Saeed Ahmad *et al.*,

2006). Bok Kim *et al.* (2009) determined apple firmness by using ultrasonic technique as a quality indicator. They measured apparent elastic modulus and rupture point by a compression test apparatus and correlated these properties with ultrasonic parameters. Salvador *et al.* (2007) studied the changes in color and texture of banana during storage at 10°C and 20°C. They found that during storage, the change in peel color from green to yellow was gradual in the *M. Cavendish* samples, whereas the *M. Paradisiacal* variety presented a different pattern, remaining green for the first 8 days and then changing rapidly to a yellow tone from day 12 onwards. While the flesh texture of the *M. Cavendish* type bananas softened quite rapidly during storage, it evolved more slowly in the *M. Paradisiacal* variety and there was little variation in the flesh hardness values over the storage time.

The objectives of this research were to study the variation of some chromatic properties (L^* , a^* and b^*), mechanical properties (energy required per unit depth of probe penetration and ultimate strength) and chemical properties (TA, TSS, and pH) of banana fruits, to determine the correlation among these properties and stages of banana ripeness and to find the best method to indicate the level of banana ripeness during ripening treatment.

2. Material and Methods

Specimens were provided from Kowsar airtight warehouse located in Abyek province in Qazvin, Iran. In this warehouse, ripening period on banana is carried out at six days. Temperature of ripening room was set up to 15.5°C. Relative humidity in warehouse was controlled between 85%-90%. During ripening, peel color varied from green to yellow. Ripeness is currently assessed visually by comparing the color of the peel with standardized color charts that describe various stages of ripeness. In trade market, seven ripening stages of bananas are usually discerned (Figure 1). Color stage was judged visually using a chart scale provided by SH Pratt & Co. Ltd (Luton, United Kingdom) to categorize bananas based on their level of ripeness. During ripening treatment at first day, banana fruits were at stage one and at the end of sixth day they were at stage six. Banana fruits (*Cavendish variety*) were selected from imported bananas (Philippine islands) that were ripened in an airtight warehouse with ethylene gas control system. Undamaged bananas of each stage were selected and cut into fingers. The experiment was set up with three replications from each stage. The laboratory tests were done at horticulture department in Faculty of Agricultural Science and Engineering, University of Tehran., Karaj (Iran). Color of banana fruits was measured by colorimeter (Model Konica Minolta CR-400). Positive a^* relates to degree of redness of peel, negative a^* indicates degree of greenness. Positive b^* defines yellowness and negative value of b^* represents the blueness. L^* is the value of lightness of banana peel ($L^* = 0$ for black and $L^* = 100$ for white).

Mechanical properties of specimens were measured by an Instron universal testing machine (Model SANTAM ST-5) controlled by a PC- based data acquisition card in a personal computer. A cylindrical probe with 8 mm diameter was used to penetrate in banana. Head speed was set at 50 mm/min (Saeed Ahmad *et al.*, 2006). The compression test results, calculations and graphs were generated automatically. As the compression initiated and progressed, a load-deformation curve was plotted.

After measuring mechanical properties, 10g of pulp was cut from a whole banana and diluted with 50g of distilled water in a blender for one minute and filtered. A hand held refractometer (Model Neerveld 14-B22550, GTEI) was employed to indicate the total solid soluble (TSS) in % Brix. The pH of diluted flesh was measured by pH meter (Ihanna pH 211; Italy). To calculate the titratable acidity (TA), the diluted pulp was titrated with 0.1N NaOH to the end point at pH= 8.1. The TA was expressed as a percentage of malic acid.

A randomized complete block experiment design was carried out on experiments. The Duncan multiple range test was employed for mean separation. The level of significance was at 5%.

3. Results and Discussion

3.1 Physical properties

Variation in mean values of L^* and b^* versus stage of banana ripeness is presented in Figure 2. Lowest value of L^* was 48.82 and the highest was 70.35 and for b^* the values were 27.4 to 45.73 (Table 1). There was a significant difference ($P \leq 0.05$) between the stages of banana ripeness for L^* and b^* . L^* increased between stages one and three and reached to 70.35 and stopped until stage six then decreased rapidly to 48.82 at stage seven. Similarly, b^* varied in this fashion. Decrease in these parameters was as a result of developing brown spots on skin. Accordingly, it was concluded that L^* and b^* are not good indicators for assessment of stage of banana ripeness. The values of a^* are presented in Figure 3. The a^* increased when banana fruits reached to a full-ripe stage. A positive correlation was observed between a^* and various stages of banana ripeness. As it was noted, an increase in a^* means the degree of greenness was decreased. These changes during ripening period (loss of greenness and increase in reddish) occurred as a result of the breakdown of the chlorophyll in the peel

tissue. It seemed that this parameter is more appropriate for predicting the level of ripeness of banana. Linear estimation of ripeness with a^* is shown in Figure 4. The correlation coefficient between stage of banana ripeness and a^* was obtained as 0.917. Results of Duncan multiple range test for these characteristics are presented in Table 1.

3.2 Mechanical properties

There was a significant difference ($P \leq 0.05$) in ultimate strength and energy required per unit depth of probe penetration at different level of ripeness of bananas, too (Table 2). Variations of these parameters are shown in Figure 5. Trend in decrease of ultimate strength and energy required per unit of penetration were similar. It was found that ultimate strength and energy of penetration decreased linearly. It was concluded that these characteristics could be good indicators in the study of banana ripeness. Mechanical properties decreased dramatically between stage one and stage three and then continued to decrease at a slower rate thereafter. This rapid softening corresponds to a commutation of pectic substances (Marriott and Lancaster, 1983). The major defect of this method is its destructivity on specimens that makes it not practical. Correlation between mechanical properties and stages of banana ripeness are presented in Figure 6. Correlation coefficient for ultimate strength and energy required per unit of penetration were -0.91044 and -0.9106, respectively.

3.3 Chemical properties

A significant difference ($P \leq 0.05$) was found between TA of each stage. Mean values of TA shows that this parameter decreases gradually until the fruit reaches to full-ripe (stage six) then increases at stage seven (Figure 7). It confirms the earlier findings by Olsen and Martin (1980) that total organic acid content declines gradually during fruit maturation, ripening and storage. But at stage seven, an increase in TA was observed because of conversion of sugars to acids. The TA showed an inconsistent pattern of variation. However, the TA varied between various stages of ripeness. It is very difficult to set a specific value of TA as an indicator of the level of ripeness. The pH measurement of data resulted in a significant difference ($P \leq 0.05$) which happened through of stages. Irregular variation occurred through ripening stages (Figure 8). The pH decreased at the first stage to stage three, and then an increase was observed until stage seven. Also it is found that acidity of fruit reached to a maximum value at stage three. Because of irregular changes, this indicator is not proper to estimate degree of ripeness. An increase in TSS pending ripening treatment was occurred as shown in Figure 9. Most of the TSS is sugar, thus this parameter is a good indicator of sweetness. During ripening the starch of banana converted to sugar so TSS is increased. This increase was reported by Marriot et al. (1981). At stage seven, TSS was the maximum (21.9 %Brix). Increase of TSS is an important trait of hydrolysis of starch into soluble sugars such as glucose, sucrose and fructose. In order to determine level of ripeness by TSS, it is necessary to destruct fruit and supply diluted pulp for measuring TSS, so this method is not practical in ripening room continually. Figure 10 shows a linear correlation between TSS and stage of banana ripeness. Correlation coefficient was obtained as 0.928. Table 3 shows the mean value of chemical properties (TA, pH and TSS) of banana fruits at different stages of ripeness.

4. Conclusion

Some physical, mechanical and chemical properties of banana fruits were investigated in this study. A significant difference was found between these properties and fruit ripeness. At different levels of ripeness, the correlation among these properties with stages of ripeness was found. Results showed a good correlation between mechanical properties and a^* existed with levels of ripeness. Extraction of mechanical properties led to destruction of samples. Experts need to enter the ripening room for ripeness distinction which increase energy used as well as a variation in warehouse environmental condition. So, it could only be a good practice in laboratory not at warehouses. The best alternative method of prediction of level of ripeness is to measure a^* since it dose not destroy the fruits. It is also a rapid method of indicating ripeness of banana fruit. Use of this technique resolves the above problem and provides an automatic control condition for airtight warehouses.

References

- Ahmad, S., Thompson, A. K., Hafiz, I. A., & ASI, A. S. (2001). Effect of temperature on the ripening behavior and quality of banana fruit. *International journal of agriculture & biology*, 3(2), 224–227.
- Ahmad, S., Perviez, M. A., Chatha, Z. A., & Thompson, A. K. (2006). Improvement of banana quality in relation to storage humidity, temperature and fruit length. *International journal of agricultural & biology*, 8(3), 377-380.
- Charles, R. J., & Tung, M. A. (1973). Physical, rheological and chemical properties of bananas during ripening. *J. Food Sci*, 38, 456-459.

- Fernandes, K. M., De Carvalho, V. D., & Cal-Vidal, J. (1978). Physical changes during ripening of silver bananas. *Journal of Food Science*, 44(4), 1254-1255.
- Finney, E., BenCela, I., & Massie, D. R. (1967). An objective evaluation of changes in firmness of ripening banana using a sonic technique. *Food Science*, 32(6), 642-646.
- Kachru, R. P., Kotwaliwale, N., & Balasubramanian, D. (1995). Physical and mechanical properties of green banana (*Musa paradisiaca*) fruit. *Journal of Food Engineering*, 26, 369-378.
- Kajuna, S.T. A. R., Bilanski, W. K., & Mittal, G. S., (1997). Textural changes of banana and plantain pulp during ripening. *J. Sci. Food Agric*, 75, 244-250.
- Kim, K. B., Lee, S., Kim, M. S., & Kwan, B. (2009). Determination of apple firmness by nondestructive ultrasonic measurement. *Postharvest Biology and Technology*, 52, 44-48.
- Li, M., David C., Slaughter, D. C., & Thompson J., F. (1997). Optical chlorophyll sensing system for banana ripening. *Postharvest Biology and Technology*, 12, 273-283.
- Marriott, J., Robinson, M., & Karikari, S. K. (1981). Starch and sugar transformation during the ripening of plantains and bananas. *Journal of Science, Food and Agriculture*, 1021-1026.
- Marriott, J., & Lancaster, P. A. (1983). Bananas and plantains. *Handbook of Tropical Foods (Harvey T. and Chan Jr., eds). Marcel Dekker, Inc. New York*. 85-143.
- Perera, O. D. A. N., Basnayake, B. M. K. M. K., & Anjani, M. (1999). Physicochemical characteristics, popularity and susceptibility to anthracnose of some local banana cultivars. *J. Natn. Sci. Foundation Sri Lanka*, 27(2), 119-130.
- Salvador, A., Sanz, T., & Fiszman, S. M. (2007). Changes in color and texture and their relationship with eating quality during storage of two different dessert bananas. *Postharvest Biology and Technology*, 43, 319-325.
- Subedi, P. P., & Walsh, K. B. (2009). Non-invasive techniques for measurement of fresh fruit firmness. *Postharvest Biology and Technology*, 51, 297-304.
- www.applegate.co.uk/food-and-agribusiness/pratt-company

Table 1. Mean values of L*, a* and b* at different stages of ripeness

Stages of banana ripeness	L*	a*	b*
1	57.44833 ^c	-14.055 ^c	32.638 ^c
2	61.985 ^{bc}	-9.07 ^b	38.443 ^b
3	70.35 ^a	-4.62 ^b	45.733 ^a
4	65.975 ^{ab}	-7.67167 ^b	40.9 ^{ab}
5	65.41667 ^{ab}	1.186667 ^a	40.41 ^{ab}
6	67.14167 ^{ab}	0.911667 ^a	40.29 ^{ab}
7	48.81833 ^d	2.645 ^a	27.35 ^d

In each column, means followed by the same letter are not significantly different ($P \leq 0.05$) according to Duncan multiple range test.

Table 2. Mean values of mechanical properties of banana fruits at different stages of ripeness

Stages of banana ripeness	Ultimate strength (N)	Energy required per unit of penetration (J/mm)
1	75.13 ^a	37.61 ^a
2	60.07 ^b	29.95 ^b
3	46.22 ^c	23.09 ^c
4	40.92 ^c	20.48 ^c
5	26.07 ^d	14.42 ^d
6	28.91 ^d	13.43 ^d
7	27.03 ^d	13.32 ^d

In each column, means followed by the same letter are not significantly different ($P \leq 0.05$) according to Duncan multiple range test.

Table 3. Mean values of chemical properties of banana fruits at different stages of ripeness

Stage of banana ripeness	TA	PH	TSS
1	0.1876 ^b	5.023 ^a	7.8 ^f
2	0.1833 ^b	4.67 ^{ef}	13.22 ^c
3	0.163 ^{bc}	4.62 ^f	16.4 ^d
4	0.1184 ^c	4.74 ^{ef}	17.41 ^c
5	0.0.125 ^c	4.77 ^{cd}	18 ^{bc}
6	0.136 ^{bc}	4.86 ^{bc}	18.6 ^{ab}
7	0.3529 ^a	4.933 ^{ab}	21.9 ^a

In each column, means followed by the same letter are not significantly different ($P \leq 0.05$) according to Duncan multiple range test.

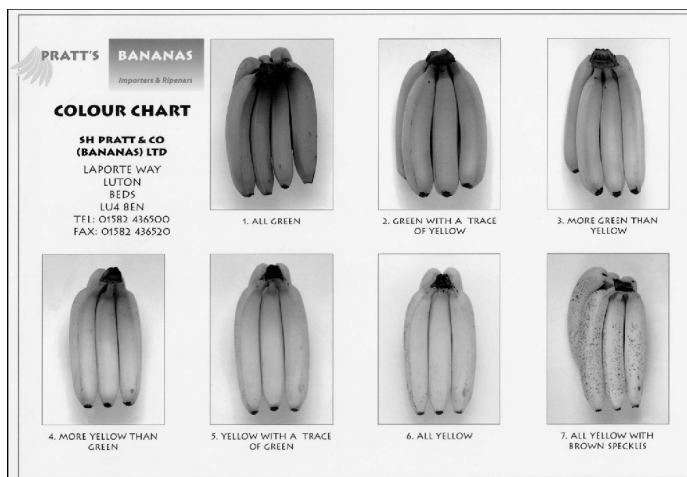


Figure 1. Color chart, SH Pratt's & co, (Luton, UK)

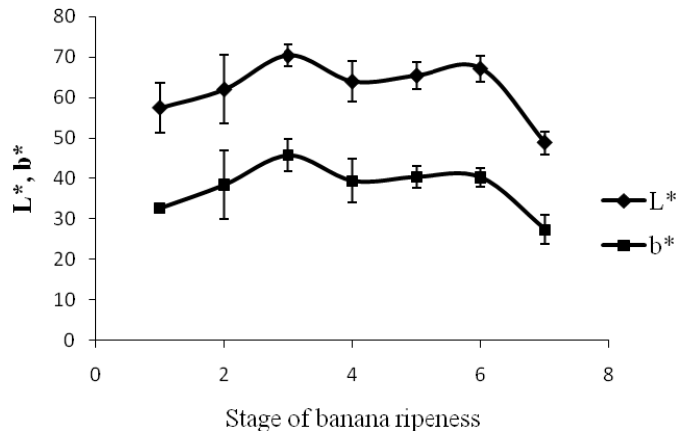


Figure 2. Variation of L* vs. banana ripeness. Vertical lines represent the 95% confidence intervals

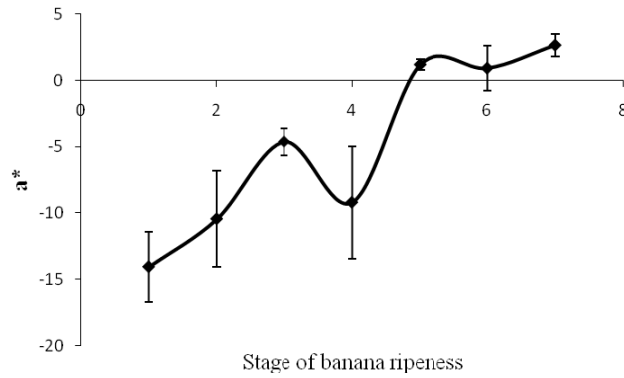


Figure 3. Variation in a* vs. banana ripeness. Vertical lines represent the 95% confidence intervals

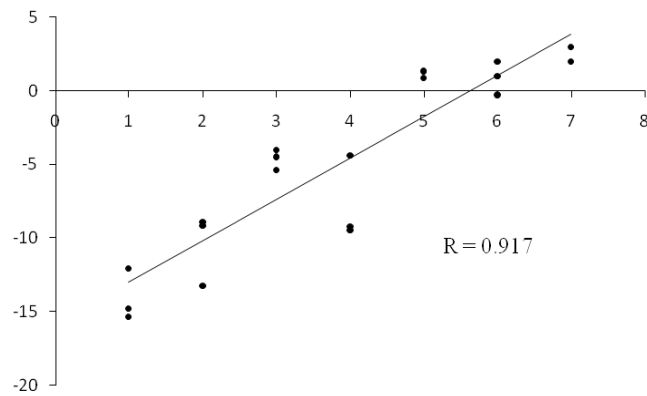


Figure 4. Correlation between a* vs. banana ripeness

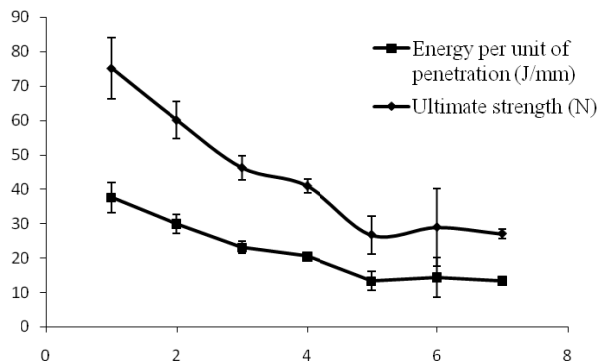


Figure 5. Relation between ultimate strength, energy per unit of penetration and banana ripeness. Vertical lines represent the 95% confidence intervals

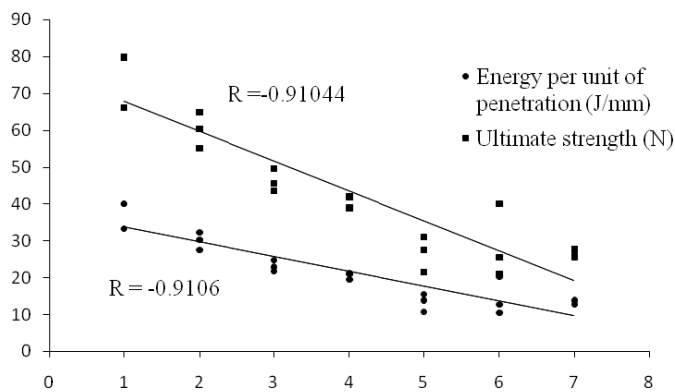


Figure 6. Relation between mechanical properties and stage of banana ripeness

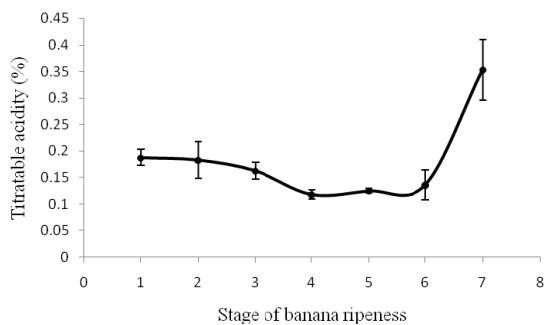


Figure 7. Variation in TA vs. banana ripeness. Vertical lines represent the 95% confidence intervals

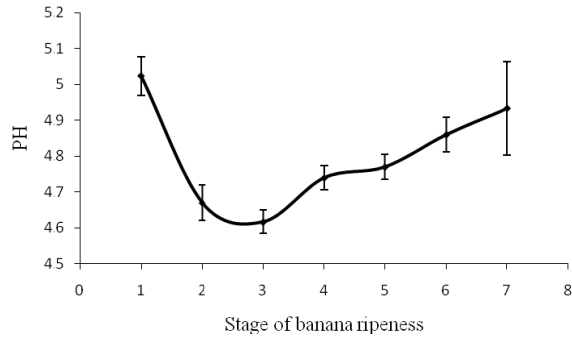


Figure 8. Change in pH vs. banana ripeness . Vertical lines represent the 95% confidence intervals

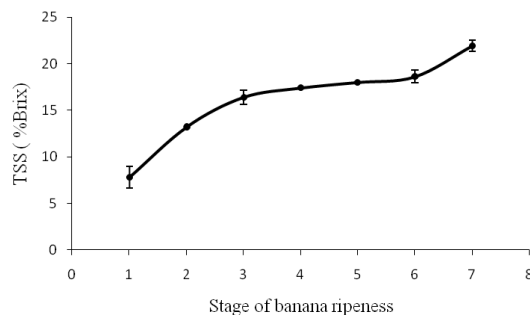


Figure 9. Change in TSS vs. banana ripeness . Vertical lines represent the 95% confidence intervals

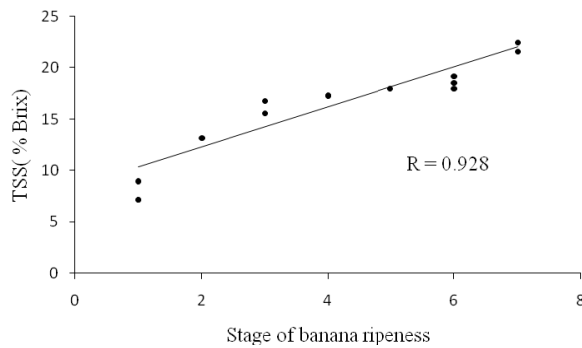


Figure 10. Correlation between TSS and stage of banana ripeness

The Drawbacks and Superiorities of Using IR-Microwave System in Cake and Bread Baking: A Review

K.A. Abbas (Corresponding author)

Department of Food Technology, Faculty of Food Science and Technology
Universiti Putra Malaysia, 43400 Serdang, Selangor, Malaysia
Tel: 60-3-8946-8534 E-mail: ali_kassim@hotmail.com

S. M. Abdulkarim

Department of Food Science, Faculty of Food Science and Technology
Universiti Putra Malaysia, 43400 Serdang, Selangor, Malaysia

M. Ebrahimian

Department of Food Technology, Faculty of Food Science and Technology
Universiti Putra Malaysia, 43400 Serdang, Selangor, Malaysia

N. Suleiman

Department of Food Technology, Faculty of Food Science and Technology
Universiti Putra Malaysia, 43400 Serdang, Selangor, Malaysia

Abstract

This review work tried to highlight and summarize the drawbacks and superiorities of three different heating methods commonly used for baking bread and cakes. These methods are *infrared heating*, *microwave heating* and *infrared-microwave heating*. The literature revealed that infrared heating method usually result in good quality food products, but the system performance is still underdeveloped to meet challenges of the current era. Whereas microwave heating method possesses superior system performance features but present many problems with the eating quality of the final food product. In order to improve both system performance and the food quality, researchers found that the *infrared-microwave system* is the best alternative. This system (halogen lamp-microwave) is a combination of the first two heating methods and at optimized conditions; the system can produce good quality food with better performance. Studies revealed that the good crust color formation and time saving are the superiorities, but the lower moisture content and lower specific volume are the drawbacks on using such system. The products were firmer as a result of the high moisture loss. Halogen lamp power, microwave power and baking time are found to be the major factors that affect the characteristics of the baked products. Based on the heating effects, it is possible to conclude that microwave heating is the dominant heating mechanism in halogen lamp–microwave combination system. However, this system was still be able to produce acceptable quality of baked products therefore researchers recommended IR-microwave for cake and bread baking.

Keywords: Bread, Cake, Baking, Infrared, Microwave, Infrared-Microwave

Introduction

Although the infrared heating is producing good eating quality baked foods, but many drawbacks are inherent regarding system performance. Therefore the microwave heating was emerging to overcome these drawbacks. However, many quality problems have come into sight again to be associated with microwave-baked products. Microwave-baked products are firm, tough in texture, rapidly staled, dry, lack of color and crust (Sevimli *et al.*, 2005). Cakes baked in a microwave oven had the lowest quality (Sumnu *et al.*, 2005^b). It was also found that insufficient starch gelatinization in microwave-baked cakes in which the degree of gelatinization ranged from 55% to 78% depending on formulation (Sakiyan *et al.*, 2009).

Microwave heating is also not commonly used in mass production. Among the drawbacks are non-uniformity of heating since it is very much depending on the geometry, thickness and the dielectric properties of the material; there is no common method to monitor or control the electromagnetic field distribution and its effect after the

microwave is switched on and high in cost (Vadivambal and Jayas, 2007). In order to reduce non-uniformity heating, carousel has been used and Geedipalli *et al.* (2007) has successfully determined the power absorbed in the food as a function of the angle of rotation of the turntable covering the entire cycle. On using various measures of heating uniformity, it was shown that the carousel helps in increasing the temperature uniformity of the food by about 40% (Geedipalli *et al.*, 2007).

Besides these drawbacks, Megahey *et al.* (2005) reported that when used singly in cake baking, the microwave oven at 250 W showed improved textural properties (springiness, moisture content, firmness) as compared to cake baked in the convective oven. However, in the recent development in baking, microwave heating has been combined with infrared (halogen-lamp) heating (Sevimli *et al.*, 2005). Combination of these two heating methods at optimized conditions resulted in better performance and quality of baked products. Fig. 1 shows the illustration of an IR-microwave combination oven.

Halogen lamp produces near-IR radiation and the electromagnetic spectrum is near visible light with higher frequency and lower penetration. IR radiation affects only the surface of the food and heat transfer through the food takes place by conduction or convection. Therefore, the radiation can cause its temperature to reach the required values for browning. On the other hand, microwave heating happens evenly throughout the food and when IR radiation is added to microwave heating, the heat transfer processes can be modified significantly (Sevimli *et al.*, 2005).

Many studies have focused on the effects of different baking methods on the physical properties of breads and cakes. For example, Keskin *et al.* (2004) compared the quality of breads baked by different methods; conventional, microwave, halogen lamp and halogen lamp-microwave combination baking methods. Sumnu *et al.* (2007) studied the same thing, but using different methods which were microwave plus infrared (MIR), microwave plus jet impingement (MJET) and jet impingement (JET). Different methods were also used in a study conducted by Ozkoc *et al.* (2009^b), which involved microwave, infrared-microwave combination and conventional baking methods, but their focus was on physicochemical properties of breads during storage.

Although IR-microwave system is preferably used in (cake and bread) baking and effective drying, but there is big lack of information about this systems in the literature. As most of the publications talk about comparison of properties of different systems but there is no review paper on the advantages and disadvantages of the IR-microwave system. Moreover there is no real picture summarizing current status of the development in this regards. In the light of above the following subsections have been prepared.

1. Advantages

The infrared-microwave combination oven was able to produce brown and crispy products which mainly due to the infrared (halogen lamp) heating. It was possible to obtain cakes with quality comparable to cakes baked in a conventional oven by using the halogen lamp-microwave combination oven.

1.1 Crust color formation

According to Sevimli *et al.* (2005), cakes baked in a halogen lamp-microwave combination oven had specific volume and color values comparable with cakes which were baked using commercial electrical oven. Results of the experiments are as shown in Table 1 (Sevimli *et al.*, 2005). They found that the upper halogen lamp power and the baking time significantly affected the color of the cakes. Sumnu *et al.* 2005^b, also confirmed that it was possible to achieve surface color formation in cakes by IR and IR-microwave combination baking.

In the study done by Keskin *et al.* (2004) it was found that all bread samples baked in microwave oven had similar colors with the dough, therefore their total color change (ΔE) values were very close to zero. The ΔE value of breads baked in IR-microwave oven increased with baking time and halogen lamp oven power (Fig. 2).

The crust color formation is affected by increase in surface temperature of the breads due to increment in halogen power. The required values for surface browning can be achieved by halogen lamp heating which is known to provide low penetration depth and concentrate radiation at the surface. Therefore, similar ΔE values with the conventionally baked breads could be achieved with halogen lamp-microwave combination heating (Keskin *et al.*, 2004). It is also supported by Demirekler *et al.* (2004). The upper halogen lamp power and time were found to be significant in affecting the color change (Demirekler *et al.*, 2004).

In halogen lamp-microwave combination baking, breads baked at 70% halogen lamp power and 30% microwave power for 3 min had ΔE value and specific volume similar to conventionally baked breads. Darker colors could be observed when the baking time was extended, while specific volume of the bread decreased and firmness increased in an unacceptably great extends (Keskin *et al.*, 2004). These disadvantages are going to be discussed further in the next section; disadvantages of halogen lamp-microwave baking system.

When comparing the effect of using different IR powers Sumnu *et al.* (2005^b) suggested the best conditions for baking of cakes in IR-microwave combination oven is at 70% halogen lamp and at 50% microwave power levels for was 5 minutes. Fig. 3 shows the effect of different IR powers to the colour. Increase in colour was faster using 70% IR power.

Tireki *et al.* (2006) also supported that ΔE values were lower in microwave drying and higher in infrared drying in their study on bread crumbs production. Infrared-assisted microwave dried crumbs generally had similar color values with the conventionally dried ones (Tireki *et al.*, 2006). However, they did not observed the effect of power on color change as shown in Fig.4.

Demirekler *et al.* (2004) had reported that increasing the upper halogen lamp power and the baking time will increase the ΔE value significantly. However, at higher upper halogen lamp powers, the increase in time was insignificant for the color change of the breads. Similarly, the increase in the microwave power did not affect the color change for short baking times. However, when the baking time was long, the increase in the microwave power increased the color change (Demirekler *et al.*, 2004).

Besides good crust color formation, IR-microwave system is time and energy saving as microwave heating produces even heating throughout the food (Sevimli *et al.*, 2005).

1.2 Time saving

The near infrared-microwave combination heating combines the colour and crust formation advantages of near infrared heating with the time saving advantage of microwave heating. When an IR-microwave combination oven was used at this condition conventional baking time of cakes was reduced by about 75% (Sumnu *et al.*, 2005^b). The increase in microwave oven power level decreased the drying time. In another study but on drying of carrot slices, Sumnu *et al.* (2005^a) concluded that the drying time can be reduced up to 98% when microwave drying was done at the highest power (using halogen lamp–microwave combination system), in comparison to conventional hot-air drying.

Tireki *et al.* (2006) studied the IR-microwave system in bread crumbs production. The moisture content of the bread crumbs dough was reduced from 40.9 to 8% in order to have a good quality product. Their findings were summarized in Table 2. Higher reduction in drying time was observed in microwave (96.5–98.6% reduction) and infrared-assisted microwave (96.8–98.6% reduction) ovens as compared to conventional baking. Infrared system alone results in 80.2–94.0% reduction in drying time. Demirekler *et al.* (2004) also agreed that baking time was significantly reduced using IR-microwave system compared to conventional system.

Microwave drying at the highest power and halogen lamp-microwave combination drying reduced the drying time significantly. It was suggested that halogen lamp-microwave combination oven can be used when the product moisture content is required to be reduced to very low values (Tireki *et al.*, 2006).

2. Disadvantages

IR-microwave combination system had reduced some of the weaknesses of single microwave heating system to a certain extend to render the product more acceptable. However, many published papers which covered the effect of the IR-microwave system had concluded that the system had resulted in less desirable baked products in term of its specific volume, moisture content and texture.

2.1 Lower specific volume

Table 3 revealed that bread samples baked in halogen lamp-microwave combination oven had the highest specific volume. However, Keskin *et al.* (2004) concluded that microwave baked breads had higher specific volume as compared to others. This is because, specific volume of breads baked in halogen lamp–microwave combination oven decreased as baking time increased (Fig. 5). The specific volume of breads also decreased with the increment of halogen lamp power. The crumb expansion is retarded because of immediate thick crust formation at the breads' surface. The crust was formed due to focused radiation provided by halogen lamp heating on the breads' surface.

In comparison, a study by Sumnu *et al.* (2007) showed that breads baked in MIR system had lowest final volume due to highest loss in moisture content, followed by samples baked in MJET and JET systems. The final volume of breads baked in MIR oven is 9.1% lower than that of baked in MJET. This is due to the faster heating of the MIR. In addition, MIR has low surface temperature such that the rigid outer crust of the breads does not develop that would allow the gas generated in the dough to expand the volume (instead the gas is released). This also explains the lower height of breads (Fig. 6) baked in MIR than breads baked in other heating modes.

Whereas, in a study on bread baked in IR-microwave oven, Demirekler *et al.*, 2004 reported that when time and the microwave power increased, a higher specific volume was observed. However, the increase in the upper halogen lamp power resulted in a decrease in the specific volume of the breads. However, the power of the lower halogen lamp did not affect any of the quality parameters significantly (Demirekler *et al.*, 2004).

2.2 Lower moisture content due to high weight loss

In the study done by Keskin *et al.* (2004), for all oven types, weight loss of breads was affected by baking time and oven power proportionally, but not significantly affected by the temperature increment (Figs. 7–9). However, in halogen lamp-microwave combination oven, increment in the microwave and halogen lamp power caused higher weight loss of the bread samples (17.86%) as shown in Fig. 9.

Higher rate of weight loss was observed in breads baked in microwave oven at 100% power compared to 50% power because during the same baking time, more microwaves were coupled to the bread samples as power was increased which resulted in more heating (Fig. 8). Whereas increase in halogen power caused the bread samples to be subjected to more radiation, thus weight loss increased, indicating moisture loss.

In halogen lamp–microwave combination baking, the microwave power was more effective on weight loss than halogen lamp power. It can be seen in Fig. 9, which shows that breads baked with 50% microwave and 60% halogen lamp power undergoes the highest weight loss.

Similarly, Sumnu *et al.* (2007) also found that MIR heating leads to higher moisture loss. But in this study, MIR was compared with MJET and JET baking methods. In each method, the loss was observed at the end of baking, where highest moisture loss was observed in bread samples that undergo MIR baking method, followed by MJET and JET methods. This is shown in Fig. 10.

However, according to Ozkoc *et al.* (2009), when both infrared-microwave combination and conventional baking methods were compared, microwave-baked breads found to have lowest moisture content (Table 5).

In an IR-microwave system, as the baking time, the upper halogen lamp power, and the microwave and halogen lamp powers increased, the weight loss of the breads increased. These findings were strongly supported by Demirekler *et al.* (2004) and Sevimli *et al.* (2005). When the microwave power and the upper halogen lamp power were compared, the microwave power was found to be more effective and significant in resulting in weight loss (Demirekler *et al.*, 2004, Sevimli *et al.*, 2005).

On the other hand, on a study on bread crumbs dough, Tireki *et al.*, 2006, reported that all IR-microwave drying methods were found to be effective in increasing water binding capacity as shown in Fig. 11, compared to conventional baking. At fixed microwave powers increase of halogen lamp power did not affect the water binding capacity in infrared-assisted microwave drying (Tireki *et al.*, 2006).

In another study by Datta and Ni (2002), heating by microwave-only was found to result in moisture build-up due to enhanced (pressure-driven) flow of moisture to the surface and cold ambient air is unable to remove moisture at a high-rate. When microwave and infrared heating (using hot-air) was combined, it was discovered that surface moisture was reduced and the reduction it is very much depending on the power level. The phenomenon is illustrated in Fig. 12. Infrared was more effective in reducing surface moisture and increasing surface temperature, compared to hot air. This is perhaps due to much lower surface heat flux for hot air compared to the infrared energy (Datta and Ni, 2002).

From the composition point of view, Keskin *et al.*, 2007, concluded that the dielectric properties and quality parameters (including moisture content) of breads baked in infrared-microwave combination oven were dependent on gum type. It depends on the water binding capacity of the gums to retain moisture in the baked products. They concluded that κ -carrageenan resulted in undesirable final bread quality as the dielectric constant and its loss factor were found to be the highest among the other gums. Thus, it results in very dry, firm and highest weight loss product. On the other hand, xanthan-guar blend addition improved bread quality. The breads formulated with xanthan-guar blend has high specific volume and porosity and low hardness values. The findings by Keskin *et al.*, 2007, were summarized in Table 6 and Fig. 13.

Sakiyan *et al.* (2007) also confirmed that dielectric constant and loss factor of cakes are dependent on formulation, baking time, and temperature. The increase in baking time decreased dielectric constant and loss factor of cakes. These parameters were measured by the porosity and moisture content of the cakes. The increase in the fat content of the cake formulations increased its dielectric properties.

However, the ability of IR-microwave heating system to reduce the moisture content the lowest possible was claimed to be good and might be applicable in the instant soups and snack foods industry. This is due to the

higher rehydration potential of microwave dried/baked products (especially starchy products) as reported by Khraisheh *et al.* (2004). Sumnu *et al.* (2005^a) found that carrot slices dried in microwave and halogen lamp–microwave combination oven also had significantly higher rehydration ratio and less colour deterioration. In addition, they also recommended halogen lamp–microwave combination oven in the production of food where its moisture content is required to be reduced to very low values (Sumnu *et al.*, 2005^a).

2.3 Firmer product

The texture and density of baked products such as bread and cakes are controlled by the way their rheology and vapor content change during the baking process (Mondal and Datta, 2008). Microwave baked products are high in weight loss, thus, having higher firmness values i.e. the cakes and breads are quite dry and hard (refer Table 1 for cakes and Table 8 for breads). This is happened due to rapid heating by microwave which enhances the evaporation process. It was possible to reduce the firmness of cakes baked in a halogen lamp–microwave combination oven by providing the required humidity within the oven during baking (Sevimli *et al.*, 2005).

Table 7 shows that bread samples baked in halogen lamp-microwave combination baking system had the highest firmness (3.05 N) compared to breads baked with other methods.

During baking at 100% power, firmness of breads increased sharply which can be related to high rate of moisture loss. The firmness was not significantly affected by the increase in halogen power. However, the crumb firmness was extremely increased in microwave power from 30% to 50%. This evidence showed that firmness of breads is more affected by microwave heating in halogen lamp–microwave combination oven (Fig. 14), similarly to the study done by Keskin *et al.* (2004), where the same factor is more dominant in affecting weight loss of the breads. At the final stages of baking, the breads undergo extreme drying which caused sudden increase in their firmness.

During halogen lamp baking, crumb firmness of breads was found to be decreased while in conventional and halogen lamp oven, firmness of breads baked was found to be negatively correlated to their specific volumes. But on using halogen lamp-microwave combination baking, the firmness of breads baked was not found to be correlated to their specific volume (Keskin *et al.*, 2004).

According to Demirekler *et al.*, 2004, baking time and microwave power were the most significant factors in increasing the firmness in an IR-microwave oven. They said at shorter baking times and lower microwave power combinations, firmness values similar to those of conventionally baked breads were observed. The increase in the firmness of the breads with respect to time may be explained by the increase in weight loss during the baking process. For constant baking time and power of the lower halogen lamp, the optimum firmness value was observed at lower microwave and upper halogen lamp powers (Demirekler *et al.*, 2004)

Keskin *et al.* (2005) applied IR-microwave heating (halogen lamp-microwave system) on cookies. They also confirmed that the hardness values of the cookies increased with increasing baking time and/or halogen power. In addition, the microwave power also contributed to cookie hardness. The best cookies baking condition in a halogen lamp–microwave combination oven was suggested at 70% halogen lamp and 20% microwave power levels for 5.5 min. The baking time of these cookies is half of that required in conventional baking (Keskin *et al.*, 2005). Fig. 15 showed the gelatinization properties of cookies (which was assessed using Rapid Visco Analyser) baked in different ovens.

Keskin *et al.* (2007) also confirmed crumb firmness of breads baked in infrared-microwave combination oven was found to be higher as compared to that of conventionally baked ones. However, they had suggested that the addition of different gums into the bread formulation would be able to prevent this problem. Different gums will have different water binding capacity. Hence, it will affect the viscosity of the solution. Thus, it influences the dielectric properties and microwave heatability of these food. Table 9 shows the water binding capacity of dough as affected by the type of gums used in the formulations. Their findings were explained earlier in the moisture content topic (page 17).

In contrary, Sumnu *et al.* (2005^b) found that IR-microwave combination baking reduced weight loss in cakes, as showed in Fig. 16. Similar pattern was also observed in the firmness of the baked cakes (Sumnu *et al.*, 2005^b).

Other relevant papers on IR-microwave system mainly focused on the starch gelatinization during baking, development of pores and the usage of NIR in the analysis and prediction of the milling and baking parameters of wheat.

Sakiyan *et al.* (2009) studied the effects of different baking ovens and different cake formulations on the degree of starch gelatinization during cake baking. Starch gelatinization levels were examined using Differential Scanning Calorimeter (DSC) and Rapid Visco Analyzer (RVA). Both DSC and RVA results showed that

increasing baking time increased gelatinization level for all baking types as shown in Table 10 and 11 (Sakiyan *et al.*, 2009). Generally, microwave heating resulted in high final viscosity due to high moisture lost in short time. Meanwhile, conventional baking took the longest baking time. IR-microwave combination oven gave the properties in between these two.

They also found that addition of fat reduced the degree of starch gelatinization in conventional baking. However, fat enhanced the gelatinization in microwave and IR–microwave combination ovens. There was insufficient starch gelatinization in microwave-baked cakes in which the degree of gelatinization ranged from 55% to 78% depending on formulation. On the other hand, it ranged from 85% to 93% in conventionally baked cakes. Combining infrared with microwaves increased degree of starch gelatinization (70–90%) (Sakiyan *et al.*, 2009).

Palav and Seetharaman (2007) did a study on the impact of microwave heating on the physico-chemical properties of a starch-water model system. They concluded that microwave heating alone leads to different mechanism of starch gelatinization compared to conduction heating. The vibrational motion and the rapid increase in temperature also result in granule rupture and formation of film polymers coating the granule surface (Palav and Seetharaman, 2007).

Ozkoc *et al.* (2009^a) analyzed the pores size (using Scanning Electron Microscope) of breads baked in different ovens. Pores of breads baked in conventional oven were found to be smaller, and had spherical, oval-like shape as compared to the ones baked in IR-microwave combination oven. Their cell structure was also more homogeneous. Meanwhile, IR-microwave combination oven resulted in pores that were so close to each other which subsequently lead to coalescence of the gas cells to form channels, thus, the pores were no longer spherical. The starch granules in conventionally baked breads were more distorted and seen as a continuous sheet of gelatinized starch. On the other hand, granular residues and continuous starch structure was observed together in IR-microwave combination heating (Ozkoc *et al.*, 2009^a).

Jirsa *et al.* (2008) found that near infrared reflectance spectroscopy (NIRS) has accurately analyzed and predicted the milling and baking parameters of wheat. The parameters measured are flour extraction, protein content, Zeleny sedimentation, deformation energy, gas volume and baking volume of wheat from many varieties. The range of spectra used was from 400 to 2500 nm. They also suggested NIRS to be used in the determination and screening performance of wheat for its rheological traits (deformation energy, gas volume and specific loaf volume).

Conclusion

The IR-microwave system is a new emerging system suggested for baking. Microwave heating was found to be the dominant heating mechanism in halogen lamp–microwave combination baking in terms of affecting weight loss and texture development. The advantages of using IR-microwave system enhance the crust and color formation with energy saving process. The IR-microwave system were noted for lower specific volume and moisture content of the baked products, even the products are also firm and hard due to high weight/moisture loss.

It is not advisable to bake breads by using only halogen lamp mode of the oven because of the formation of the very thick bread crust. Halogen lamp–microwave combination baking provided color similar to the conventionally baked products but the weight loss and firmness of breads were still higher as compared to conventionally baked products. Nevertheless, many researchers recommended IR-microwave for cake and bread baking.

References

- Datta, A.K. and Ni, H. (March 2002). Infrared and hot-air-assisted microwave heating of foods for control of surface moisture. *Journal of Food Engineering* 51(4):355-364.
- Demirekler, P., Sumnu, G. and Sahin, S. (2004). Optimization of bread baking in a halogen lamp–microwave combination oven by response surface methodology. *European Food Research Technology* 219:341–347. DOI 10.1007/s00217-004-0969-3.
- Geedipalli, S.S.R., Rakesh, V. and Datta, A.K. (2007). Modeling the heating uniformity contributed by a rotating turntable in microwave ovens. *Journal of Food Engineering* 82:359–368.
- Jirsa, O., Hrušková, M. and Švec, I. (2008). Near-infrared prediction of milling and baking parameters of wheat varieties. *Journal of Food Engineering* 87: 21–25.
- Keskin, S.O., Sumnu, G. and Sahin, S. (2004). Bread baking in halogen lamp-microwave combination oven. *Food Research International* 37:489-495.

- Keskin, S.O., Oztürk, S., Sahin, S., Koksel, H. and Sumnu, G. (2005). Halogen lamp–microwave combination baking of cookies. *European Food Research Technology* 220:546–551. DOI 10.1007/s00217-005-1131-6.
- Keskin, S.O., Sumnu, G. and Sahin, S. (2007). A study on the effects of different gums on dielectric properties and quality of breads baked in infrared-microwave combination oven. *European Food Research Technology* 224:329–334. DOI 10.1007/s00217-006-0334-9.
- Khraisheh, M.A.M., McMinn, W.A.M. and Magee, T.R.A. (2004). Quality and structural changes in starchy foods during microwave and convective drying. *Food Research International* 37:497–503.
- Megahey, E.K., McMinn, W.A.M. and Magee, T. R. A. (2005). Experimental study of microwave baking of Madeira cake batter. *Food and Bioproducts Processing* 83(C4): 277–287.
- Mondal, A. and Datta, A.K. (2008). Bread baking – A review. *Journal of Food Engineering* 86:465–474.
- Ozkoc, S.O., Sumnu, G. and Sahin, S. (2009^a). The effects of gums on macro and micro-structure of breads baked in different ovens. *Food Hydrocolloids* 23:2182–2189.
- Ozkoc, S.O., Sumnu, G., Sahin, S., and Turabi, E. (2009^b). Investigation of physicochemical properties of breads baked in microwave and infrared-microwave combination ovens during storage. *European Food Research Technology* 228:883-893.
- Palav, T. and Seetharaman, K. (2007). Impact of microwave heating on the physico-chemical properties of a starch–water model system. *Carbohydrate Polymers* 67:596–604.
- Sakiyan, O., Sumnu, G. Sahin, S. and Meda, V. (2007). Investigation of dielectric properties of different cake formulations during microwave and infrared–microwave combination baking. *Journal of Food Science* 72(4):E205-E213.
- Sakiyan, O., Sumnu, G., Sahin, S., Meda, V., Koksel, H. and Chang, P. (May 2009). A study on degree of starch gelatinization in cakes baked in three different ovens. *Food Bioprocess Technology* DOI 10.1007/s11947-009-0210-2.
- Sevimli, K.M., Sumnu, G. and Sahin, S. (2005). Optimization of halogen lamp–microwave combination baking of cakes: a response surface methodology study. *European Food Research Technology* 221:61–68.
- Sumnu, G., Turabi, E. and Oztop, M. (2005^a). Drying of carrots in microwave and halogen lamp–microwave combination ovens. *LWT* 38:549–553.
- Sumnu, G., Sahin, S., and Sevimli, M. (2005^b). Microwave, infrared and infrared-microwave combination baking of cakes. *Journal of Food Engineering* 71:150–155.
- Sumnu, G., Datta, A.K., Sahin, S., Keskin, S.O., and Rakesh, V. (2007). Transport and related properties of breads baked using various heating modes. *Journal of Food Engineering* 78:1382-1387.
- Tireki, S., Sumnu, G. and Esin, A. (2006). Production of bread crumbs by infrared-assisted microwave drying. *European Food Research Technology* 222:8–14. DOI 10.1007/s00217-005-0109-8.
- Vadivambal, R. and Jayas, D.S. (2007). Changes in quality of microwave-treated agricultural products – a review. *Biosystems Engineering* 98:1 – 16.

Table 1. Response values for cakes baked in the halogen lamp–microwave combination oven and control cakes (ref: K. Melike Sevimli et al., 2005b)

Response	Halogen lamp-microwave combination baked cakes	Control cakes (conventionally baked for 24 min)
Weight loss (%)	7.500	10.290
Specific volume (ml/g)	1.660	1.650
Firmness (N)	0.330	0.440
Color (ΔE)	54.00	67.820
Springiness (mm)	2.756	2.793
Gumminess (kgf)	0.017	0.019
Adhesiveness (kgf mm)	0.002	0.001

Table 2. Drying times for different drying treatments (ref: Tireki et al., 2006)

Drying method	Drying time (s)
Conventional	7560
30% microwave power only	265
50% microwave power only	148
70% microwave power only	106
30% halogen power only	1500
50% halogen power only	780
70% halogen power only	450
30% microwave power and 30% halogen power	240
30% microwave power and 50% halogen power	202
30% microwave power and 70% halogen power	195
50% microwave power and 30% halogen power	142
50% microwave power and 50% halogen power	139
50% microwave power and 70% halogen power	135
70% microwave power and 30% halogen power	111
70% microwave power and 50% halogen power	105
70% microwave power and 70% halogen power	103

Table 3. Effects of different baking methods on weight loss (%) of breads (ref: Keskin et al., 2004)

Baking methods	Specific volume (ml/g)
Conventional	1.60
Microwave	2.04
Halogen lamp	1.44
Halogen lamp-microwave combination	2.57

Table 4. Effects of different baking methods on weight loss (%) of breads (ref: Keskin et al., 2004)

Baking methods	Weight loss (%)
Conventional	4.06
Microwave	10.80
Halogen lamp	8.20
Halogen lamp-microwave combination	17.86

Table 5. Moisture content of control breads baked in different ovens during staling at 0 hour (ref: Ozkoc et al., 2009)

Oven type	Moisture content (%)
Microwave-control	35.2 ± 0.12
Combination-control	36.0 ± 0.17
Conventional-control	38.2 ± 0.11

Table 6. Moisture content data for breads formulated with different gums baked in infrared-microwave combination oven (ref: Keskin et al., 2007)

Bread type	Moisture content (%)
Control	35.98 a *
Xanthan	36.07 a
Guar	35.81 a
Xanthan-guar	36.04 a
κ -carrageenan	35.78 a

* Different letters are significantly different $p \leq 0.05$

Table 7. Effects of different baking methods on firmness (N) of breads (ref: Keskin et al., 2004)

Baking methods	Firmness (N)
Conventional	0.67
Microwave	2.88
Halogen lamp	0.80
Halogen lamp-microwave combination	3.05

Table 8. Comparison of responses for conventionally baked breads and responses calculated for the optimum point for halogen lamp–microwave combination oven baked bread (ref: Demirekler et al., 2004).

Responses	Conventional baking	Halogen lamp–microwave combination oven baking
Weight loss (%)	4.06	4.39
ΔE	35.7	34.8
Specific volume (ml/g)	1.63	1.70
Firmness (N)	0.71	0.86
Porosity	64.1	65.3
Chewiness (N mm)	1.05	1.38
Springiness (mm)	2.92	3.00

Table 9. Water binding capacity values for dough samples formulated with different gums (ref: Keskin et al., 2007)

Dough type	WBC (w\w)
Control	0.551 b *
Xanthan	0.910 a
Guar	0.621 b
Xanthan-guar	0.887 a
κ -carrageenan	0.571 b

*Different letters are significantly different $p \leq 0.05$

Table 10. RVA characteristics of non-fat cake samples baked in different ovens (ref: Sakiyan et al., 2009)

Baking type	Baking time (min)	Peak viscosity (cp)	Trough (cp)	Break down (cp)	Final viscosity (cp)	Setback	Peak time (s)
Batter		190.00	162.00	28.00	376.00	214.00	6.20
Conventional	22	92.00 b	71.00 b	21.00 a	135.00 b	64.00 a	6.80 a
Conventional	28	74.00 b	60.00 b	14.00 a	124.00 b	64.00 a	6.87 a
Microwave	2	176.00 a	161.00 a	15.00 a	233.50 a	72.50 a	6.17 a
Microwave	2.5	163.50 a	130.00 a	33.50 a	232.50 a	102.50 a	5.97 a
Microwave	3	127.50 a	110.50 a	17.00 a	199.00 a	88.50 a	6.43 a
IR-MW Comb	3.5	149.00 ab	116.00 ab	33.00 a	208.00 ab	85.00 a	6.40 a
IR-MW Comb	4.5	123.33 ab	99.67 ab	23.67 a	171.67 ab	72.00 a	6.80 a
IR-MW Comb	5.5	97.33 ab	81.00 ab	16.33 a	123.00 ab	42.00 a	6.93 a

Baking types with different letters (a, b) are significantly different ($p \leq 0.05$)

IR-MW Comb infrared-microwave combination

Table 11. RVA characteristics of cake samples containing 25 g fat/100 g flour baked in different ovens (ref: Sakiyan et al., 2009)

Baking type	Baking time (min)	Peak viscosity (cp)	Trough (cp)	Break down (cp)	Final viscosity (cp)	Set back	Peak time (s)
Batter		198.00	183.00	15.00	356.00	173.00	6.57
Conventional	22	94.00 b	78.00 b	16.00 a	124.00 b	46.00 a	6.93 a
Conventional	28	80.00 b	57.00 b	23.00 a	129.00 b	72.00 a	6.53 a
Microwave	2	175.00 a	158.00 a	17.00 a	264.00 a	106.00 a	6.00 b
Microwave	2.5	172.00 a	127.00 a	45.00 a	236.50 a	109.50 a	5.93 b
Microwave	3	147.33 a	117.33 a	30.00 a	212.00 a	94.67 a	6.04 b
IR-MW Comb	3.5	136.00 b	117.00 ab	19.00 a	210.00 ab	93.00 a	6.60 a
IR-MW Comb	4.5	116.00 b	81.50 ab	34.50 a	143.00 ab	61.50 a	6.93 a
IR-MW Comb	5.5	96.50 b	73.00 ab	23.50 a	132.50 ab	59.50 a	6.63 a

Baking types with different letters (a, b) are significantly different ($p \leq 0.05$)

IR-MW Comb infrared-microwave combination

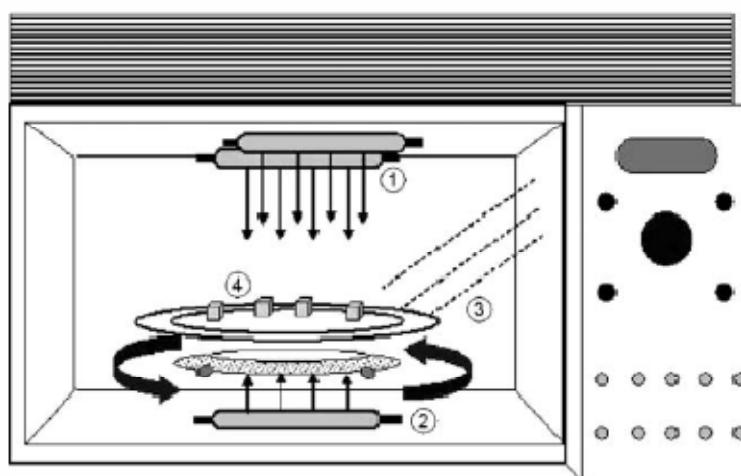


Figure 1. Illustration of IR-microwave combination oven.

(1) Upper halogen lamps, (2) Lower halogen lamp, (3) Microwaves, (4) Turntable (ref: Sumnu et al., 2005^b)

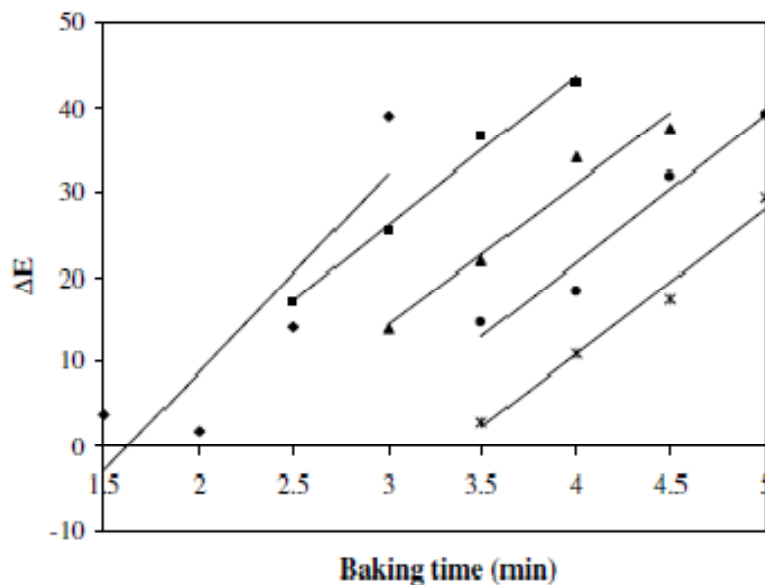


Figure 2. Changes of color (ΔE value) of breads during halogen lamp– microwave combination baking at different at different halogen lamp (H) and microwave (MW) powers. (◆) H, 60% and MW, 50%; (■) H, 70% and MW, 30%; (▲) H, 60% and MW, 30%; (●) H, 50% and MW, 30%; (*) H, 40% and MW, 30% (ref: Keskin et al., 2004)

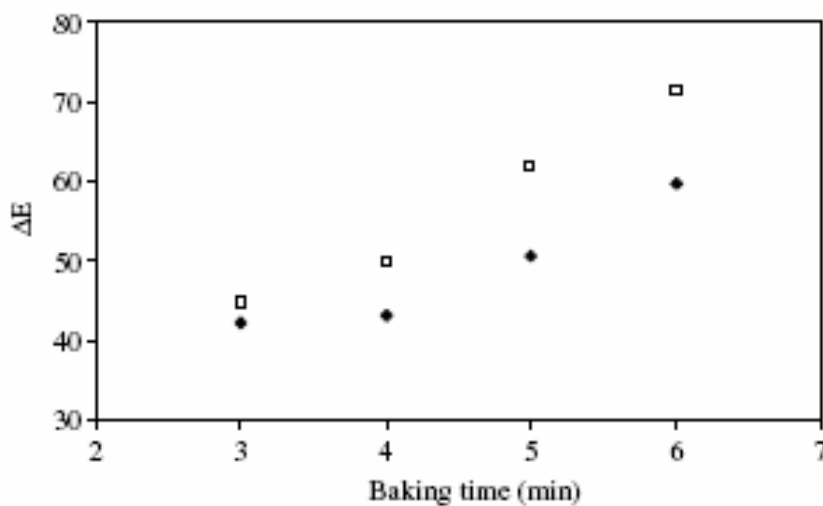


Figure 3. Changes in colour (ΔE value) of cakes during IR-microwave combination baking at 50% microwave power and at different IR powers. (◆): 50%, (□): 70% (ref: Sumnu et al., 2005b).

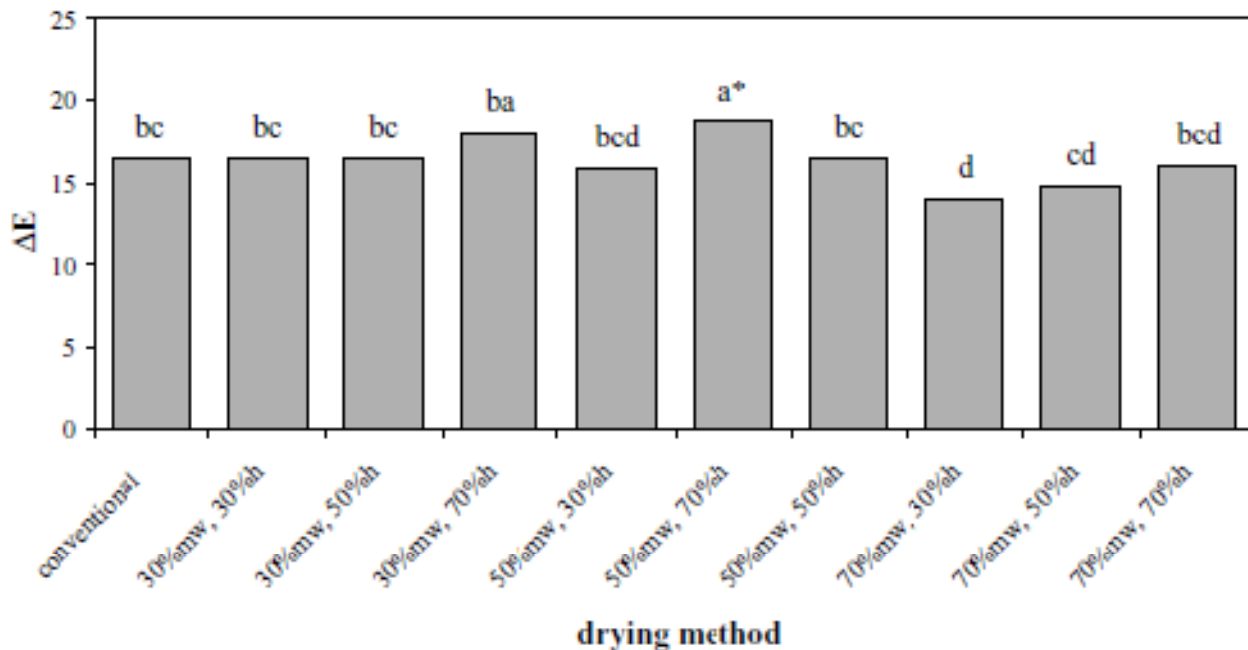


Figure 4. Effect of infrared-assisted microwave drying on ΔE values of bread crumbs.

*Means bars containing different letters are significantly different ($p \leq 0.05$) (ref: Tireki et al., 2006)

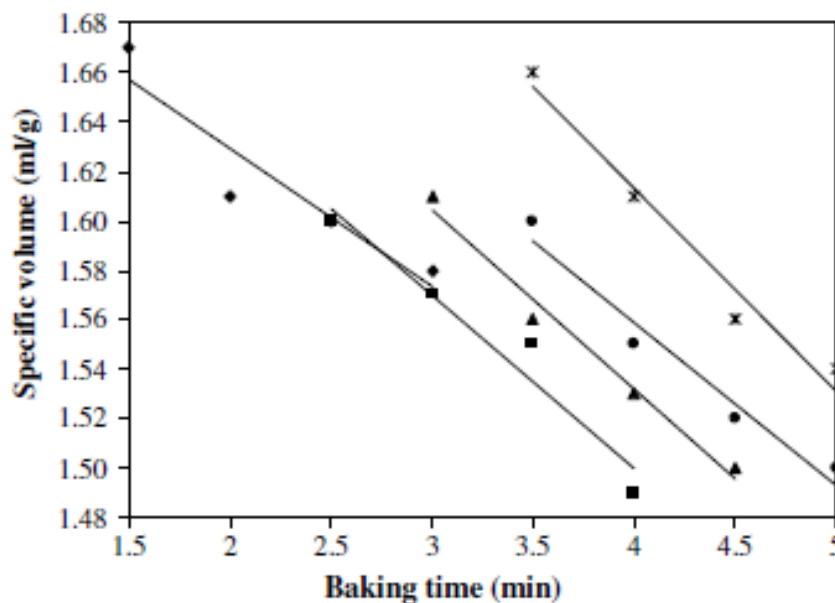


Figure 5. Changes of specific volume of breads during halogen lamp–microwave combination baking at different halogen lamp (H) and microwave (MW) powers. (◆) H, 60% and MW, 50%; (■) H, 70% and MW, 30%; (▲) H, 60% and MW, 30%; (●) H, 50% and MW, 30%; (*) H, 40% and MW, 30% (ref: Ozge Keskin et al., 2004)

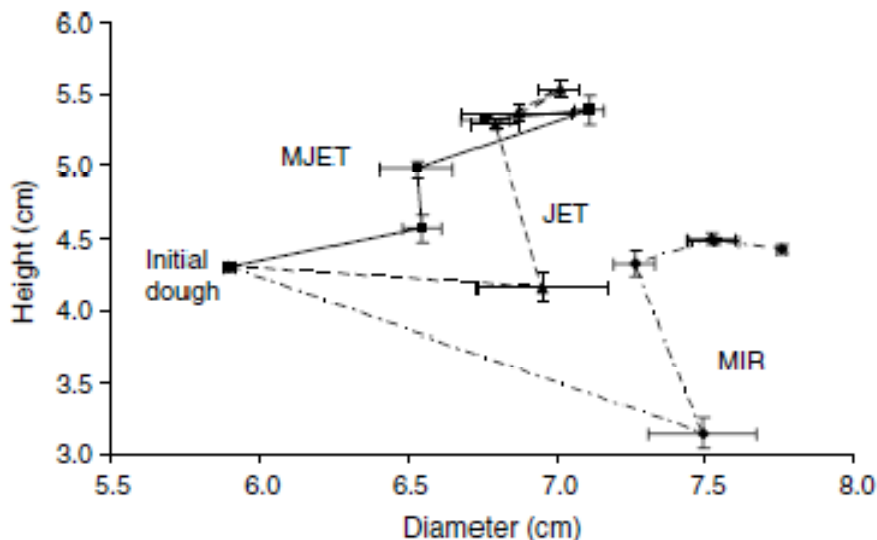


Figure 6. History of dimension changes in bread during baking using different heating modes. The baking times for MJET are 0, 2, 3.5 and 6.5 min, for JET are 0, 2, 3.5, 6 and 8 min, and for MIR are 0, 2, 3, 4, 6 and 8 min, respectively. Error bars represent range of height and diameter in replicates (ref: Sumnu et al., 2007)

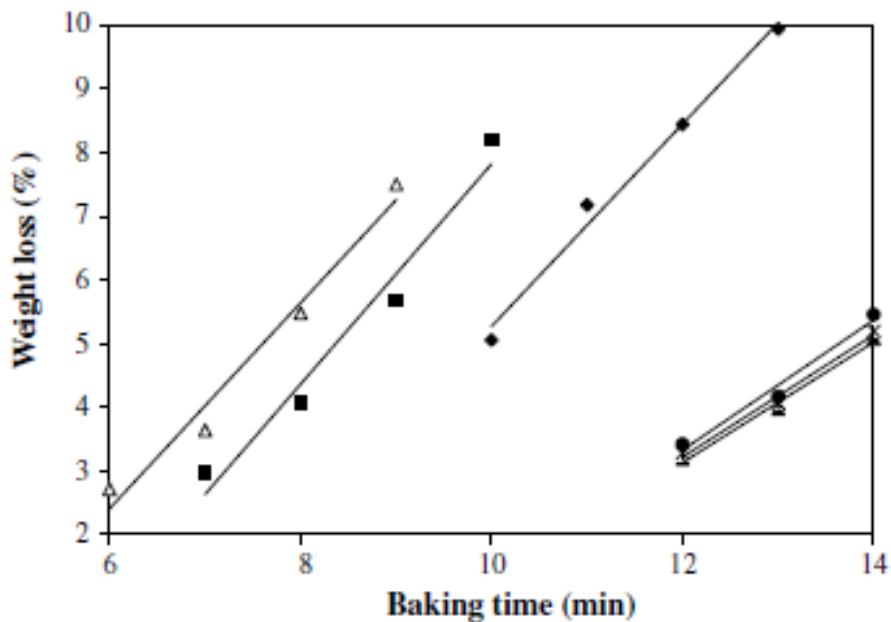


Figure 7. Weight losses of breads during conventional oven and halogen lamp baking at different temperatures and oven powers, respectively. (▲) 175 °C; (*) 200 °C; (●) 225 °C; (◆) 50%; (■) 60%; (Δ) 70% (ref: Keskin et al., 2004)

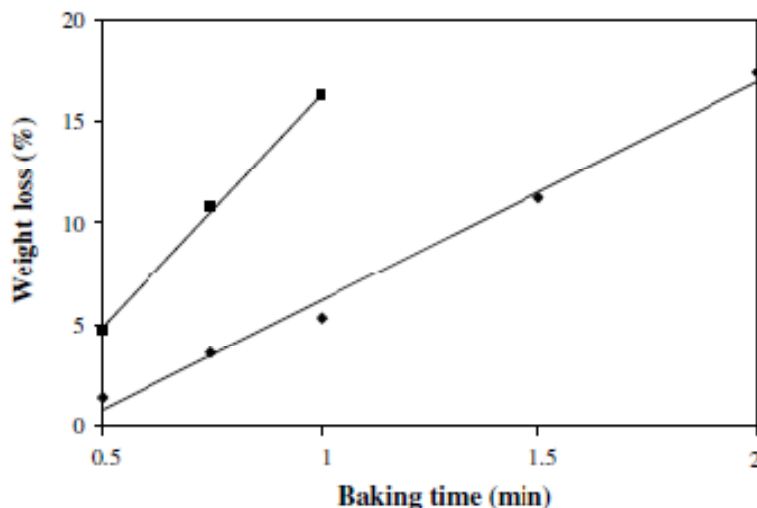


Figure 8. Weight losses of breads during microwave baking at different powers. (◆) 50%; (■) 100%. (ref: Keskin et al., 2004)

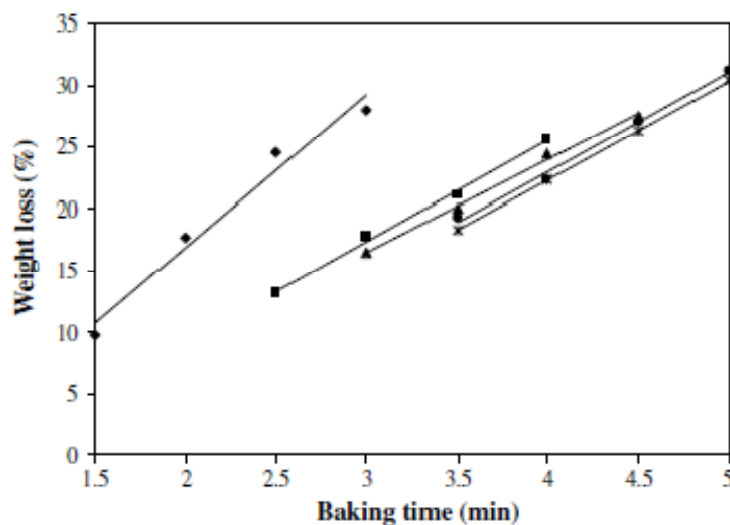


Figure 9. Weight losses of breads during halogen lamp–microwave combination baking at different halogen lamp (H) and microwave (MW) powers. (◆) H, 60% and MW, 50%; (■) H, 70% and MW, 30%; (▲) H, 60% and MW, 30%; (●) H, 50% and MW, 30%; (*) H, 40% and MW, 30% (ref: Keskin et al., 2004)

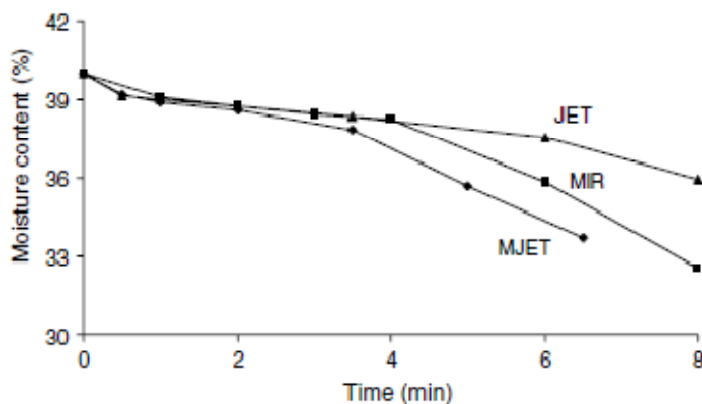


Figure 10. Transient moisture content of breads during baking in different heating modes (ref: Sumnu et al., 2007)

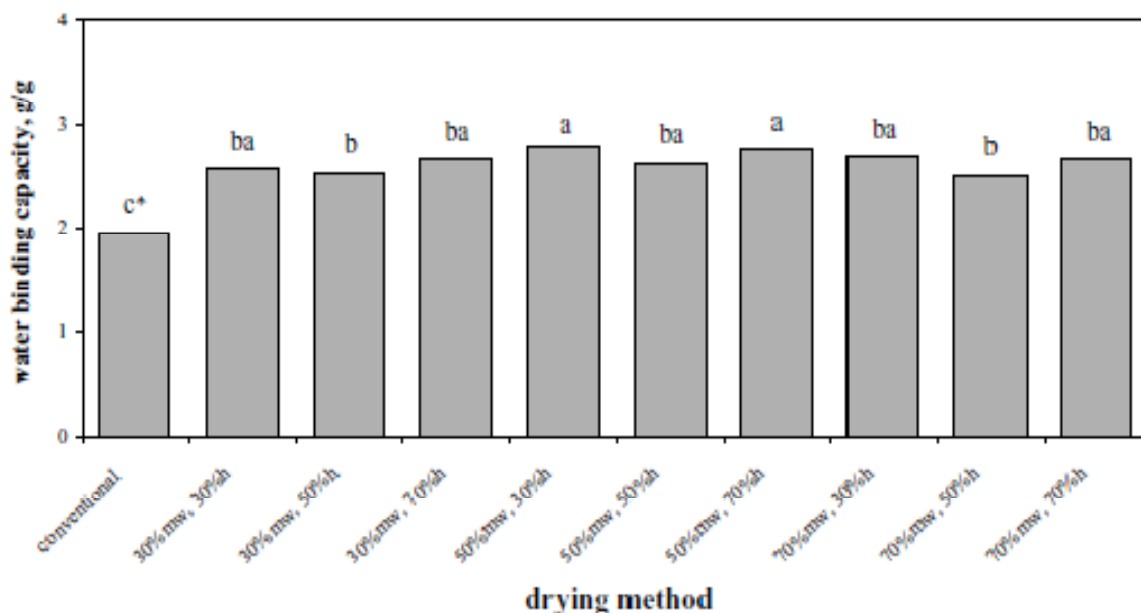


Figure 11. Effect of infrared-assisted microwave drying on water binding capacity of bread crumbs. *Means bars containing different letters are significantly different ($p \leq 0.05$) (ref: Tireki et al., 2006)

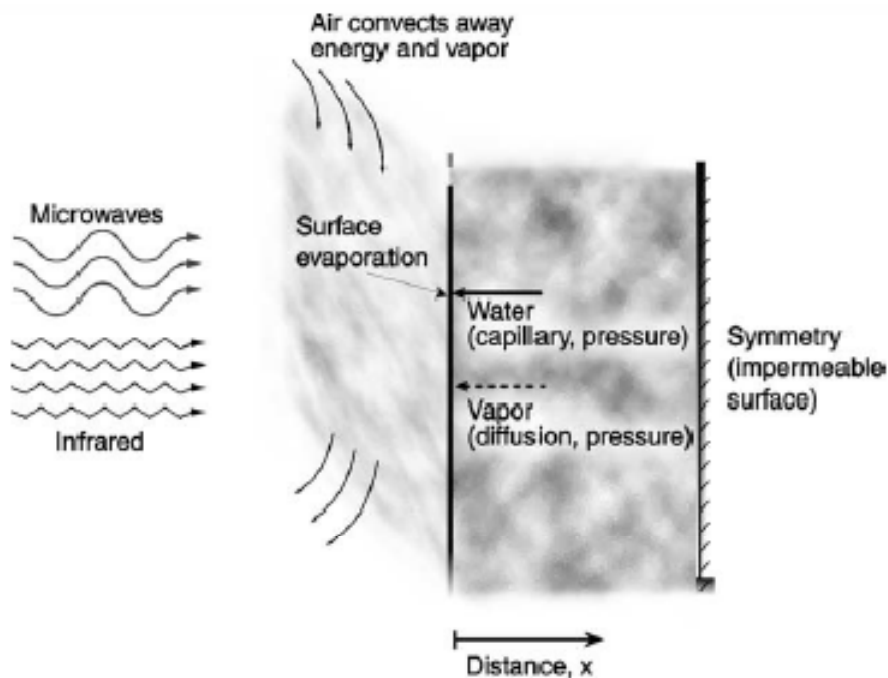


Figure 12. Schematic diagram of the heating process showing transport of liquid water and vapour to the surface from inside, evaporation of liquid water at the surface and convection transport of energy and vapour at the surface (ref: Datta and Ni, 2002)

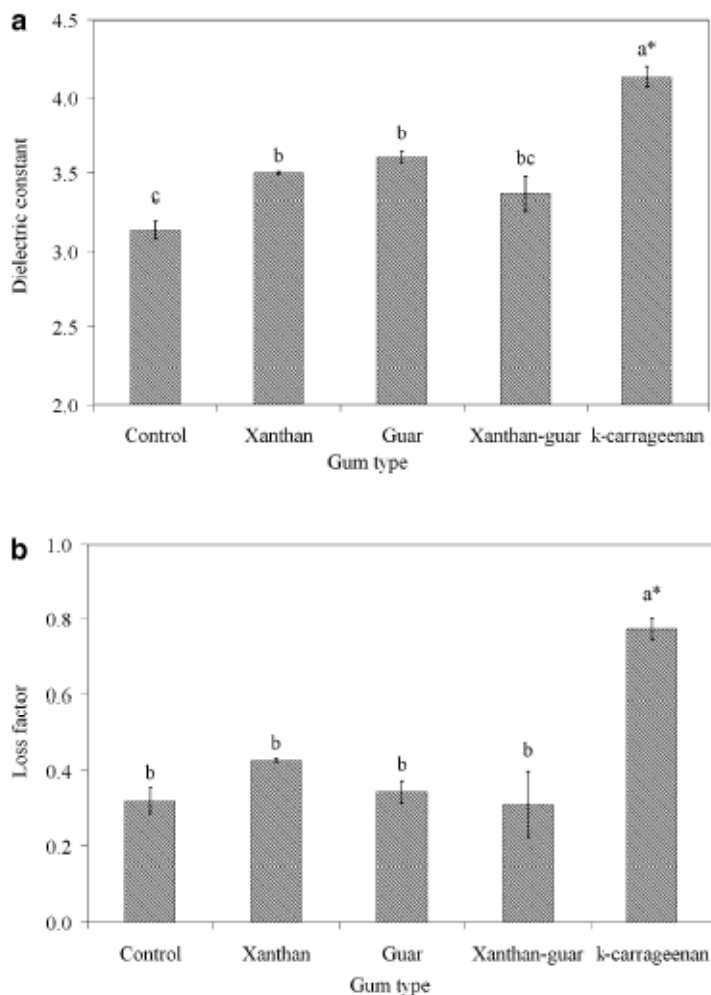


Figure 13. a The effects of different gums on dielectric constant of breads baked in infrared-microwave combination oven (*Bars with different letters (a, b, c, d) are significantly different $p \leq 0.05$); b The effects of different gums on loss factor of breads baked in infrared-microwave combination oven (*Bars with different letters (a, b, c, d) are significantly different $p \leq 0.05$) (ref: Keskin et al., 2007)

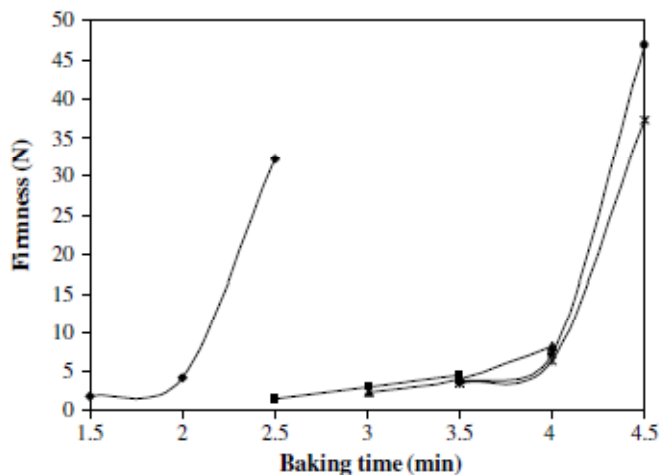


Figure 14. Changes of firmness of breads during halogen lamp-microwave combination baking at different halogen lamp (H) and microwave (MW) powers. (◆) H, 60% and MW, 50%; (■) H, 70% and MW, 30%; (▲) H, 60% and MW, 30%; (●) H, 50% and MW, 30%; (*) H, 40% and MW, 30% (ref: Keskin et al., 2004)

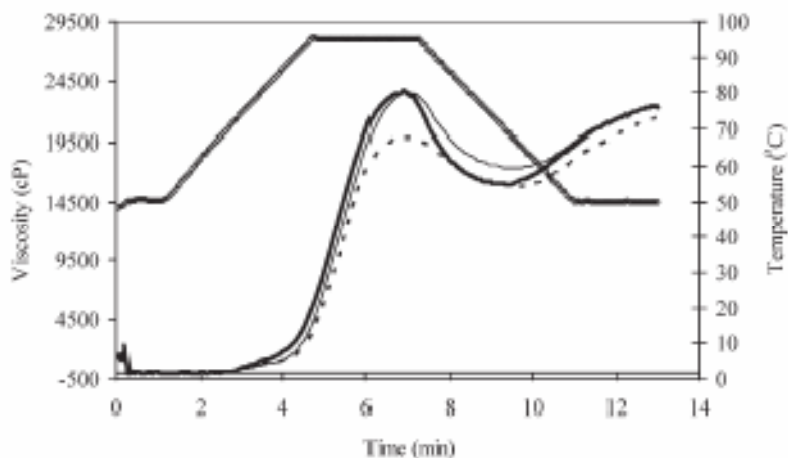


Figure 15. Rapid Visco Analyzer curve for different baking conditions of cookies: conventional (....), microwave (thick continuous line) and halogen lamp–microwave combination (—) baking for 5 min at 70% halogen power and 20% microwave power (ref: Semin Ozge Keskin et al., 2005)

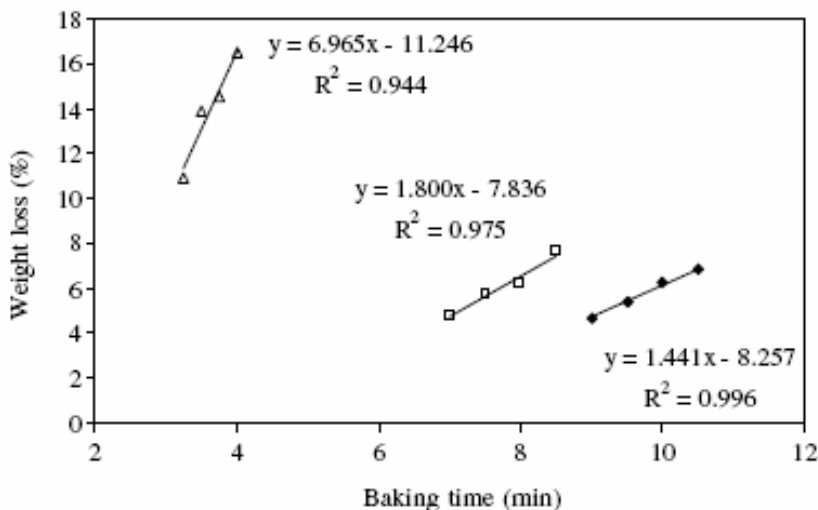


Figure 16. Weight losses of breads during baking by different methods. (Δ): Microwave baking at 50% power, (◆): IR baking at 50% power, (◻): IR baking at 70% power. Markers represent data points and lines represent model equation (ref: Sumnu et al., 2005b)

Study of Two-level P2P Model on Self-adaptive Dynamic Network

Feixue Huang

Department of Economics, Dalian University of Technology, Dalian 116024, China

Tel: 86-411-8470-7210 E-mail:software666@163.com

Zhijie Li

School of Computer Science & Engineering, Dalian Nationalities University, Dalian 116600, China

Tel: 86-411-8765-6179 E-mail:lizhijie@dlnu.edu.cn

Abstract

This study's objective was to solve the problem that the structured P2P model was not appropriate for dynamic network. A self-adaptive dynamic P2P model of two-level is proposed. Super peers compose to a self-adaptive Distribute Hash Table network on the top layer, and lower ordinary peers take super peer in the same group as their center server to form a cluster. When super peer join or leave, it does not maintain the consistency of entire network's logic topology. Only updating routing table of its predecessor and successor, super peers update their routing table cache when they transmit messages. The experimental results indicate that if k is average amount of peers in each group, then search in self-adaptive P2P model of two-level only brings $1/k$ hops compared to Chord of same net size. When peer join or leave it produce messages at constants level. The conclusion indicates that the model could be more applicable in ad hoc P2P network with high churn rate compared with Chord network.

Keywords: Peer-to-Peer(P2P), Fault tolerance, Distribute hash table, Ad hoc P2P

1. Introduction

Based on the new computing infrastructure—grid technology(LI Z J,2009) (OLESZKIEWICZ J,2006): such as, Zhu G H(2004) discussed environment of China's knowledge grid; Li M L(2006) built a grid project of Shanghai's information services; WANG Y f (2007) built a grid framework for testing the engine. this thesis focuses on how to optimize the grid resource allocation using economic theory. Thus, resource management is a complex process (BERTEN V,2006). All existing P2P model can be classify to three categories by network logic topology: Centralized model, Decentralized unstructured model and Decentralized structured model. However such rigid structured model was not appropriate for dynamic network as it brings large number of messages when peer churns. Decentralized unstructured model is ineffective for its flooding search mechanism, and Decentralized structured model based on DHT (Distribute Hash Table) enjoys great advantage of simplicity and extensibility. CHEN H h(2006) proposed Semre X, a Semantic Similarity Based P2P Overlay Networks. In fact, P2P networks are focused on the sharing of resources (LING B,2005)(DOU W,2004)(WU K,2006)(LI Z Y,2006).Currently, Consistent hashing and DHT (Distribute Hash Table are often used in P2P networks, such as Chord (STOICA I ,2003), CAN (RATSANAMY S,2001), Tapestry(ZHAO B Y,2004), etc.

To address the above issues, a dynamic network which is more suitable for adaptive two-level P2P model is proposed. The model is organized into an adaptive DHT networks for the upper super-peer, and the organizational structure of lower ordinary peer is similar to Napster(SAROIU S,2003), which take the super-peers in the present group as the central directory server to form a cluster. The data actually is stored in an ordinary peer, and the super peers save data and deal with the requests from ordinary peers. When peers join or leave, the upper super-peer networks temporarily do not to maintain the consistency of the networks logical topology, only update routing table of its predecessor and successor, and the super peers update their routing table cache when they transmit messages. The lower peers retain the backup of super-peer; and generate a new super-peer when the super-peer fails. Adaptive two-level P2P system model has a better search performance, one query produces $O(\log N)$ (N is number of super peers)hops, and when peers join or left, it take relatively lower cost to maintain the networks topology, also has a certain degree of failure recovery mechanism. As the networks operate, it voluntarily adjusts load-balance and selects the high-capacity peer as the super-peer, so that the overall structure tended to be optimized.

2. Variables and principle of Model

Data format used in the system is similar with the general DHT Networks, is (key, value), key is the keywords corresponding to the data, key and the upper super-peer identifier (ID) are all m -bit identifier distributed by the

consistent hash function. System provides function of the releasing the value, as well as inquiring the corresponding value of a given key. The format of Data Index is (key, routing): key is for corresponding keywords to the data, routing is for data storage of peer routing information. The overall structure of the system shown in Figure 1: System will voluntarily select the high-capacity peer as the super-peer. The upper super-peer networks are similar to Chord, the peer ID uniformly distributed in the identifier space, and form a ring in accordance with the peer ID.

The value of key is the index to the key value of K , stored in the peer whose first ID is equal to K , or a successor to K in the ring, namely the first encountered peer K start from the ring in clockwise direction. This peer becomes the successor of key. In addition, super-peer saved M-bit Rooting Table (becoming the Finger Table) to speed up the query. The difference with the Chord is that: the upper super-peer networks did not timely update the networks and synchronize the other peers in the Finger Table to reflect changes in the peer when peers join and leave, that is, the system allows the networks topology being inconsistent with the logic topology, at the same time only to update the peer's predecessor and successor peers, and to ensure the correctness of ring connectivity. And then when message transmitted between the super peers, each peer dynamically adjust the local Finger Table according to sources, so that the networks logical topology tends to be consistent. Also, the upper peers keep all routing information of ordinary peers in this group.

Lower ordinary peers take super peer in the same group as their center server to form a cluster, and the ordinary peers only keep routing information of upper peers in this group. Ordinary peer (key, routing) sent data index stored in the local to super-peers of the group, then according to the rules super-peer posted the index of the key value to a peer in the ring, namely, the successor to the key. When query, an ordinary peer transmits a query message to super-peer, and the super-peer only transmit the message on the super-peer ring, until finding the index of the data looked for, it will return the request message to the query peer, and then query peer voluntarily connect the destination peer to get data.

In each group, the super-peer select a ordinary peer in this group (does not contain itself) as a backup peer in accordance with peer ability, backup peer cache super-peer information, which include: the index to the key value, routing information of ordinary peers in this group, the super peer ID, the successor peer on the upper ring, predecessor peer. Backup peer can generate a new super-peer when super-peer invalid. To balance the load of super-peer in the system, system sets the minimum and maximum number of peers for each group. When number of ordinary peers under a super-peer exceeds the maximum, they split into two new groups. When number of normal peers is less than the minimum number of peers, the group will voluntarily merge into successor peer group of the super-peer on the Chord ring.

3. Algorithm Description

3.1 Data distribution and data query

The process of peer to publish data is described as follows:

- 1) The key value data to be released is calculated by consistent hash function.
- 2) To generate data indexing, such as (key, peer routing).
- 3) Sent to super-peer of this group.
- 4) The super-peer sent the index to the successor super-peer of the key value to save.

The search algorithm of peer is described as follows:

- 1) The value of the key data to be inquired is calculated by consistent hash function.
- 2) Transmit the query request of key value to super-peer of the group.
- 3) The super-peer transmits to the key's successor peer.
- 4) The peer returns the message, which contains the corresponding index of the key.
- 5) The query peer voluntarily connects to data- storing peer.

3.2 Algorithm of Peers' joining and leaving

Peers will issue a join request to the upper super-peer in the system when joining, the super-peer process the request. If number of ordinary peers under a super-peer in the group reaches the maximum the system allows, it splits a new group. This would avoid that the group is too great and the super-peers are overloaded and can make system more robustness. After received returning message of the request, ordinary peers obtain routing information from the super-peer, and are set as group servers routing that means it join the networks. The flow

that Super-peer processes the leaving request: peers sent leaving request to super peer of the group when leaving the networks, super peer processes the request. If number of ordinary peers under a super-peer in the group reaches the minimum allowed by the system, the group will voluntarily merge to successor peer group of the super-peer on the Chord ring. This will avoid too many super-peers caused by too many small groups in the system.

3.3 Recovery Algorithm of Peer Failure

A variety of operation in system mainly carried out on the upper super-peer, ordinary peer only depends on the super-peer. It can be seen that ordinary peer failure does not produce any effect on the entire networks topology, at most when searching for the early release of data index of the failed peer, it fails when other peers acquire data. The operation of the entire networks will not be affected, so here only the super-peer failure recovery mechanism is considered.

Each group in the system has an ordinary peer to back up certain essential information of super-peer, including: index of the key value cached by super peer, routing information of ordinary peer, super-peer ID, successor peer of super-peer in the upper ring, routing information of precursor peer. Therefore, when a super-peer fails, the backup peer has enough information to restore a new super-peer.

In order to maintain the effectiveness of the backup peer information, when the above information of super-peer changes, the backup peer must simultaneously be updated, and when there are ordinary peers joining the group, the super-peer select the ordinary peer of the largest capacity for backup.

The backup peer takes the way of interval of time period checking to monitor super-peer, once a super-peer is not connected, the backup peer transform into a new super-peer, while selecting a new backup peer in the group.

The algorithm of recovery process of backup peer is described as follows:

- 1) Backup peer transform into a super-peer.
- 2) Add the backup information to itself.
- 3) Inform the super-peer on Chord ring to change the successor peer into its own route, and inform successor peer to change its predecessor into its own route.
- 4) Inform the ordinary peer within the group update the super-peers routing into itself.

3.4 Analysis of System performance

In Chord model, each peer store $O(\log N)$ routing information of other peers, a query hops are kept at $O(\log N)$, N is the networks size. Table 1 lists the comparison of hops for self-adaptive Chord and Chord.

When peers join or leave, due to update the other peers in the networks, regardless of under what circumstances Chord need launch at least $\log N$ queries, and a query generate $O(\log N)$ hops, it totally has generated $O(\log^2 N)$ hops. As the super-peer of upper ring temporarily stops real-time maintenance of networks, a major operation of Self-Adaptive Chord at this point is to find the predecessor peer to be joined, and then transmit two messages. Therefore, in the best case, the peer requests its predecessor to join the networks, peers produced only two hops. The worst and the general cases result in $O(\log N)$ hop. Compared to Chord, Self-Adaptive Chord can effectively reduce the number of messages caused by the peers join or leave, at the same time as the networks operates, the query efficiency become closer to Chord.

When query, in the best circumstances, when a query peer key is stored in constant successor peers after the initiated peer, Chord and Self-Adaptive Chord only produce constant hops. In the worst case, if the query key's precursor is the query peer, Chord needs to transmit message among $\log N$ peers to the destination peer.

If all the peers of the Self-Adaptive Chord are newly joined the networks, and they are all directly request their predecessor peer to join, then all peers only have successor peer routing and self-routing in the Finger Table, so the peer will traverse to find the destination peer along the ring through its successor peer, resulting in N hops. Under general case, because Self-Adaptive Chord will constantly adjust the networks logical topology, a query hops of Chord and Self-Adaptive Chord both is $O(\log N)$.

Self-Adaptive Chord is only the upper layer of adaptive P2P mode, the networks size increase significantly compared to Chord, making n as the average number of peers in each group, if the efficiency of P2P model is similar to Chord, the networks size increases by n times; In addition, as the system ensures that the number of ordinary peers of each group is kept with a certain range, so it not only avoids the excessive group creating a overload super-peer, or a large area networks paralyzed after a single peer failure, but also avoids too many

groups with too few peers and purposefully limit the number of super-peers, so that system performance can be further enhanced.

4. Experiments

4.1 Comparison of query efficiency between Adaptive two-level P2P model and Chord model

The experimental procedures are the new 500-peer in Chord networks and sequential implementation of the 20 Sections respectively in 500 super-peer adaptive two-level P2P model, 500 queries in each section.

As the results shown in Figure 2, the query implementation efficiency of Chord is more stable, and every 500 queries generated more than 3,000 messages, with average 6 messages each query, this is because the number of messages a Chord query produces is $O(\log N)$. But the adaptive two-level P2P model's efficiency of query is worse than Chord in the first groups, because in the newly generated networks, the Finger Table of most peers is initialized in relation to its successor, these peers do not know the whole the logic of the networks topology, and is likely to transverse the entire ring peer by peer by the successor peer, therefore less efficient than Chord. But, after some inquiries, the peer updates local routing information by transmitting the message dynamically, and we can see the more lately implemented the query is, the more closer the number of messages is to Chord. At this point in adaptive P2P networks model the number of all the peers is about 4000, showing that when the size of two-level P2P model adaptive networks is approximately 8 times of Chord, its query efficiency is still close to Chord.

4.2 Analysis of the distribution of the peer capacity in Adaptive two-level P2P model

The purpose of this experiment was to analyze the distribution of the peer capacity in Adaptive two-level P2P model. Experimental procedures is to generate a network with 5000 peers, capacity of each peer is a random number between 1 and 10. Then check distribution of the super peer capacity.

As the results shown in Figure 3, the capacity of most super-peers is a value around 8,9,10. It can be seen that Adaptive two-level model P2P optimize network's structure, dynamically adjust networks structure, and select the peer of large capacity as the super peer.

5. Conclusion

The experimental results indicate that if k is average amount of peers in each group, then search in self-adaptive P2P model of two-level only brings $1/k$ hops compare to Chord of same net size, when peers join or leave it produce messages at constants level. It also has effective mechanism for fault tolerance. The conclusion indicates that the model can be more applicable in ad hoc P2P network with high churn rate.

Acknowledgments

This work is supported by the funds project under the Ministry of Education of the PRC for young people who are devoted to the researches of humanities and social sciences under Grant No. 09YJC790025; software + X research of Dalian University of Technology under Grant No. 842301.

References

- BERTEN V, GOOSSENS J, JEANNOT E. (2006). on the distribution of sequential jobs in random brokering for heterogeneous computational grids. *IEEE Transactions on Parallel and Distributed Systems*, 17 (2): 113 – 124.
- CHEN H h, JIN H, NING X m, et al. (2006). SemreX: A Semantic Similarity Based P2P Overlay Networks. *Journal of Software*, 17(5):1170-1181.
- DOU W ,WANG H M, JIA Y, et al. (2004). A Recommendation-Based Peer-to-Peer Trust Model. *Journal of Software*, 15(4):571-583.
- LI M L, WU M Y, LI Y, et al. (2006). ShanghaiGrid: an Information Service Grid. *Concurrency and Computation: Practice & Experience*, 18(1): 111-135.
- LI Z J, CHENG C T. (2009). An Evolutionary Game Algorithm for Grid Resource Allocation under Bounded Rationality. *Concurrency and Computation: Practice and Experience*, 21(9): 1205-1223.
- LI Z J, CHENG C T, HUANG F X. (2009). Utility-driven solution for optimal resource allocation in computational grid. *Computer Languages, Systems and Structures*, 35(4): 406-421.
- LI Z Y, XIE G G, MIN Y H, et al. (2006). Topology Matching Method for Structured P2P Systems. *JOURNAL OF SYSTEM SIMULATION*, 18(5):1181-1185.
- LING B, WANG X y, ZHOU A y, et al. (2005). A Collaborative Web Caching System Based on Peer-to-Peer Architecture. *CHINESE JOURNAL OF COMPUTERS*, 28(2):170-178.

OLESZKIEWICZ J, LI X, LIU Y H. (2006). Effectively Utilizing Global Cluster Memory for Large Data-Intensive Parallel Programs. *IEEE Transactions on Parallel and Distributed Systems*, 17(1): 66-77.

RATSANAMY S, FRANCIS P, HANDLEY M, et al. (2001). A scalable content-addressable network. *ACM SIGCOMM Computer Communication Review*, 31 (4): 161 - 172.

SAROIU S, GUMMADI K P, GRIBBLE S D. (2003). Measuring and analyzing the characteristics of Napster and Gnutella hosts. *Multimedia Systems*, 9 (2): 170 - 184.

STOICA I, MORRIS R, LIBEN-NOSTRONG D, et al. (2003). Chord: a scalable peer-to-peer lookup protocol for internet applications. *IEEE/ACM Transactions on Networking*, 11 (1): 17-32.

WANG Y f, DONG X s, HE X q, et al. (2007). Grid Testing Engine:a Infrastructure for Constructing Grid Testing Environment. *JOURNAL OF XI'AN JIAOTONG UNIVERSITY*, 41(8):884-888.

WU K, DAI H, YE B l, et al. (2006). Research on NS2-Based P2P Networks Simulation Platform. *JOURNAL OF SYSTEM SIMULATION*, 18(8):2152-2157, 2169.

ZHAO B Y, HUANG L, STRIBLING J, et al. (2004). Tapestry: A Resilient Global-scale Overlay for Service Deployment. *IEEE Journal on Selected Areas in Communications*, 22(1):41-53.

ZHUGE H. (2004). China's e-science knowledge grid environment. *IEEE Intelligent Systems*, 19 (1): 13-17.

Table 1. Comparison of hops for self-adaptive Chord and Chord

Peer Operation	networks	Chord	Self-Adaptive Chord
inquire	Best case	$O(1)$	$O(1)$
	worst case	$O(\log N)$	$O(N)$
	General case	$O(\log N)$	$O(\log N)$
join or leave	Best case	$O(\log^2 N)$	$O(1)$
	worst case	$O(\log^2 N)$	$O(\log N)$
	General case	$O(\log^2 N)$	$O(\log N)$

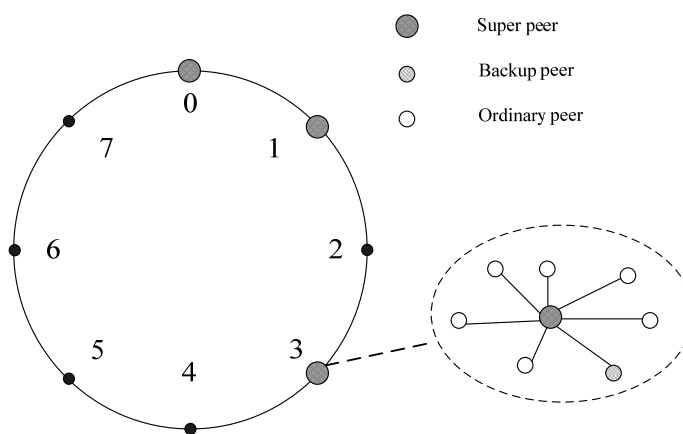


Figure 1. The overall structure of the system

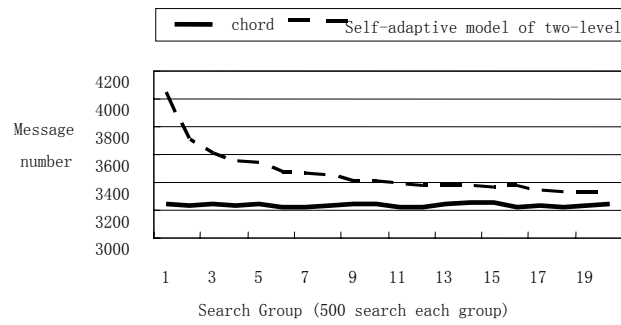


Figure 2. Comparison of query performance for self-adaptive model of two-level and Chord

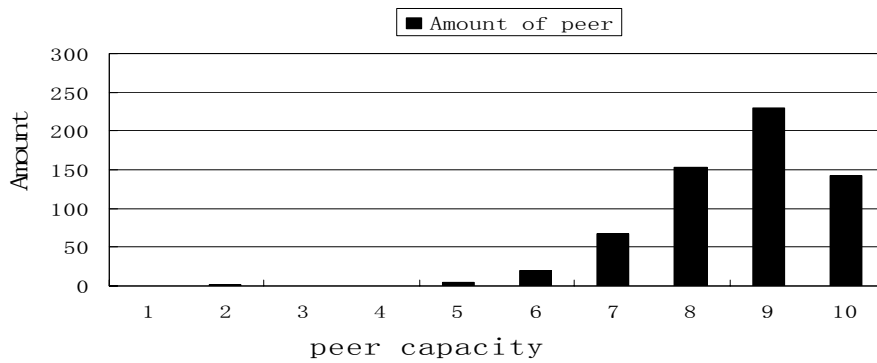


Figure 3. The ability distribution of super-peer for self-adaptive model of two-level

Mass Transfer Coefficient Studies in Bubble Column Reactor

D.Devakumar (Corresponding author)

Assistant Professor, Department of Mechanical Engineering
Excel College of Engineering and Technology, Komarapalayam
Namakkal – 638183, Tamilnadu, India
E-mail: devakumarand@yahoo.com

Dr.K.Saravanan

Professor and Head, Department of Chemical Engineering
Kongu Engineering College, Perundurai, Erode – 638052, Tamilnadu, India
E-mail: rumisivaesh@yahoo.com

Dr.T.Kannadasan

Director - Research, Anna University- Coimbatore
Coimbatore-641047, Tamilnadu, India
E-mail: tkannadasan56@yahoo.com

B.Meenakshipriya

Senior Lecturer, Department of Mechatronics Engineering
Kongu Engineering College, Perundurai, Erode – 638052, Tamilnadu, India
E-mail: b.meenakshipriya@gmail.com

Abstract

Stirred bubble column are widely used in chemical and allied processes industries. Stirred bubble column reactor promotes significant liquid hold-up and long liquid residence time. It is used when a large mass transfer area and high mass transfer coefficient in both phases are desired. These columns can operate continuously with a concurrent and counter current phase flow where high interfacial areas between phases are possible with low investment cost. An experimental work was undertaken to focus the effect of various parameters like Height to Diameter ratio (H/D), Gas flow rate and Speed of the stirrer (N) on mass transfer coefficient in stirred bubble column reactor. For this purpose, experiments were conducted in 0.14 m i.d column having 2 m height. The column with ring sparger having 67% active area is used as sparger for dispersing the dispersed phase into the continuous phase. For the optimized sparger plate, the effect of various parameters on mass transfer coefficient was studied based on CO₂ –absorption Technique.

Keywords: Stirred bubble column reactor, Mass transfer coefficient, Sparged column

1. Introduction

Bubble columns are widely used in the chemical industry, where heterogeneous gas -liquid (or) gas- solid reaction take place, particularly in which the liquid phase controls mass transfer process due to relative insolubility of gases (Lye et al., 2001). Important applications of bubble column include oxidation, hydrogenation, ozonolysis, alkylation, column floatation and waste water treatment (Yang et al., 2001). To design a bubble column as a reactor, Studies like fractional holdup, mixing time and mass transfer characteristics are needed (Ali Abdul R. N. Jasim, 2009). Many works on bubble column for holdup, mixing time and mass transfer characteristics have been reported in the literature (Shah et al., 1982; Pandit and Joshi, 1984; Thorat et al., 2004; Mashelkar, 1970; Deckwer et al., 1974; Urza and Jackson, 1975; Burekhardt and Deckwer, 1976; Maclean et al., 1977; Schugerl et al., 1977; Shiaya and Duna, 1978; Alvarez - cunca at al., 1980; Mangertz and Pilhofer, 1981; Koide et al., 1984; Haque et al., 1987; Ozturk et al., 1987; Akita and Yoshida, 1973; Kawase and Moo-young, 1987; Hikita et al., 1981; Kang et al., 1999; Schumpe and Grund, 1986). The efficiency of mixing in bubble column can be enhanced by employing stirrer in the conventional bubble column. The only work reported in the literature stirred bubble column is by

(Shanmugam et al., 2008). Knowing the importance of mass transfer characteristics in the design of stirred bubble Column, the present work focus on the determination of mass transfer characteristics in the stirred bubble column.

2. Experimental set up and methods

Mass transfer experiments were carried out using the experimental setup as shown in Figure 1. It consists of 0.14 m i.d in diameter and 2 m in height. In order to visualize the flow, the column is made up of transparent perspex (Acrylic). The compressed air from the compressor is sparged in to the bubble column through sparger. The sparger plate is made up of acrylic having an active area of 67%. The design details pertaining to sparger is shown in Table 1 and details of column is shown in Table 2. Mass transfer coefficient was determined based on the Denckwards methods. The gas flow rate was measured using recalibrated rotameter.

3. Results and discussions

3.1 Effect of mass transfer coefficient on H/D ratio

The effect of mass transfer coefficient was studied for stirred bubble column. Since the H/D ratio is also one of the vital parameter which influence the mass transfer characteristics, a systematic work was undertaken to vary the H/D ratio from 2 to 5. The graph was drawn between H/D ratio and mass transfer coefficient ($K_L a$) is shown in Figure 2. From this figure, it can be seen that mass transfer coefficient increases with decrease in H/D ratio. As a mass transfer characteristic depends on phase holdup, hence increase in holdup shows high mass transfer coefficient.

3.2 Effect of mass transfer coefficient on speed of the stirrer

Speed of the stirrer was varied in the range of 50 rpm to 200 rpm. The speed of the stirrer was found to affect the mass transfer coefficient marginally. The stirrer plays a vital role in breaking of large bubbles into smaller ones. The effect of speed of the stirrer on mass transfer coefficient ($K_L a$) is shown in Figure 3. From the figure, it could be seen that, with the increase in the speed of the stirrer, the mass transfer coefficient increases. This may be due to the breakage of the larger bubbles into smaller ones; hence the contact area available for mass transfer between the two phases increases.

3.3 Effect of mass transfer coefficient on superficial gas velocity

The effect of gas flow rate on mass transfer coefficient for constant H/D ratio is shown in the Figure 4. From the figure, it can be seen that mass transfer coefficient ($K_L a$) increases with increase in superficial gas velocity (V_G). More and more gas bubbles occupy the column as the superficial gas velocity increase. Thus column shows more $K_L a$ for higher V_G .

4. Comparison of mass transfer coefficient in bubble column with and without stirrer

4.1 Comparison of effect of mass transfer coefficient on H/D ratio

From the Figure 5, it seems that the addition of an external stirrer in the bubble column reactor increases the mass transfer coefficient values to a certain extent. This is due to the breaking of the gas bubbles which provides more contact area available for mass transfer between the phases. The external stirrer, which is responsible for agitation and creation of large interfacial area between the phases, increases the mass transfer coefficient.

4.2 Comparison of effect of mass transfer coefficient on superficial gas velocity

The variation of mass transfer coefficient for different superficial gas velocity was studied in 0.14 m i.d bubble column fitted with three Ruston turbine impeller having 0.046 m diameter. This effect is shown in Figure 6 for both with and without stirrer. From this figure, it can be seen that mass transfer coefficient increases as superficial gas velocity increases. The mass transfer coefficient is 20% more for stirred bubble column than compared to conventional bubble column. This may be due to additional effect of stirring which ensures uniform mixing in the vessel. Also, for stirred system, column is fully occupied by gas bubbles and more number of circulation loops is formed which makes stirred bubble column having high mass transfer coefficient.

5. Conclusion

- The mass transfer coefficient is more for stirred bubble column than conventional bubble column for the same scale up factors
- The mass transfer coefficient is found to decrease with increase in the H/D ratio.
- The mass transfer coefficient increases with an increase in impeller speed
- The mass transfer coefficient increases with increase in superficial gas velocity

References

Akita, K. and Yoshida, F. (1973). Gas hold-up and volumetric mass transfer coefficients in bubble columns. *Ind. Eng. Chem. Process. Des. Dev.*, 12, 76-80.

- Ali Abdul R. N. Jasim (2009). Studies on gas hold-up, mass transfer coefficient, mixing time and circulation time in bubble columns with draught tube for pseudo plastic (carboxymethyl) cellulose and glycerol solutions. *Eng. & Tech. Journal*, 27 (12), 2245-2256.
- Alvarez-cunca, M. and Nerenbreg, M. A. (1980). Oxygen mass transfer in bubble columns working at an liquid flow rates. *AICHE, J.*, 27, 66.
- Burekhardt, R. and Deckwer, W. D. (1976). Bubble size distribution and interfacial areas of electrolyte solutions in bubble columns. *Chem. Eng. Sci.*, 30, 35.
- Deckwer, W. D., Burckhart, R. and Zoll, G. (1974). Mixing and mass transfer in tall bubble columns. *Chem. Eng. Sci.*, 29, 2177-2188.
- Haque, M. N., Nigam, K. D. P., Joshi, J. B. and Viswanathan, K. (1987). Studies on mixing time in bubble columns with pseudo plastic (carboxymethyl cellulose) solution. *Ind. Eng.*, 26, 82-86.
- Hikita, H., Asal, S., Kikukawa, H., Zalke, T. and Ohue, M. (1981). Heat transfer coefficient in bubble column. *Ind. Eng. Chem. Process Des. Dev.*, 20, 540-545.
- Kang, Y., Cho, Y. J., Woo, K. J. and Kim, S. D. (1999). Diagnosis of bubble distribution and mass transfer in pressurized bubble columns with viscous liquid Medium. *Chem. Eng. Sci.*, 54, 4887.
- Kawase, Y. and Moo-Young, M. (1987). Heat transfer in bubble column reactors with Newtonian and non-Newtonian fluids. *Chem. Eng. Res. Des.*, 65, 121-126.
- Koide, K., Takazawa, A., Komura, M. and Matsunage, H. (1984). Gas hold-up of volumetric liquid phase mass transfer in solid suspended bubble columns. *J. Chem. Eng. Japan*, 17 (5), 459-466.
- Lye and Stuckey (2001). Extraction of Erthromycin- a using colloidal liquid aphrons: part 2. *Mass Transfer Kinetics, Chemical Engineering Science*, 56, 97-108.
- Maclelan, G. F., Erickson, L. E., Hsu, K. H. and Fan, L. T. (1977). Oxygen transfer and axial dispersion in an aeration tower containing Static mixers. *Biotechn. Bioengng.*, 19, 493.
- Mangertz K.H. and Pilhofer (1981). Interpretation of mass transfer measurements in bubble columns considering dispersion of both phases. *Chem. Eng. Sci.*, 36, 1069.
- Mashelkar, R. A. and Sharma, M. M. (1970). Mass transfer in bubble columns. *Trans. Inst. Chem. Eng.*, 48, T162.
- Ozturk, S. S., Schumpe, A. and Deckwer, W. D. (1987). Organic liquids in a bubble column: holdups and mass transfer coefficients. *AIChE, J.*, 33, 1473-1480.
- Pandit, A. B. and Joshi, J. B. (1984). Three phase sparged reactions, some design aspects. *Rev. Chem. Eng.*, 2, 1-84.
- Schugerl, K., Lucke, J. and Oels, U. (1977). Bubble column bioreactions. *Adv. Biochem. Eng.*, 7, 1.
- Schumpe, A. and Grund, G. (1986). The gas disengagement technique for studying gas holdup structure in bubble columns. *Can. J. Chem. Eng.*, 64, 891-896.
- Shah, Y. T., Kelkar, B.G., Godbole, S. P. and Deckwer, W. D. (1982). Design parameters estimations for bubble column reactors. *AIChE, J.*, 28 (3), 353-379.
- Shanmugam, K., Saravanan, K., Ramamoorthy, V. & Balasubramani, R. (2008). Hydrodynamic studies in stirred bubble column. *Journal of the University of Chemical Technology and Metallurgy*, 43 (1), 113-118.
- Shiaya, S. and Duna, I. J. (1978). Dynamic oxygen mass transfer coefficient measurement method for column reactors. *Chem. Eng. Sci.*, 33, 1529.
- Thorat, B. N and Joshi, J. B. (2004). Regime transition in bubble columns: experimental and predictions. *Exp. Therm. Fluid Sci.*, 28, 423-30.
- Urza, I. J. and Jackson (1975). Pressure aeration in a 55-ft bubble column. *Ind. Eng. Chem. Process Des. Dev.*, 14, 106.
- Yang, W., Wang, J. and Jin, Y. (2001). Gas-Liquid Mass Transfer in a slurry Bubble Column Reactor under High Temperature and High Pressure. *Chinese Journal of Chemical Engineering*, 9 (3), 253-257.

Table 1. Details for Sparger design

Total area of sparger	0.0154 m ²
Active area of sparger	0.0158 m ²
Free area of sparger	0.0138 m ²
Effective area of sparger	67%
Diameter of hole for square and triangular pitch	6.7 x 10 ⁻³ m
Diameter of hole for single orifice	4.5 x 10 ⁻³ m
Number of holes in distributor for square and triangular pitch	45
Material	Mild steel
Sparger vessel thickness	0.003 m

Table 2. Details for column design

Column diameter	0.14 m
Column length	2 m
Material of column	Acrylic
Number of impellers	3
Type of impeller	Rushton Impeller
Gap between the impeller	0.046 m
Clearance of impeller from vessel bottom	0.046 m

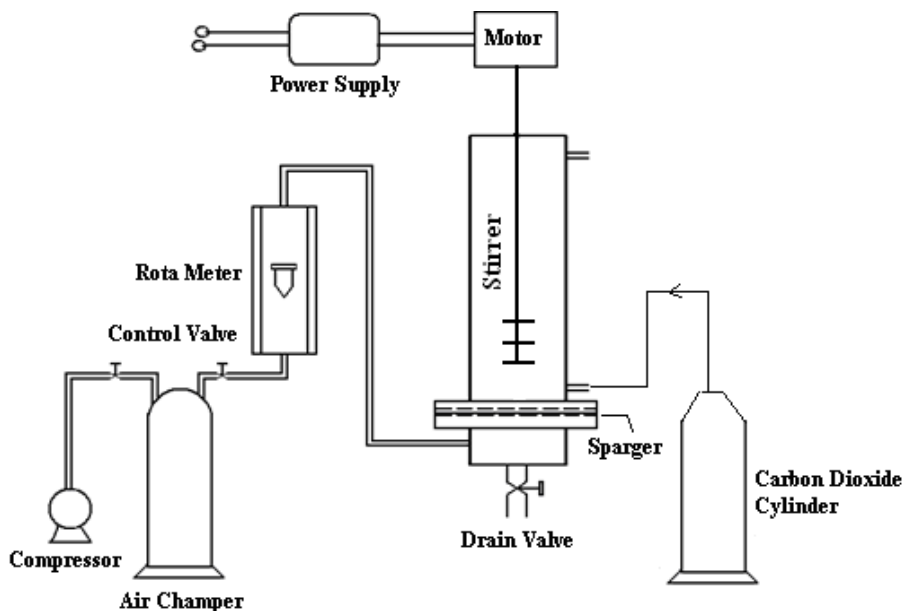


Figure 1. Experimental setup for stirred bubble column reactor

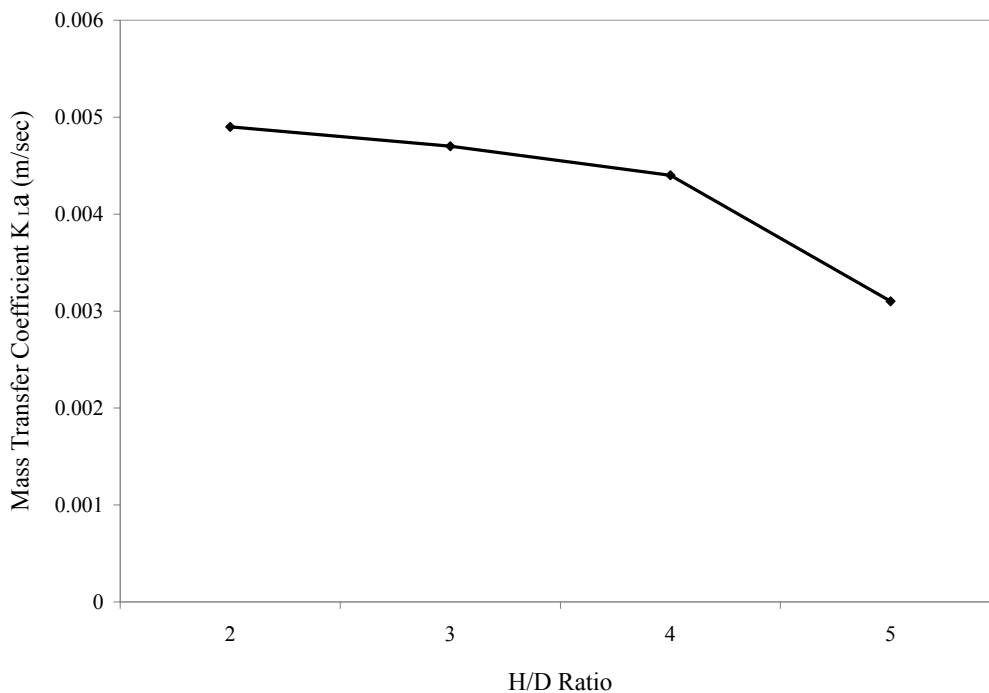


Figure 2. Effect of mass transfer coefficient on H/D ratio (Air flow rate = 0.42 lpm, Speed of the stirrer = 100 rpm)

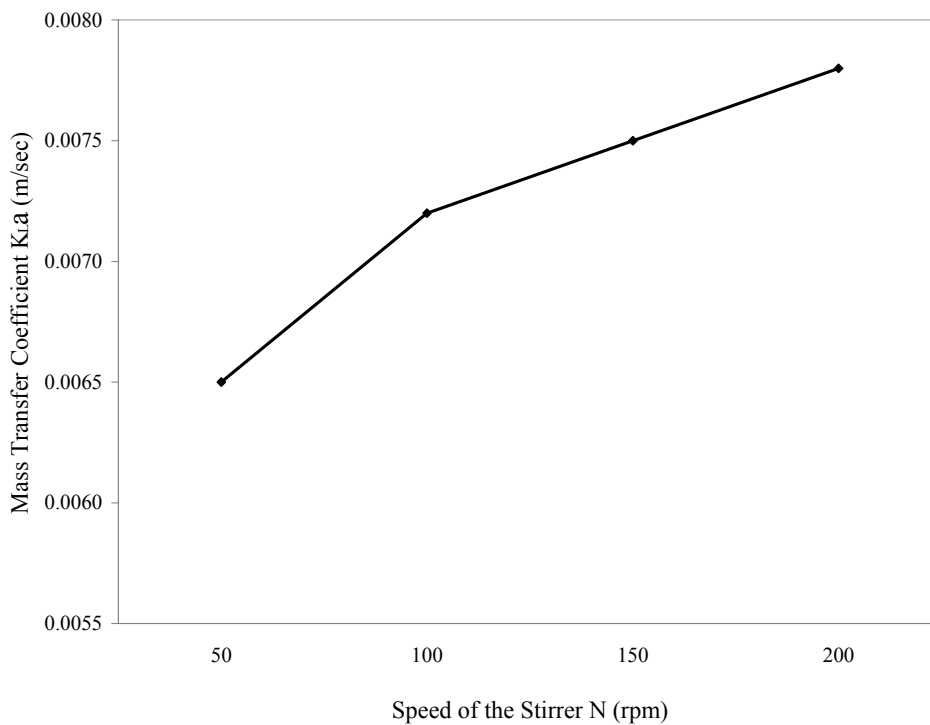


Figure 3. Effect of mass transfer coefficient on speed of the stirrer (H/D ratio = 4, Air flow rate = 0.42 lpm)

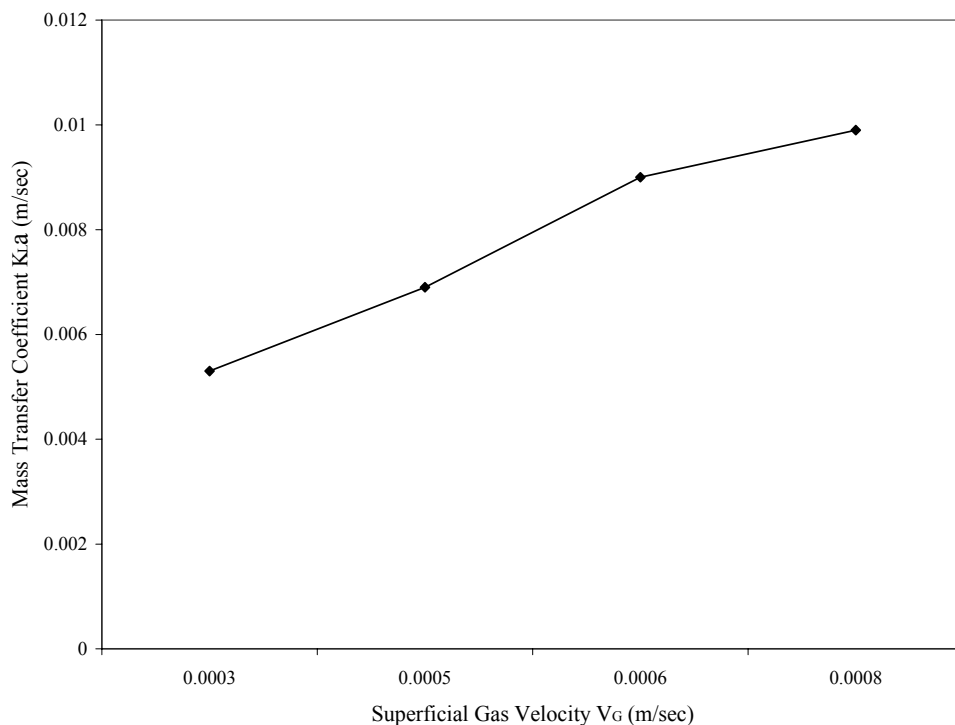


Figure 4. Effect of Mass transfer coefficient on superficial gas velocity (H/D ratio = 4, Speed of the stirrer = 100 rpm)

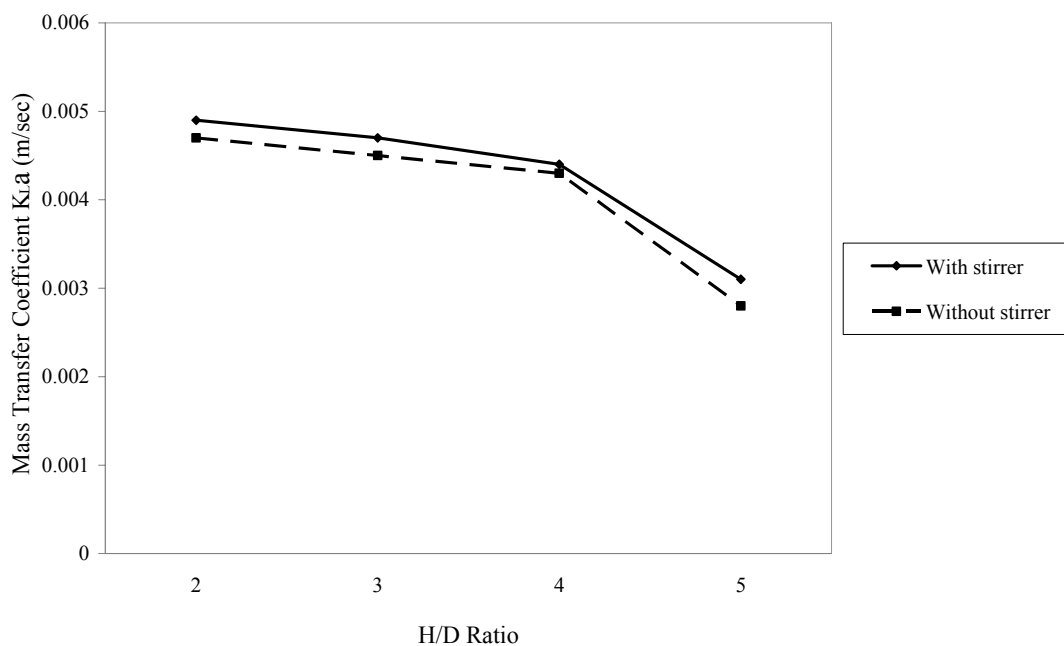


Figure 5. Comparison of effect of mass transfer coefficient on H/D ratio (Speed of the stirrer = 100 rpm, Air flow rate = 0.42 lpm)

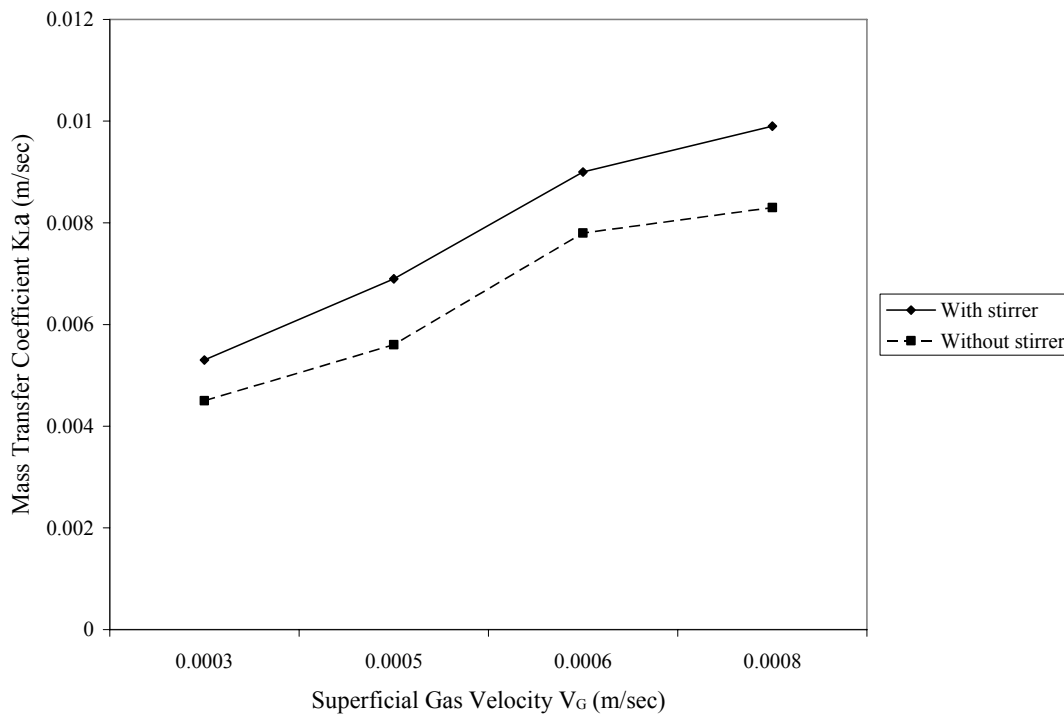


Figure 6. Comparison of effect of mass transfer coefficient on superficial gas velocity (H/D ratio = 4, Speed of the stirrer = 100 rpm)

Land Suitability Evaluation Using Fuzzy Continuous Classification (A Case Study: Ziaran Region)

Ali Keshavarzi (Corresponding author)

Department of Soil Science Engineering, University of Tehran

P.O.Box: 4111, Karaj 31587-77871, Iran

Tel: 98-261-223-1787 E-mail: aliagric@gmail.com, alikeshavarzi@ut.ac.ir

Fereydoon Sarmadian

Department of Soil Science Engineering, University of Tehran

P.O.Box: 4111, Karaj 31587-77871, Iran

Tel: 98-261-223-1787 E-mail: fsarmad@ut.ac.ir

Ahmad Heidari

Department of Soil Science Engineering, University of Tehran

P.O.Box: 4111, Karaj 31587-77871, Iran

Tel: 98-261-223-1787 E-mail: ahaidari@ut.ac.ir

Mahmoud Omid

Department of Agricultural Machinery Engineering, University of Tehran

P.O.Box: 4111, Karaj 31587-77871, Iran

Tel: 98-261-280-8138 E-mail: omid@ut.ac.ir

The research is financed by Department of Soil Science Engineering, University of Tehran

Abstract

Because conventional Boolean retrieval of soil survey data and logical models for assessing land suitability treat both spatial units and attribute value ranges as exactly specifiable quantities, they ignore the continuous nature of soil and landscape variation and uncertainties in measurement which can result in the misclassification of sites that just fail to match strictly defined requirements. The objective of this research is to apply fuzzy set theory for land suitability evaluation in Ziaran region in Qazvin province, Iran. The study area was divided into 15 land units and 9 land characteristics considered to be relevant to irrigated wheat. The weight contributions of individual characteristics to observed yield were determined using the analytic hierarchy process (AHP). The use of the fuzzy technique is helpful for land suitability evaluation and classification of continuous variation, especially in applications in which subtle differences in land characteristics are of a major interest.

Keywords: Fuzzy set, Continuous classification, AHP, Land index, Irrigated wheat, Ziaran

1. Introduction

Making effective decisions regarding agricultural land suitability problems are vital to achieve optimum land productivity and to ensure environmental sustainability (Kurtener et al., 2004). Land evaluation procedures focus increasingly on the use of quantitative procedures to enhance the qualitative interpretation of land resource surveys. Crucial to the estimation of land suitability is the matching of land characteristics with the requirements of envisaged land utilization types. Land evaluation results from a complex interaction of physical, chemical and bioclimatic processes and evaluation models are reliable enough to predict accurately the behaviour of land (Held et al., 2003; Ball and De la Rosa, 2006; Shahbazi et al., 2009).

Land evaluation is carried out to estimate the suitability of land for a specific use such as arable farming or irrigated agriculture. Land evaluation can be carried out on the basis of biophysical parameters and/or socio-economic conditions of an area (FAO, 1976). Biophysical factors tend to remain stable, whereas socio-economic factors that are affected by social, economic and political performances (Dent and Young, 1981; Triantafilis et al., 2001). Thus, physical land suitability evaluation is a prerequisite for land-use planning and

development (Sys, 1985; Van Ranst et al., 1996). It provides information on the constraints and opportunities for the use of the land and therefore guides decisions on optimal utilization of land resources (FAO, 1984).

In 1976, FAO is provided a general framework for land suitability classification. In this framework, doesn't have been proposed a specific method for doing this classification. In later years, the collection of methods was presented based on the above framework (FAO, 1984). From the variation of these methods can be pointed maximum limitation and parametric methods. In parametric method, a quantitative classification is allocated to each characteristic of land. If a characteristic of land for a specific product was completely desired and provided optimum conditions for that, maximum degree 100 would belong to that characteristic and if it has limitation, the lower degree will be given to it. Later, allocated ranks will be used in calculation of the land index. In parametric method, different classes of land suitability are defined as completely separate and discrete groups and are separated from each other by distinguished and consistent range. Thus, land units that have moderate suitability can only choose one of the characteristics of predefined classes of land suitability. Fuzzy sets theory for the first time defined by Zadeh (1965) in order to quantitative defining and determining of some classes that are expressed vaguely such as "very important" and so on. In fuzzy thinking, determination of specific border is difficult and belonging of various elements to various concepts and issues are relative. In fuzzy theory, the membership was not two-valued, but it can allocate the range of numbers from zero to one. A function that expresses degree of membership is called membership function. In land evaluation with fuzzy method, mainly bell-shape functions, such as sigmoid, cauchy and kandel functions were used. Fuzzy model has been used by many researchers in land suitability evaluation (Tang et al., 1991; Van Ranst et al., 1996; Keshavarzi and Sarmadian, 2009). Most of the researchers, have been compared the results of this evaluation with other conventional methods such as maximum limitation, parametric and multiple regression methods in order to predicting the yield of production. Fritz and See (2005) studied the comparison of land cover maps using fuzzy agreement. The spatial fuzzy agreement between the two land cover products is provided. The results showed that fuzzy agreement can be used to improve the overall confidence in a land cover product. Sicat et al. (2005) used fuzzy modeling incorporating the farmers' knowledge to assign the weights of the membership functions. The final objective was to make land suitability maps for agriculture in Nizamabad district of Andhra Pradesh State in India. Tang et al. (1991) used fuzzy method for evaluation of Hamen lands in Liaoning province in China in order to cultivating corn. These researchers were obtained the final matrix of suitability with constituting weight matrix and land characteristics matrix and multiplication of them and finally were calculated the land index. In this study, they were used multiple regression to determination of weights. Tang et al. (1992) did the land suitability evaluation in the region of Aitayi in Liaoning province in China for dry maize using fuzzy, parametric and limitation methods and studied regression relationships between obtained suitability indices and the observed yield. The results of their investigation showed that indices obtained from fuzzy method had more correlation with the observed yield ($r=0.96$). After fuzzy method, parametric method ($r=0.9$) and finally limitation method had lowest correlation ($r=0.8$). They were used simulation method for selecting appropriate weights. Sanchez (2007) in his study for the investigation of land suitability for dry rice and rubber, used three methods including the investigation of land suitability using farmer's knowledge, land suitability classification with two-valued method using ALES model and evaluation based on fuzzy logic. He used AHP method for weighting in his study. The results of this study showed that obtained proportions from three methods had differences in some cases. Also integration of farmer's knowledge with evaluation methods increases the correlation of evaluations with region conditions. The selection of appropriate membership function for land evaluation depends on the degree of characteristics changes in transition zone and boundary of classes. After the selection of membership function, determination of transition zone's width is one of the most important and critical stages of decision in fuzzy sets theory and accuracy of results is indebted these decision.

Hence, the present study was carried out with objective to application of fuzzy continuous classification for evaluation of agricultural land suitability using Analytic Hierarchy Process in Ziaran region. Wheat yield information obtained from users (farmers) and policy makers (government officials) who are responsible for rural development.

2. Materials and methods

2.1 Study area

The land investigated in the research is located in Ziaran (Qazvin province in Iran) which has the area about 5121 hectares; between latitudes of $35^{\circ} 58'$ and $36^{\circ} 4' N$ and between longitudes of $50^{\circ} 24'$ and $50^{\circ} 27' E$. The average, minimum and maximum heights points of Ziaran region are 1204, 1139 and 1269 meters from the sea level, respectively. Figure1 shows the study area in Iran. The soil moisture and temperature regimes of the region by means of Newhall software are Weak Aridic and Thermic, respectively. Based on soil taxonomy (USDA,

2010), this region has soils in Entisols and Aridisols orders (Table 1).

2.2 Data collection and soil sample analysis

After preliminary studies of topographic maps (1:25000), using GPS, studying location was appointed. 70 soil samples were collected from different horizons of 15 soil profiles located in Ziaran region in Qazvin Province. Measured soil parameters included texture (determined using Bouyoucos hydrometer method), Organic Carbon (OC) was determined using Walkley-Black method (Nelson and Sommers, 1982). The Clod method (Blake and Hartge, 1986) was used to determine Bulk density (Bd). The moisture contents at field capacity and wilting point were determined with a pressure plate apparatus (Cassel and Nielsen, 1986) at -33 and -1500 kPa, respectively. Water saturation percentage (SP) was determined using Gravimetry method, CaCO_3 content was determined using Calcimetry method, gypsum content was determined using Acetone method and CEC (cation exchange capacity in $\text{cmol}^c \text{kg}^{-1}$ soil) determined by the method of Bower (Sparks et al., 1996). pH, electrical conductivity (EC), dissolved Ca^{2+} , Mg^{2+} , Na^+ and K^+ were determined using standard methods (USDA, 1998).

2.3 Fuzzy sets theory

It is well known that many elements of land properties have uncertainties. Uncertainty is inherent in decision-making processes, which involve data and model uncertainty. These range from measurement errors, to inherent variability, to instability, to conceptual ambiguity or to simple ignorance of important factors. Fuzzy sets theory is a mathematical method used to characterize and propagate uncertainty and imprecision in data and functional relationships. Fuzzy sets are especially useful when insufficient data exist to characterize uncertainty using standard statistical measures (e.g., mean, standard deviation and distribution type). An underlying philosophy of the fuzzy sets theory is to provide a strict mathematical framework, where the imprecise conceptual phenomena in decision making may be precisely and rigorously studied, in particular for knowledge management (Kurtener et al., 2004). The fuzzy sets theory includes fuzzy mathematics, fuzzy measures, fuzzy integrals, etc. Fuzzy logic is a minor aspect of the whole field of fuzzy mathematics. In classical sets theory, the membership of a set is defined as true or false, 1 or 0. Membership of a fuzzy set, however, is expressed on a continuous scale from 1 (full membership) to 0 (full non-membership).

Definition 1. Let X be a set (universe). D is called a fuzzy subset of X if D is a set of ordered pairs: $D = [(x, \mu D(x)), x \in X]$, where $\mu D(x)$ is the grade of membership of X in D . $\mu D(x)$ takes its values in the closed interval $[0, 1]$. The closer $\mu D(x)$ is to 1, the more x belongs to D ; the closer it is to 0 the less it belongs to D . If $[0, 1]$ is replaced by the two element set $\{0, 1\}$, then D can be regarded as a subset of X (Kurtener et al., 2004).

2.4 Application of fuzzy set theory in land suitability evaluation

The irrigated wheat requirements were determined using FAO framework for land evaluation (Sys, 1985). The studied area was divided into 15 land units and 9 land characteristics considered to be relevant to irrigated wheat. They included Slope (%), Soil depth (cm), Climate (index), EC (dSm^{-1}), Exchangeable Sodium percentage (ESP), Volumetric content of gravel (%), OC content in soil (%), Soil texture (class) and Gypsum content (%). (Table 2)

To determine the land suitability classes for irrigated wheat via land biophysical characteristics, fuzzy method was used. To determined degree of membership for each land characteristic and via square root method, land index in each land unit was obtained. Finally, land suitability classes were determined. In fuzzy method, based on irrigated wheat requirements, the sigmoid (Torbert et al., 2008) and Kandel (Sarmadian et al., 2009) membership functions were used to determine the degree of membership of each land characteristic to land suitability classes (Figures 2 and 3) and the results were put in a matrix R (called characteristic matrix).

Then, via Analytic Hierarchy Process (AHP) the weight of each effective land characteristic in irrigated wheat yield was calculated and put in weights matrix (W). The AHP is characterized by pairwise comparisons among decision elements for generation of relative matrix. In this method, pairwise comparisons are considered as inputs and relative weights are as outputs. The Saaty scale (2003) was used for generation of pairwise comparison matrix which relatively rates priorities for two criteria (Table 3). It was supposed that comparison matrix was reverse and reciprocal that means if a criterion A in comparison with criteria B has a double priority, it could be inferred that criteria B has a priority half of criteria A. The criteria priorities are defined according to expert's judgments. After generation of pairwise comparison matrix, the criteria weights are calculated that includes sum of each column of pairwise comparison matrix and division of each component by the result of each relevant column sum. The resulted matrix is known as normalized pairwise comparison matrix. The average of each row of the pairwise comparison matrix is calculated and these average values indicate relative weights of compared criteria.

To determine the final land suitability class in each land unit, a multiple operator (combination) was used. The

final matrix of land suitability (E) was calculated after multiplying the characteristic matrix (R) in each land unit by weights matrix (W).

The components of E indicate the degree of membership of relevant land unit to land suitability classes. This matrix is calculated as below (Eq.1):

$$E = W \circ R \quad (1)$$

Where: \circ is fuzzy operator created from Triangular norm T (as minimum) and Triangular conorm T* (as maximum) (Ruan, 1990) (Table 4).

According to these norms, the best result for final land suitability matrix is achieved via formula presented as below (Keshavarzi and Sarmadian, 2009):

$$e_j = \min(a_1 + a_2 + \dots + a_n, 1) \quad (2)$$

$$a_i = \max(0, w_i + r_{ij} - 1), \quad i = 1, 2, \dots, n \quad (3)$$

Where:

r: components of characteristic matrix (R) for land characteristic of i under the land suitability class of j

w: components of weights matrix (W) for land characteristic of i

e: components of final land suitability matrix (E) for land suitability classes of S₁ to N

The final land suitability matrix for land unit 10 (E₁₀) is shown as an example in below:

S₁ S₂ S₃ N

$$E_{10} = [0.74 \quad 0.23 \quad 0.09 \quad 0]$$

In order to calculate land index, the sum of components of land suitability matrix (E) is set to one (standardized) and the new components of matrix are multiplied by average of indices of land suitability classes, respectively, based on the following formula (Sarmadian et al., 2009):

$$LI = \sum [d(E_j) \times A_j] \quad (4)$$

Where:

LI: land index

d: normalized (standardized) value of land suitability matrix (E)

A: average of maximum and minimum indices of land suitability classes

3. Results and discussion

Pairwise comparison matrix and normalized pairwise comparison matrix with criteria weights are shown in Tables 5 and 6, respectively. Due to higher weight, gravel volume percentile in soil was the most significant characteristic (criteria). The soil depth was the least significant criteria among all effective criteria in irrigated wheat yield. By the determined land characteristic weights, the weight matrix (W) was generated as the matrix below:

$$W = [0.239 \quad 0.024 \quad 0.044 \quad 0.154 \quad 0.213 \quad 0.129 \quad 0.086 \quad 0.066 \quad 0.045]$$

The weight matrix (W) multiplied by characteristic matrix (R) for each land unit based on fuzzy operator (combination) and resulted in the final land suitability matrix (E). Then, land indices were calculated based on final E matrix in each land unit. Table 7, shows the observed irrigated wheat yield, land suitability classes and land indices obtained by fuzzy method for different land units in Ziaran region. According to table 7, maximum and minimum observed yield were 5.30 and 0.00 (Ton.ha⁻¹) respectively. In land unit 9, due to high EC (43.9 dSm⁻¹) and ESP (42.3%), the irrigated wheat yield is near to zero. The calculated regression between land index and observed irrigated wheat yield (Figure 4) were 0.91 for fuzzy method.

Major limitations to wheat yield were gravel and organic carbon. Emphasis should be placed on soil management techniques that conserve organic matter and enhance nutrient and water-holding capacity of the soil. A comparison between results of this research and other investigators (Tang et al., 1991; Tang et al., 1992; Van Ranst et al., 1996; Sanchez, 2007; Joss et al., 2008; Keshavarzi and Sarmadian, 2009) indicated that the fuzzy method with higher correlation factor, had more accuracy and capability of predicting yield, since fuzzy set method considered the continual land changes and is more efficient in reflecting spatial variability of soil characteristic rather than Boolean's two-valued logic that overlooks a considerable section of useful information

during land evaluation processing. Nonetheless, the accuracy of the results is mainly dependant on the designated weights to different land characteristics. Although in land suitability evaluation, nowadays the emphasis is on quantitative (numerical) methods, because the fuzzy sets theory's problem in land suitability evaluation needs a high volume of calculations. On the other hand, increasing the number of land characteristic increases the number of pairwise comparisons and decision making on spatial variability of different characteristics in each land unit becomes difficult, because different characteristics has different weights and designation of weight to characteristics needs more experience and criteria precedence. The weakest part of the fuzzy set methodology for land evaluation is the way in which membership functions, class centers, cross-over values and weight values are chosen (Burrough, 1989; Keshavarzi and Sarmadian, 2009). Davidson et al. (1994) also stated that one critical issue in the application of fuzzy set theory to land suitability assessment is the choice of membership functions. This is not a straightforward task since decisions have to be made on membership values according to degree of suitability. The problem of how to define the parameters of the fuzzy membership functions is more complicated than the Boolean equivalent because it requires not only specifications of what kind of membership function and class boundary values, but also the widths of the transition zones. Another critical issue is the choice of weights which clearly have a major impact on results. Some guidance can be obtained from the literature and expert experience on land properties relevant to particular crops, but ultimately subjective decisions have to be made. The strength of the fuzzy set approach in land evaluation is that it starts from the promise that nature may be inherently vague or imprecise, and does not try to pretend that the real world, which has been modeled by data entitles created by human or machine observation, is more exact, or more perfect than it really is (Burrough, 1989).

4. Conclusion

Fuzzy logic is an attempt to extend the concept of continuous variation of soil properties from the geographic space to the attribute space (Burrough et al., 1997). The use of fuzzy technique in this study produced land suitability for irrigated wheat in a continuous scale. Land suitability indices reflect inherent fertility of the soils (Brimoh et al., 2004). The approach in this research is well applicable for applications in which subtle differences in land characteristic is of the major interests. Usage of SI model permits the evaluation of the land characteristics limitations to wheat in the study area. Considering major constraints to the use of fuzzy technique for land suitability evaluation, it results valuable information for identifying major limitations to crops production and strategies for overcoming them. The most important factor that complicates a decision making problem, is domination of uncertainty situation. Decision making under uncertainty situation is complex and difficult, thus achieving a suitable and optimum choice demands compliance with rules, values and different description aspects of decision process. Fuzzy set theory can continually show land continuity in different land classes and this one is of its advantages. The other advantage is that it allows the environment to be inherently vague and does not try to limit soil continual system to the data measured by soil science researchers (Burrough et al., 1992).

References

- Ball, A., & De la Rosa, D. (2006). Modelling possibilities for the assessment of soil systems. In N. Uphoff, A. Ball, E. Fernandes, H. Herren, O. Husson, M. Laing, Ch. Palm, J. Pretty, P. Sanchez, N. Sanginga, J. Thies (Eds.), *Biological Approaches to Sustainable Soil Systems*. CRC Press, BocaRaton, FL, USA.
- Blake, G. R., & Hartge, K. H. (1986). Particle density. In A. Klute (Eds.), *Methods of soil analysis*. Part 1. Agron. Monogr. 9. ASA, Madison, WI. pp. 377–382.
- Brimoh, A. K., & Stein, A. (2004). Land evaluation for Maize based on Fuzzy set and interpolation. *Journal of Environmental Management*, 33(2), 226–238.
- Burrough, P. A. (1989). Fuzzy mathematical methods for soil survey and land evaluation. *Journal of Soil Science*, 40, 477-492.
- Burrough, P. A., MacMillan, R. A., & Van Densen, W. (1992). Fuzzy classification methods for determining land suitability from soil profile observations and topography. *Journal of Soil Science*, 43, 193-210.
- Burrough, P. A., Van Gaans, P. F. M., & Hootsmans, R. (1997). Continuous classification in soil survey: spatial correlation, confusion and boundaries. *Geoderma*, 77, 115–135.
- Cassel, D. K., & Nielsen, D. R. (1986). Field capacity and available water capacity. In A. Klute, (Eds.), *Methods of Soil Analysis*. Part 1, second ed. Agron. Monogr. 9. ASA and SSSA, Madison, WI, pp. 901-926.
- Davidson, D. A., Theocharopoulos, S. P., & Bloksma, R. J. (1994). A land evaluation project in Greece using GIS and based on Boolean and fuzzy set methodologies. *International Journal of Geographic Information*

- Systems*, 8(4), 369–384.
- Dent, D., & Young, A. (1981). *Soil survey and land evaluation*. George Allen and Uniwin: Boston.
- FAO. (1976). *A framework for land evaluation*. FAO Soils Bulletin 32, Rome.
- FAO. (1984). *Guidelines: Land evaluation for rainfed agriculture*. FAO Soils Bulletin 52, Rome.
- Fritz, S., & See, L. (2005). Comparison of land cover maps using fuzzy agreement. *International Journal of Geographical Information Science*, 19(7), 787-807.
- Held, M., Imeson, A., & Montanarella, L. (2003). *Economic Interests and Benefits of Sustainable Use of Soils and Land Management*. Joint Res. Centre Press, Ispra, Italy.
- Joss, B. N., Hall, R. J., Sidders, D. M., & Keddy, T. J. 2008. Fuzzy-logic modeling of land suitability for hybrid poplar across the Prairie Provinces of Canada. *Earth and Environmental Science*, 141, 79-96.
- Keshavarzi, A., & Sarmadian, F. (2009). Investigation of fuzzy set theory's efficiency in land suitability assessment for irrigated wheat in Qazvin province using Analytic hierarchy process (AHP) and multivariate regression methods. *Proc. 'Pedometrics 2009' Conf*, August 26-28, Beijing, China.
- Kurtener, D., Krueger-Shvetsova, E., & Dubitskaia, I. (2004). *Quality estimation of data collection*. In UDMS, UDMS Press, Gioggia-Venice. pp. 9101–9109.
- Nelson, D.W., & Sommers, L. E. (1982). Total carbon, organic carbon, and organic matter. In A. L. Page, R. H. Miller, & D.R. Keeney (Eds.), *Methods of Soil Analysis*. Part II, 2nd ed. American Society of Agronomy, Madison, WI, USA. pp. 539-580.
- Ruan, D. (1990). A critical study of widely used fuzzy implication operators and their influence on the inference rules in fuzzy expert systems. Doctoral Thesis, State University of Gent, Belgium. 155 pp.
- Saaty, T. L. (2003). Decision-making with the AHP: Why is the principal eigenvector necessary? *European Journal of Operational Research*, 145, 85-91.
- Sanchez, J. F. (2007). Applicability of knowledge-based and Fuzzy theory-oriented approaches to land suitability for upland rice and rubber. M.Sc. Thesis, ITC, the Netherland.
- Sarmadian, F., Keshavarzi, A., Rajabpour, B., & Rajabpour, A. (2009). Multi-Criteria Decision Making in Fuzzy Modeling of Land Suitability Evaluation (Case Study: Takestan area of central Iran). *Proc. 'Pedometrics 2009' Conf*, August 26-28, Beijing, China.
- Shahbazi, F., Jafarzadeh, A. A., Sarmadian, F., Neyshaboury, M. R., Oustan, S., Anaya-Romero, M., Lojo, M., & De la Rosa D. (2009). Climate change impact on land capability using MicroLEIS DSS. *Int. Agrophysics*, 23, 277-286.
- Sicat, R. S., Carranza, E. J. M., & Nidumolu, U. B. (2005). Fuzzy modeling of farmers' knowledge for land suitability classification. *Agricultural systems*, 83, 49-75.
- Sparks, D. L., Page, A. L., Helmke, P. A., Leoppert, R. H., Soltanpour, P. N., Tabatabai, M. A., Johnston, G. T., & Summer, M. E. (1996). *Methods of soil analysis*. Soil Sci. Soc. of Am. Madison, Wisconsin.
- Sys, C. (1985). *Land evaluation*, part I, II, III. ITC, University of Ghent, Belgium, 343 pp.
- Tang, H., Debaveye, J., Ruan, D., & Van Ranst, E. (1991). Land suitability classification based on fuzzy set theory. *Pedologie*, 3, 277-290.
- Tang, H., Van Ranst, E., & SYS, C. (1992). An approach to predict land production potential for irrigated and rainfed winter wheat in Pinan County, China. *Soil Technology*, 5, 213-224.
- Torbert, H. A., Krueger, E., & Kurtener, D. (2008). Soil quality assessment using fuzzy modeling. *Int. Agrophysics*, 22, 365-370.
- Triantafilis, J., Ward, W. T., & McBratney, A. B. (2001). Land suitability assessment in the Namoi Valley of Australia, using a continuous model. *Amsterdam Journal of Soil Research*, 39, 273–290.
- USDA. (1998). *Field book for describing and sampling soils*. Version 1.1, Lincoln: Nebraska. NRCS.
- USDA. (2010). Soil Survey Staff. *Keys to Soil Taxonomy*. 11 th edition.
- Van Ranst, E., Tang, H., Groenemans, R., & Sinthurath, S. (1996). Application of Fuzzy logic to land suitability for rubber production in Peninsular Thailand. *Geoderma*, 70, 1-19.
- Zadeh L. A. (1965). Fuzzy sets. *Information and control*, 8, 338-353.

Table 1. Soil classification in the study area based on soil taxonomy (2010)

Soil mapping unit	Soil classification
1	Fine-loamy, mixed, super active, thermic, Xeric Haplocambids
2	Coarse-loamy over fragmental, mixed, super active, calcareous, shallow, thermic, Xeric Torrifuvents
3	Coarse-loamy, mixed, super active, thermic, Xeric Torrifuvents
4	Coarse-loamy, mixed, super active, thermic, Xerofluentic Haplocambids
5	Sandy-skeletal over coarse loamy, mixed, super active, calcareous, thermic, Xeric Torrifuvents
6	Fine, mixed, semi active, thermic, Xeric Haplocalcids
7	Fine-loamy, mixed, active, thermic, Xeric Haplocalcids
8	Fine-loamy over clayey, mixed, active, thermic, Sodic xeric Haplocambids
9	Fine-loamy, mixed, super active, thermic, Gypsic Aquisalids
10	Fine-loamy, mixed, super active, thermic, Typic Haplogypsid
11	Fine, mixed, active, thermic, Xeric Haplocalcids
12	Fine-loamy, mixed, super active, thermic, Xeric Haplocalcids
13	Fine, mixed, active, thermic, Xeric Haplocalcids
14	Fine-loamy, mixed, super active, thermic, Xeric Haplocalcids
15	Coarse-loamy over fragmental, mixed, super active, calcareous, shallow, thermic, Xeric Torriorthents

Table 2. Selected land characteristics in Ziaran region

Land Unit	Land Characteristics								
	Slope (%)	ESP	OC (%)	EC (dSm ⁻¹)	Gypsum (%)	Soil texture (class)*	Climate (index)	Gravel (%)	Soil depth (cm)
1	1.50	1.53	0.37	1.18	0.00	C.L	92.30	5.88	170
2	2.50	1.42	0.61	1.16	0.00	S.L	92.30	25.63	50
3	1.50	1.19	0.61	0.94	0.00	L	92.30	0.00	200
4	1.50	9.18	0.76	1.40	0.00	L	92.30	1.88	175
5	1.50	2.34	1.04	1.20	0.00	S.L	92.30	23.38	170
6	0.75	7.49	0.75	2.35	0.00	C	92.30	0.00	170
7	0.75	9.10	0.94	3.47	0.00	L	92.30	0.10	180
8	1.50	23.50	0.75	6.03	0.00	C.L	92.30	0.00	180
9	0.75	42.30	0.66	43.90	4.97	S.C.L	92.30	0.00	120
10	4.00	1.95	0.67	2.00	9.37	S.C.L	92.30	0.00	170
11	1.50	9.09	0.47	2.34	0.00	C	92.30	0.00	190
12	0.75	7.05	0.56	1.67	0.00	S.C.L	92.30	0.70	170
13	1.50	1.83	0.38	1.06	0.00	C.L	92.30	1.39	160
14	1.50	8.98	0.57	1.92	0.00	S.L	92.30	1.04	180
15	2.50	1.14	0.76	0.96	0.00	L	92.30	14.05	40

*C=Clay, L= Loam, C.L= Clay Loam, S.L= Sandy Loam, S.C.L= Sandy Clay Loam

Table 3. The Saaty scale (2003) was used for generation of pairwise comparison matrix

Intensity of importance	Definition
1	Equal importance
2	Equal to moderate importance
3	Moderate importance
4	Moderate to strong importance
5	Strong importance
6	Strong to very strong importance
7	Very strong importance
8	Very to extremely strong
9	Extreme importance

Table 4. Examples of triangular norm T and triangular conorm T* (Ruan, 1990)

Triangular norm T	Triangular conorm T*
Minimum $T(a,b) = \min(a,b)$	Maximum $T^*(a,b) = \max(a,b)$
Product $T(a,b) = a.b$	Probabilistic sum $T^*(a,b) = a+b-a.b$
Bounded product $T(a,b) = \max(0,a+b-1)$	Bounded sum $T^*(a,b) = \min(a+b,1)$

Table 5. Pairwise comparison matrix

Criteria	Gravel (%)	Soil depth (cm)	Gypsum (%)	Texture (class)	OC (%)	EC (dSm ⁻¹)	ESP	Slope (%)	Climate (index)
Gravel (%)	1.00	6.00	5.00	2.00	2.00	3.00	3.00	4.00	3.00
Soil depth (cm)	0.17	1.00	0.33	0.20	0.16	0.20	0.25	0.16	0.50
Gypsum (%)	0.20	3.00	1.00	0.25	0.16	0.20	0.25	0.50	2.00
Texture (class)	0.50	5.00	4.00	1.00	0.33	2.00	3.00	4.00	3.00
OC (%)	0.50	6.00	6.00	3.00	1.00	2.00	3.00	5.00	3.00
EC (dSm ⁻¹)	0.33	5.00	5.00	0.50	0.50	1.00	2.00	3.00	4.00
ESP	0.33	4.00	4.00	0.33	0.33	0.50	1.00	2.00	2.00
Slope (%)	0.25	6.00	2.00	0.25	0.20	0.33	0.50	1.00	2.00
Climate (index)	0.33	2.00	0.50	0.33	0.33	0.25	0.50	0.50	1.00

Table 6. Normalized pairwise comparison matrix with criteria weights

Criteria	Gravel (%)	Soil depth (cm)	Gypsum (%)	Texture (class)	OC (%)	EC (dSm ⁻¹)	ESP	Slope (%)	Climate (index)	Weight
Gravel (%)	0.276	0.158	0.180	0.254	0.397	0.316	0.222	0.198	0.146	0.239
Soil depth (cm)	0.046	0.026	0.012	0.025	0.033	0.021	0.019	0.008	0.024	0.024
Gypsum (%)	0.055	0.079	0.036	0.032	0.033	0.021	0.019	0.025	0.098	0.044
Texture (class)	0.138	0.132	0.144	0.127	0.066	0.211	0.222	0.198	0.146	0.154
OC (%)	0.138	0.158	0.216	0.381	0.199	0.211	0.222	0.248	0.146	0.213
EC (dSm ⁻¹)	0.092	0.132	0.180	0.064	0.099	0.105	0.148	0.149	0.195	0.129
ESP	0.092	0.105	0.144	0.042	0.066	0.053	0.074	0.099	0.098	0.086
Slope (%)	0.069	0.158	0.072	0.032	0.040	0.035	0.037	0.050	0.098	0.066
Climate (index)	0.092	0.053	0.018	0.042	0.066	0.026	0.037	0.025	0.049	0.045

Table 7. Observed irrigated wheat yield, land suitability classes and land indices obtained by fuzzy approach for different land units in Ziaran region

Land unit No.	Observed yield (Ton/ha)	Land suitability classes evaluation for irrigated wheat
		Fuzzy approach (index)
1	4.20	S ₁ (76.23)
2	3.10	S ₂ (70.36)
3	4.80	S ₁ (85.70)
4	4.50	S ₁ (83.14)
5	3.60	S ₁ (76.55)
6	5.30	S ₁ (89.65)
7	4.80	S ₁ (88.43)
8	4.30	S ₁ (80.36)
9	0.00	N (17.20)
10	5.20	S ₂ (74.60)
11	4.50	S ₁ (81.50)
12	5.00	S ₁ (82.14)
13	4.80	S ₁ (84.60)
14	4.30	S ₁ (79.08)
15	3.30	S ₂ (74.30)

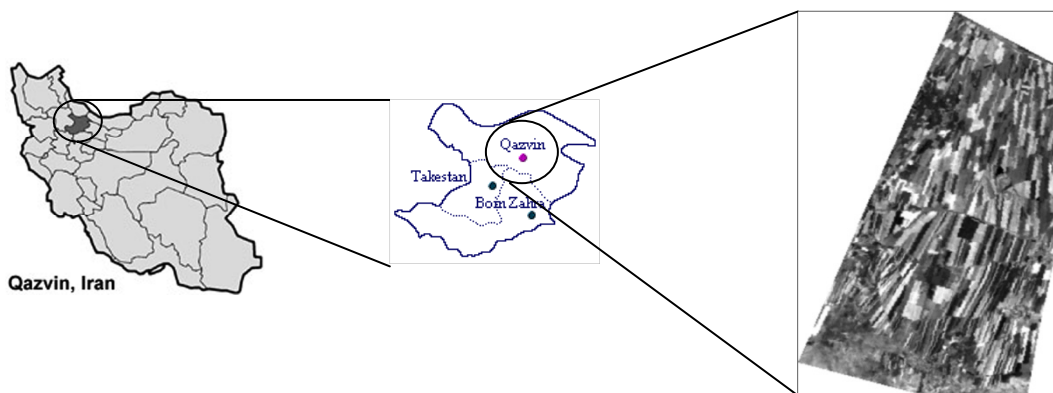


Figure 1. Location of the study area

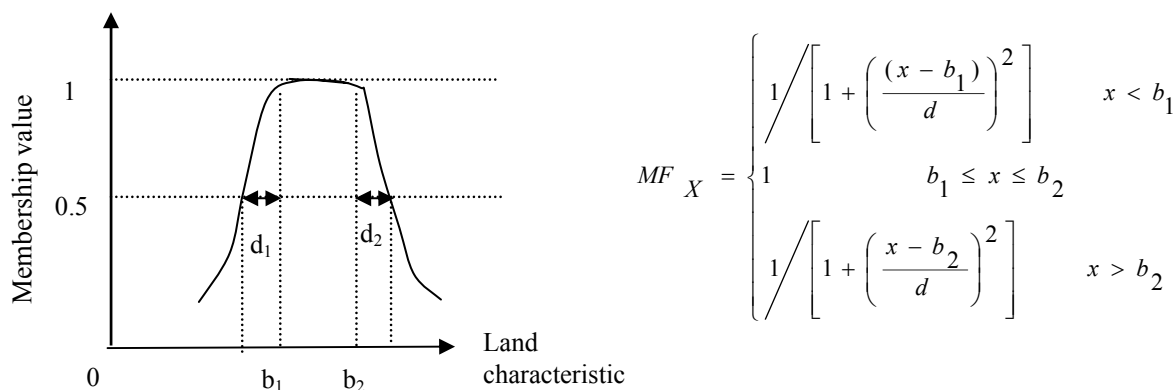


Figure 2. Kandel membership function and its equation (b_1 and b_2 are the lower limit and upper limits, respectively, and d_1 and d_2 are transitional zone widths)

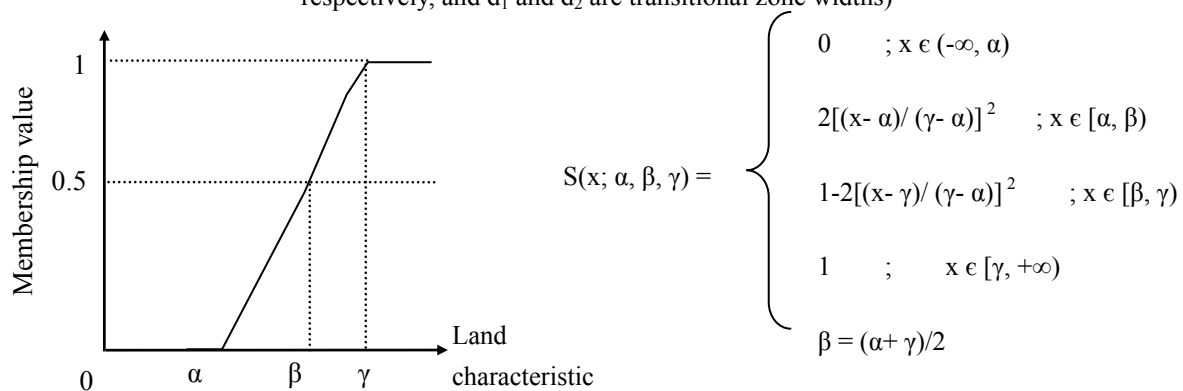


Figure 3. Sigmoid membership function and its equation

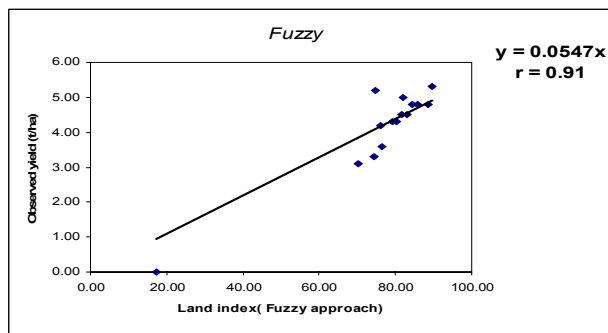


Figure 4. Linear regression between land suitability index and observed irrigated wheat yield in fuzzy approach in Ziaran region

Strongly Multiplicative Labeling for Some Cycle Related Graphs

S K Vaidya (Corresponding author)

Department of Mathematics, Saurashtra University, Rajkot 360 005, Gujarat, India

E-mail: samirkvaidya@yahoo.co.in

K K Kanani

Mathematics Department, L E College, Morbi 363 642, Gujarat, India

E-mail: kananikkk@yahoo.co.in

Abstract

In this paper we discuss strongly multiplicative labeling of some cycle related graphs. We prove that cycle with one chord, cycle with twin chords and cycle with triangle are strongly multiplicative graphs. In addition to this we prove that the graphs obtained by fusion and duplication of vertices in cycle admit strongly multiplicative labeling.

Keywords: Strongly multiplicative labeling, Strongly multiplicative graph, Cycle

1. Introduction

We begin with simple, finite, connected and undirected graph $G = (V(G), E(G))$. Here elements of sets $V(G)$ and $E(G)$ are known as vertices and edges respectively. In the present work C_n denotes cycle with n vertices and $N(v)$ denotes the set of all neighboring vertices of v . For all other terminology and notations we follow (Harary F., 1972). We will give brief summary of definitions which are useful for the present investigations.

Definition 1.1 A chord of a cycle C_n is an edge joining two non-adjacent vertices of cycle C_n .

Definition 1.2 Two chords of a cycle are twin chords (consecutive chords) if they form a triangle with an edge of the cycle C_n .

For positive integers n and p with $3 \leq p \leq n - 2$, $C_{n,p}$ is the graph consisting of a cycle C_n with a pair of twin chords with which the edges of C_n form cycles C_p , C_3 and C_{n+1-p} without chords.

Definition 1.3 Cycle with triangle is a cycle with three chords which by themselves form a triangle.

For positive integers p, q, r and $n \geq 6$, with $p + q + r + 3 = n$ then $C_n(p, q, r)$ denote a cycle with triangle whose edges form the edges of cycles C_{p+2} , C_{q+2} and C_{r+2} without chords.

Definition 1.4 If the vertices of the graph are assigned values subject to certain conditions is known as graph labeling.

For detailed survey on graph labeling we refer to 'A Dynamic Survey of Graph Labeling' by (Gallian, J., 2009).

Definition 1.5 A graph $G = (V(G), E(G))$ with p vertices is said to be multiplicative if the vertices of G can be labeled with distinct positive integers such that label induced on the edges by the product of labels of end vertices are all distinct.

Multiplicative labeling was introduced by Beineke and Hegde (Beineke L., 2001, p. 63-75). In the same paper they proved that every graph G admits multiplicative labeling and defined strongly multiplicative labeling as follows.

Definition 1.6 A graph $G = (V(G), E(G))$ with p vertices is said to be strongly multiplicative if the vertices of G can be labeled with p distinct integers $1, 2, \dots, p$ such that label induced on the edges by the product of labels of the end vertices are all distinct.

There are three types of problems that can be considered in the above context.

- (i) Construct new families of strongly multiplicative graphs;
- (ii) How strongly multiplicative labeling is affected under various graph operations;
- (iii) Given a graph theoretic property P characterize the class of graphs with property P that are strongly multiplicative.

In (Beineke L., 2001, p. 63-75) authors have extensively studied some problems of the types (i) and (iii) and they proved that

- Every cycle C_n is strongly multiplicative.
- Every wheel W_n is strongly multiplicative.
- Complete graph K_n is strongly multiplicative if and only if $n \leq 5$.
- Complete bipartite graph $K_{n,n}$ is strongly multiplicative if and only if $n \leq 4$.
- Every spanning subgraph of a strongly multiplicative graph is strongly multiplicative.
- Every graph is an induced subgraph of a strongly multiplicative graph.

The present work is intended to discuss problems of the types (i) and (ii). Here we investigate three new families of strongly multiplicative graphs and strongly multiplicative labeling is discussed in the context of graph operations namely duplication and fusion of vertices in cycle C_n .

Definition 1.7 Let u and v be two distinct vertices of a graph G . A new graph G_1 is constructed by *fusing* (identifying) two vertices u and v by a single vertex x is such that every edge which was incident with either u or v in G is now incident with x in G_1 .

Definition 1.8 Duplication of a vertex v_k of graph G produces a new graph G_1 by adding a vertex v_k' with $N(v_k') = N(v_k)$.

In other words a vertex v_k' is said to be duplication of v_k if all the vertices which are adjacent to v_k are now adjacent to v_k' also.

2. Main Results

Theorem 2.1 Every cycle with one chord is strongly multiplicative.

Proof: Let G be the cycle C_n with one chord and v_1, v_2, \dots, v_n be the consecutive vertices of C_n arranged in the clockwise direction. Let $e = v_1v_i$ be the chord of cycle C_n .

Let us define labeling $f: V(G) \rightarrow \{1, 2, \dots, n\}$ as follows.

$$f(v_1) = 1$$

$$f(v_i) = p_1 \text{ where } p_1 \text{ is the highest prime number such that } p_1 \leq n.$$

$$f(v_n) = p_2 \text{ where } p_2 \text{ is the second highest prime number such that } 1 < p_2 < p_1 \leq n.$$

Now label the remaining vertices starting from v_2 consecutively in clockwise direction from the set $\{1, 2, \dots, n\}$ except $1, p_1$ and p_2 as these numbers are already used as labels.

Then f is a strongly multiplicative labeling for G . That is, G is a strongly multiplicative graph.

Illustration 2.2 Consider a cycle C_6 with one chord. The labeling is as shown in Fig 1.

Theorem 2.3 Every cycle with twin chords is strongly multiplicative.

Proof: Let G be the cycle C_n with twin chords. Let v_1, v_2, \dots, v_n be the consecutive vertices of C_n arranged in the clock-wise direction. Let $e_1 = v_1v_i, e_2 = v_1v_{i+1}$ be two chords of C_n .

Let us define labeling $f: V(G) \rightarrow \{1, 2, \dots, n\}$ as follows.

$$f(v_1) = 1$$

$$f(v_i) = p_1 \text{ where } p_1 \text{ is the highest prime number such that } p_1 \leq n$$

$$f(v_{i+1}) = p_2 \text{ where } p_2 \text{ is the second highest prime number such that } 1 < p_2 < p_1 \leq n$$

$$f(v_n) = p_3 \text{ where } p_3 \text{ is the third highest prime number such that } 1 < p_3 < p_2 < p_1 \leq n$$

Now label the remaining vertices starting from v_2 consecutively in clockwise direction from the set

$$\{1, 2, \dots, n\} - \{1, p_1, p_2, p_3\}.$$

Then the graph G under consideration admits strongly multiplicative labeling. That is, every cycle with twin chords is strongly multiplicative

Illustration 2.4 Consider a cycle C_7 with twin chords. The labeling is as shown in Fig 2.

Theorem 2.5 Every cycle with triangle $C_n(1, 1, n-5)$ is strongly multiplicative. That is

Proof: Let G be the cycle C_n with triangle. Let e_1, e_2 and e_3 be three chords of cycle C_n . Let v_1 and v_3 be the end vertices of e_1 . Let v_3 and v_{n-1} be the end vertices of e_2 . Let v_{n-1} and v_1 be the end vertices of e_3 .

To define labeling $f: V(G) \rightarrow \{1, 2, \dots, n\}$ we will consider following cases.

Case 1: If n is odd

In this case we define labeling as

$$f(v_i) = 2i - 1; 1 \leq i \leq (n+1)/2$$

$$= 2(n - i + 1); (n+1)/2 < i \leq n$$

Case 2: If n is even

In this case we define labeling as

$$f(v_i) = 2i - 1; 1 \leq i \leq n/2$$

$$= 2(n - i + 1); n/2 < i \leq n$$

In each case described above the graph G under consideration admits strongly multiplicative labeling. That is, cycle with triangle $C_n(1, 1, n - 5)$ is strongly multiplicative.

Remark 2.6 In above Theorem 2.5 we discuss strongly multiplicative labeling for $C_n(1, 1, n - 5)$ but it is also possible to develop strongly multiplicative labeling when three chords make all possible triangle in accordance with Definition 1.3. For the sake of brevity this discussion is not reported here.

Illustration 2.7 Consider a cycle C_{10} with triangle. The labeling is as shown in Fig 3.

Theorem 2.8 The graph obtained by duplication of an arbitrary vertex in cycle C_n admits strongly multiplicative labeling.

Proof: Let C_n be the cycle with n vertices. Let v_k be the vertex of cycle C_n and v_k' is duplication and G be the resultant graph. We define labeling $f: V(G) \rightarrow \{1, 2, \dots, n + 1\}$ as follows.

Case 1: n is odd.

In this case we define labeling f as

$$f(v_k') = 1$$

For $1 \leq i \leq n - k + 1$

$$f(v_{k+i-1}) = 2i + 1; 1 \leq i \leq (n-1)/2$$

$$= 2(n - i + 1); (n-1)/2 < i \leq n.$$

For $n - k + 2 \leq i \leq n$

$$f(v_{k+i-n-1}) = 2i + 1; 1 \leq i \leq (n-1)/2$$

$$= 2(n - i + 1); (n-1)/2 < i \leq n.$$

Case 2: n is even.

In this case we define labeling f as

$$f(v_k') = 1$$

For $1 \leq i \leq n - k + 1$

$$f(v_{k+i-1}) = 2i + 1; 1 \leq i \leq n/2$$

$$= 2(n - i + 1); n/2 < i \leq n.$$

For $n - k + 2 \leq i \leq n$

$$f(v_{k+i-n-1}) = 2i + 1; 1 \leq i \leq n/2$$

$$= 2(n - i + 1); n/2 < i \leq n.$$

In each case described above the graph G under consideration admits strongly multiplicative labeling. That is, the graph obtained by duplication of an arbitrary vertex in cycle C_n admits strongly multiplicative labeling.

Illustration 2.9 Consider a graph G obtained by duplicating a vertex v_1 in cycle C_6 . The labeling is as shown in Fig 4.

Theorem 2.10 The graph resulted from fusion of two vertices v_i and v_j (where $d(v_i, v_j) \geq 3$) in cycle C_n admits strongly multiplicative labeling.

Proof: Let C_n be the cycle with vertices v_1, v_2, \dots, v_n . Let the vertex v_1 be fused with v_m where $m \leq \lceil n/2 \rceil$. Let G be the graph obtained by fusing v_1 and v_m . It is obvious that fusion of two vertices in cycle C_n produces a connected graph which includes two edge-disjoint cycles C_{m-1} and C_{n-m+1} .

We define labeling $f: V(G) \rightarrow \{1, 2, \dots, n-1\}$ as follows.

Case 1: n is odd.

Subcase I: m-1 is an even number and n-m+1 is an odd number.

In this case we define labeling f as

$$\begin{aligned} f(v_1) &= m-2 \\ f(v_i) &= m-2i; 1 < i \leq (m-1)/2 \\ &= 2i-m+1; (m-1)/2 < i \leq m-1 \\ &= 2i-m-2; m < i \leq (m+n)/2 \\ &= 2n-2i+m+1; (m+n)/2 < i \leq n \end{aligned}$$

Subcase II: m-1 is an odd number and n-m+1 is an even number.

In this case we define labeling f as

$$\begin{aligned} f(v_1) &= m-1 \\ f(v_i) &= m-2i+1; 1 < i \leq m/2 \\ &= 2i-m; m/2 < i \leq m-1 \\ &= 2i-m-1; m+1 \leq i \leq (n+m-1)/2 \\ &= 2n-2i+m; (n+m-1)/2 < i \leq n \end{aligned}$$

Case 2: n is even.

Subcase I: m-1 and n-m+1 both are odd numbers.

In this case we define labeling f as

$$\begin{aligned} f(v_1) &= m-1 \\ f(v_i) &= m-2i+1; 1 < i \leq m/2 \\ &= 2i-m; m/2 < i \leq m-1 \\ &= 2i-m-1; m < i \leq (n+m)/2 \\ &= 2n-2i+m; (n+m)/2 < i \leq n \end{aligned}$$

Subcase II: m-1 and n-m+1 both are even numbers.

In this case we define labeling f as

$$\begin{aligned} f(v_1) &= m-2 \\ f(v_i) &= m-2i; 1 < i \leq (m-1)/2 \\ &= 2i-m+1; (m-1)/2 < i \leq m-1 \\ &= 2i-m-2; m < i \leq (n+m+1)/2 \\ &= 2n-2i+m+1; (n+m+1)/2 < i \leq n. \end{aligned}$$

In each possibility described above the graph G under consideration admits strongly multiplicative labeling.

That is, the graph resulted from fusion of two vertices v_i and v_j (where $d(v_i, v_j) \geq 3$) in cycle C_n admits strongly multiplicative labeling.

Remark 2.11

(i) when $m > \lceil n/2 \rceil$ the fusion of two vertices will repeat all the graphs which are already considered earlier.

(ii) when $d(v_i, v_j) < 3$ then fusion yields a graph which is not simple and it is not desirable for strongly multiplicative labeling.

Illustration 2.12 Consider a graph G obtained by fusing vertex v_1 with v_6 in the cycle C_{11} . The labeling is as shown in Fig 5.

3. Concluding Remarks

On account of its diversified applications, labeled graph is the topic of contemporary interest. We have derived five new results on strongly multiplicative labeling. It is possible to investigate similar results for other graph families. There is a scope to derive analogous results in the context of different graph labeling techniques.

References

Beineke, L. W. and Hegde, S. M. (2001). Strongly Multiplicative Graphs, *Discuss. Math. Graph Theory*, 21, 63-75.
 Gallian, J. A. (2009). A dynamic survey of graph labeling, *The Electronic Journal of Combinatorics*, 16, #DS 6.
 Harary, F. (1972). *Graph Theory*, Massachusetts, Addison Wesley.

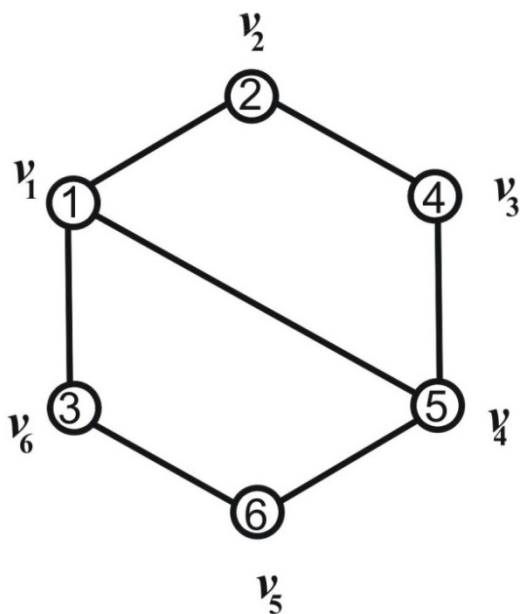


Figure 1. Cycle C_6 with one chord and its strongly multiplicative labeling

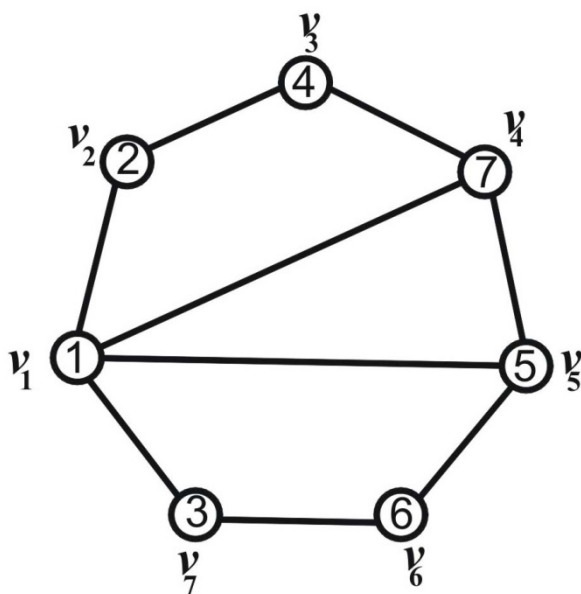


Figure 2. Cycle C_7 with twin chords and its strongly multiplicative labeling

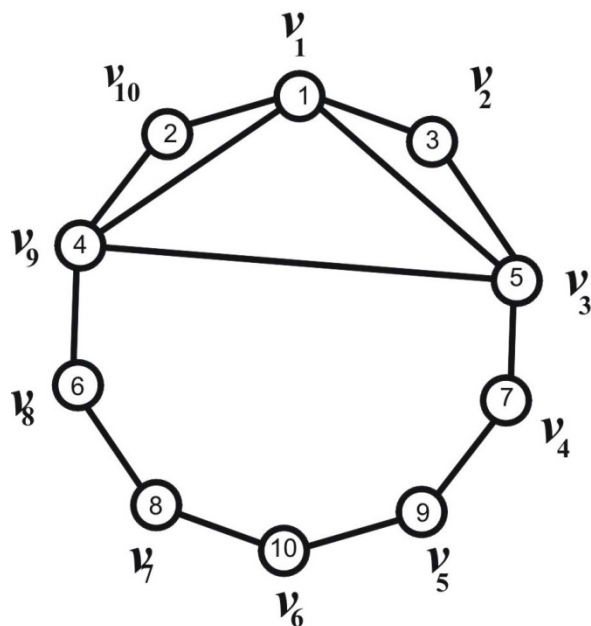


Figure 3. Cycle C_{10} with triangle and its strongly multiplicative labeling

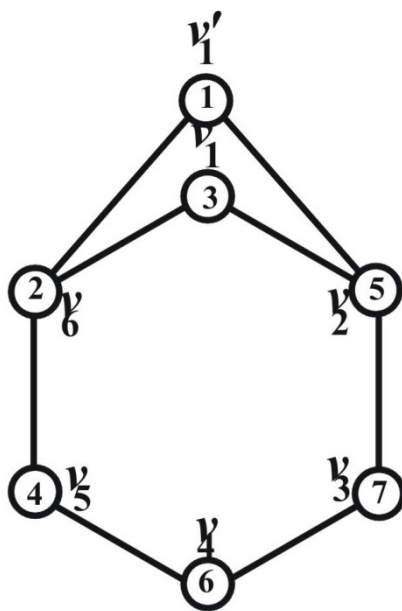


Figure 4. Duplication of a vertex v_1 in Cycle C_6 and its strongly multiplicative labeling

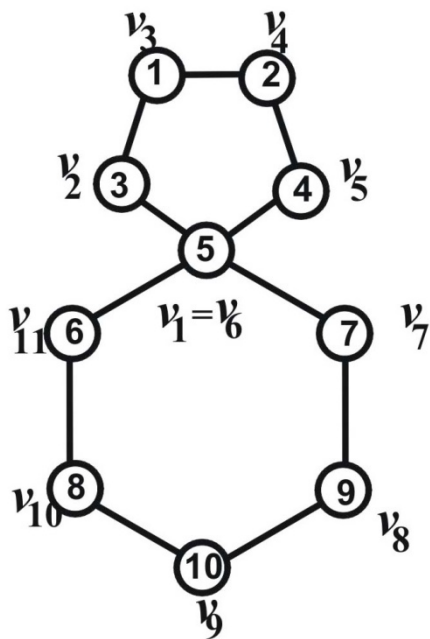


Figure 5. Fusion of v_1 with v_6 in Cycle C_{11} and its strongly multiplicative labeling

Equivalent Resistance of $5 \times n$ -laddered Network

Xingpeng Yang, Xingcheng Dong, Zhongyong Chen & Yingkai Liu (Corresponding author)

Department of Physics, Yunnan Normal University

298 One two one street, Kunming 650092, Yunnan Province, China

&

Center of Super-Diamond and Advanced Films (COSDAF), City University of Hong Kong

Tat Chee Avenue, Knowloon, Hong Kong

Tel: 86-138-8863-4539 E-mail: ykliu@cityu.edu.hk

Zhang Xiong (Corresponding author)

Department of Physics, Yunnan Normal University

298 One two one street, Kunming 650092, Yunnan Province, China

Tel: 86-871-551-6057 E-mail: ynzx@yeah.net

This work is supported in part by National Science Foundation of China through Grant (10764005), Natural Science Foundation of Yunnan Province (06A0025Q, 2007PY01-41), and from the Excellent Talent Supporting Project in the New Century of Chinese Education Ministry(NCET-08-0926).

Abstract

The basic structure of $5 \times n$ -step network was studied by matrix transform method. Thus, the resistances of both the infinite and finite network were obtained. In addition, the resistances of the finite $5 \times n$ -laddered network were measured experimentally by NI Multisim 10 when n equals to positive integer such as one,two,three ... ,and so on. It is found that the measured values of the equivalent resistances of finite $5 \times n$ -laddered networks are consistent with the calculated ones.

Keywords: Equivalent Resistance, $5 \times n$ -laddered Network, NI Multisim 10, Kirchhoff's current law

1. Introduction

Equivalent Resistance of $n \times n$ -laddered network is a general problem in introductory physics. With the development of communication technology, network technologies have become more and more important in many fields such as resistance network and self-control systems. Lots of actual network technological problems can also be simulated by resistance network. This stimulates the research of network's resistance. Up to now, studies have been devoted to the equivalent resistance of different resistance networks,¹⁻⁹ but those results have no experimental foundations. Unfortunately, some results are even wrong.³ Therefore, it is necessary to develop an effective method (matrix transform) to calculate the equivalent resistance of resistance network.

Matrix transform is commonly used in mathematics and theoretical physics, especially in quantum physics. However, students trained in the algebra-based physics course are used to matrix transform only in linear equations, but not in mechanics,electromagnetism,and difference equations. In this paper, we will construct difference equations of closed circuits and find relation of matrix transform and difference equations to calculate the equivalent resistance of $5 \times n$ -laddered network. Furthermore, we measured its resistance by using NI Multisim 10 simulation software. Agreement is achieved between the measured values and the theoretical ones.

2. The Differential Equation Model on Current

2.1 The development of the differential equation on current

Figure 1 is a schematic diagram of $5 \times n$ -laddered resistance network ($n \rightarrow \infty$). The equivalent resistance of between **a** and **f** nodes was assumed to be R_{af} .

Suppose each resistor has the same value r . The direction of the steady current is from nodes **f** to **a** as shown in Fig 1. Each branch current and its flowing direction were marked in Fig. 2, which is a part of $5 \times n$ -laddered resistance network (hereafter denoted as $5 \times n$ -laddered resistance sub-networks). Assume the currents of the

horizontal resistances in the second rank are $I_{ak}, I_{bk}, I_{ck}, I_{dk}, I_{ek},$ and I_{fk} ($1 \leq k \leq n$) respectively as shown Fig.

2. Accordingly, the currents of the vertical resistance are $I_k, I'_k, I''_k, I'''_k,$ and I''''_k respectively.

Kirchhoff's current law¹⁰ is used for the all nodes in the second rank. Differential current equations were obtained as follows:

$$I_{ak} - I_{ak-1} = -I_k \tag{1}$$

$$I_k - I'_k = I_{bk} - I_{bk-1} \tag{2}$$

$$I'_k - I''_k = I_{ck} - I_{ck-1} \tag{3}$$

$$I''_k - I'''_k = I_{dk-1} - I_{dk} \tag{4}$$

$$I'''_k - I''''_k = I_{ek-1} - I_{ek} \tag{5}$$

In terms of the symmetry, we obtain the following equations

$$I_{ak} = I_{fk}; I_{bk} = I_{ek}; I_{ck} = I_{dk}; I_k = I''''_k; I'_k = I'''_k \tag{6}$$

Trace all the meshes in the (k-1)-th rank and apply Kirchhoff's voltage law (KVL).¹⁰

$$I_k r + I_{ak-1} r - I_{k-1} r - I_{bk-1} r = 0 \tag{7}$$

$$I'_k r + I_{bk-1} r - I_{ck-1} r - I_{k-1} r = 0 \tag{8}$$

$$I''_k r + I_{ck-1} r + I_{dk-1} r - I_{k-1} r = 0 \tag{9}$$

In the same manner, trace the all meshes in the k-th rank and apply KVL.

$$I_{ak} r + I_{k+1} r - I_k r - I_{bk} r = 0 \tag{10}$$

$$I_{bk} r + I'_{k+1} r - I_{ck} r - I'_k r = 0 \tag{11}$$

$$I_{ck} r + I''_{k+1} r + I_{dk} r - I''_k r = 0 \tag{12}$$

Eq. (9) subtracted from Eq. (12) gives

$$(I_{ck} - I_{ck-1}) + (I''_{k+1} + I''_{k-1}) + (I_{dk} - I_{dk-1}) - (I''_k - I''_{k-1}) = 0$$

Considering $I_{ck} = I_{dk}, I_{ck-1} = I_{dk-1},$ we get

$$2(I_{ck} - I_{ck-1}) + I''_{k+1} + I''_{k-1} = 0 \tag{13}$$

Substituting Eq. (3) into Eq. (13) yields

$$2(I'_k - I''_k) + I''_{k+1} + I''_{k-1} = 0 \tag{14}$$

Eq. (14) is simplified as this

$$I''_{k+1} + I''_{k-1} = 4I''_k - 2I'_k \tag{15}$$

Eq. (11) subtracted from Eq. (8) gives,

$$I_{bk} + I'_{k+1} - I_{ck} - I'_k - I'_{k-1} - I_{bk-1} + I_{ck-1} + I'_{k-1} = 0 \tag{16}$$

Substituting Eqs. (2),(3) into Eq. (16) produces

$$I'_{k+1} - I'_k + I_k - I'_k - I'_k + I'_{k-1} - I'_k + I''_k = 0 \tag{17}$$

Eq. (17) can further be simplified as

$$I'_{k+1} + I'_{k-1} = 4I'_k - I_k - I''_k \tag{18}$$

And then Eq. (10) subtracted from Eq. (7) gives,

$$I_{ak} + I_{k+1} - I_k - I_{bk} - I_k - I_{ak-1} + I_{k-1} + I_{bk-1} = 0 \tag{19}$$

Similarly, substituting Eqs. (1), (2) into Eq. (19) yields

$$I_{k+1} + I_{k-1} = 4I_k - I'_k \tag{20}$$

Eqs. (15), (18), and (20) can be written in matrix form, therefore we get

$$\begin{bmatrix} I_{k+1} \\ I'_{k+1} \\ I''_{k+1} \end{bmatrix} = \begin{bmatrix} 4 & -1 & 0 \\ -1 & 4 & -1 \\ 0 & -2 & 4 \end{bmatrix} \begin{bmatrix} I_k \\ I'_k \\ I''_k \end{bmatrix} - \begin{bmatrix} I_{k-1} \\ I'_{k-1} \\ I''_{k-1} \end{bmatrix} \tag{21}$$

Eq. (21) is differential equation model of current parameters. We provide a new method to solve such problems by using matrix transform method and constructing new differential equations model.

Multiply both sides of the matrix (21) by three order undetermined matrix on the left, we have

$$\begin{bmatrix} \lambda_1 & \lambda_4 & 1 \\ \lambda_2 & \lambda_5 & 1 \\ \lambda_3 & \lambda_6 & 1 \end{bmatrix} \begin{bmatrix} I_{k+1} \\ I'_{k+1} \\ I''_{k+1} \end{bmatrix} = \begin{bmatrix} \lambda_1 & \lambda_4 & 1 \\ \lambda_2 & \lambda_5 & 1 \\ \lambda_3 & \lambda_6 & 1 \end{bmatrix} \begin{bmatrix} 4 & -1 & 0 \\ -1 & 4 & -1 \\ 0 & -2 & 4 \end{bmatrix} \begin{bmatrix} I_k \\ I'_k \\ I''_k \end{bmatrix} - \begin{bmatrix} \lambda_1 & \lambda_4 & 1 \\ \lambda_2 & \lambda_5 & 1 \\ \lambda_3 & \lambda_6 & 1 \end{bmatrix} \begin{bmatrix} I_{k-1} \\ I'_{k-1} \\ I''_{k-1} \end{bmatrix} \tag{22}$$

Assuming the existence of constants t_1, t_2, t_3 , and let the following matrix equation be correct.

$$\begin{bmatrix} \lambda_1 & \lambda_4 & 1 \\ \lambda_2 & \lambda_5 & 1 \\ \lambda_3 & \lambda_6 & 1 \end{bmatrix} \begin{bmatrix} 4 & -1 & 0 \\ -1 & 4 & -1 \\ 0 & -2 & 4 \end{bmatrix} = \begin{bmatrix} t_1 & 0 & 0 \\ 0 & t_2 & 0 \\ 0 & 0 & t_3 \end{bmatrix} \begin{bmatrix} \lambda_1 & \lambda_4 & 1 \\ \lambda_2 & \lambda_5 & 1 \\ \lambda_3 & \lambda_6 & 1 \end{bmatrix} \tag{23}$$

Expand the matrix (23) and simplify, we achieve

$$\begin{cases} 4\lambda_1 - \lambda_4 = t_1\lambda_1 \\ -\lambda_1 - 4\lambda_4 - 2 = t_1\lambda_4 \\ -\lambda_4 + 4 = t_1 \end{cases} \begin{cases} 4\lambda_2 - \lambda_5 = t_2\lambda_2 \\ -\lambda_2 - 4\lambda_5 - 2 = t_2\lambda_5 \\ -\lambda_5 + 4 = t_2 \end{cases} \begin{cases} 4\lambda_3 - \lambda_6 = t_3\lambda_3 \\ -\lambda_3 - 4\lambda_6 - 2 = t_3\lambda_6 \\ -\lambda_6 + 4 = t_3 \end{cases}$$

The solutions of the above equations are

$$\lambda_1 = 1, \quad \lambda_2 = 1, \quad \lambda_3 = 1, \tag{24}$$

$$\lambda_4 = \sqrt{3}, \quad \lambda_5 = -\sqrt{3}, \quad \lambda_6 = \sqrt{3}, \tag{25}$$

$$t_1 = 4 - \sqrt{3}, \quad t_2 = 4 + \sqrt{3}, \quad t_3 = 4 - \sqrt{3} \tag{26}$$

Substitute Eqs. (23), (24), (25), and (26) into Eq. (16), hence the matrix equation can be written as

$$\begin{bmatrix} I_{k+1} + \sqrt{3}I'_{k+1} + I''_{k+1} \\ I_{k+1} - \sqrt{3}I'_{k+1} + I''_{k+1} \\ I_{k+1} + \sqrt{3}I'_{k+1} + I''_{k+1} \end{bmatrix} = \begin{bmatrix} t_1 & 0 & 0 \\ 0 & t_2 & 0 \\ 0 & 0 & t_3 \end{bmatrix} \begin{bmatrix} I_k + \sqrt{3}I'_k + I''_k \\ I_k - \sqrt{3}I'_k + I''_k \\ I_k + \sqrt{3}I'_k + I''_k \end{bmatrix} - \begin{bmatrix} I_{k-1} + \sqrt{3}I'_{k-1} + I''_{k-1} \\ I_{k-1} - \sqrt{3}I'_{k-1} + I''_{k-1} \\ I_{k-1} + \sqrt{3}I'_{k-1} + I''_{k-1} \end{bmatrix} \tag{27}$$

Let $I_k + \sqrt{3}I'_k + I''_k = x_k$, Simplify the matrix (23), we hold

$$x_{k+1} = t_1x_k - x_{k-1} \tag{28}$$

where t_1 is the known constant, based on the definition of differential equation, Eq. (28) is obviously second order linear differential equation with fixed coefficients. Let $x_k = x^k$, substituting it into Eq. (28) yields the following characteristic equation

$$x^2 = t_1 x - 1 \quad (29)$$

Note that for $I_k - \sqrt{3}I_k' + I_k'' = y_k$, and simplify the matrix (27), we get

$$y_{k+1} = t_2 y_k - y_{k-1} \quad (30)$$

Let $y_k = y^k$, substitute it into Eq. (30), we also obtain the following characteristic equation.

$$y^2 = t_2 y - 1 \quad (31)$$

Similarly, we have

$$z^2 = t_3 z - 1 \quad (32)$$

Therefore, the characteristic equation of differential equation is

$$\begin{bmatrix} x^2 \\ y^2 \\ z^2 \end{bmatrix} = \begin{bmatrix} t_1 & 0 & 0 \\ 0 & t_2 & 0 \\ 0 & 0 & t_3 \end{bmatrix} \begin{bmatrix} x \\ y \\ z \end{bmatrix} - \begin{bmatrix} 1 \\ 1 \\ 1 \end{bmatrix} \quad (33)$$

Suppose the roots of the equation with respect to x are α and β , the roots of the equation with respect to y are γ and δ , and those of the equation with respect to z are μ and ν , the solutions of characteristic Eq. (33) are as follows:

$$\begin{bmatrix} \alpha \\ \beta \end{bmatrix} = \begin{bmatrix} \frac{1}{2}(4 - \sqrt{3} + \sqrt{15 - 8\sqrt{3}}) \\ \frac{1}{2}(4 - \sqrt{3} - \sqrt{15 - 8\sqrt{3}}) \end{bmatrix} \quad (34)$$

$$\begin{bmatrix} \gamma \\ \delta \end{bmatrix} = \begin{bmatrix} \frac{1}{2}(4 + \sqrt{3} + \sqrt{15 + 8\sqrt{3}}) \\ \frac{1}{2}(4 + \sqrt{3} - \sqrt{15 + 8\sqrt{3}}) \end{bmatrix} \quad (35)$$

$$\begin{bmatrix} \mu \\ \nu \end{bmatrix} = \begin{bmatrix} \frac{1}{2}(4 - \sqrt{3} + \sqrt{15 - 8\sqrt{3}}) \\ \frac{1}{2}(4 - \sqrt{3} - \sqrt{15 - 8\sqrt{3}}) \end{bmatrix} \quad (36)$$

Due to $x_{k+1} = t_1 x_k - x_{k-1}$, and $\alpha + \beta = 4 - \sqrt{3} = t_1$, $\alpha \cdot \beta = 1$, hence

$$x_{k+1} = (\alpha + \beta)x_k - \alpha \cdot \beta \cdot x_{k-1} \quad (37)$$

Rewriting x_{k+1} expression and transposing yields

$$\begin{aligned} x_{k+1} - \alpha x_k &= \beta(x_k - \alpha \cdot x_{k-1}) = \beta^{k-1}(x_2 - \alpha x_1) \\ x_{k+1} - \beta x_k &= \alpha(x_k - \beta \cdot x_{k-1}) = \alpha^{k-1}(x_2 - \beta x_1) \end{aligned} \quad (38)$$

From the matrix equation we obviously see that $\alpha \neq \beta$, and then subtracting Eq. (38) from Eq. (37) gives

$$x_k = \frac{1}{\alpha - \beta} [(x_2 - \beta x_1)\alpha^{k-1} - (x_2 - \alpha x_1)\beta^{k-1}] \quad (39)$$

In the same manner, we get

$$y_k = \frac{1}{\gamma - \delta} [(y_2 - \delta y_1) \gamma^{k-1} - (y_2 - \gamma y_1) \delta^{k-1}] \tag{40}$$

$$z_k = \frac{1}{\mu - \nu} [(z_2 - \nu z_1) \mu^{k-1} - (z_2 - \mu z_1) \nu^{k-1}] \tag{41}$$

Eqs. (39), (40), and (41) can be written in matrix form

$$\begin{bmatrix} x_k \\ y_k \\ z_k \end{bmatrix} = \begin{bmatrix} \frac{1}{\alpha - \beta} [(x_2 - \beta x_1) \alpha^{k-1} - (x_2 - \alpha x_1) \beta^{k-1}] \\ \frac{1}{\gamma - \delta} [(y_2 - \delta y_1) \gamma^{k-1} - (y_2 - \gamma y_1) \delta^{k-1}] \\ \frac{1}{\mu - \nu} [(z_2 - \nu z_1) \mu^{k-1} - (z_2 - \mu z_1) \nu^{k-1}] \end{bmatrix} \tag{42}$$

where $x_k = I_k + \sqrt{3}I'_k + I''_k$, $y_k = I_k - \sqrt{3}I'_k + I''_k$, $z_k = I_k + \sqrt{3}I'_k + I''_k$ ($k=1, 2, 3, \dots$). Characteristic equation (42) gives the current properties of vertical resistance r in any sub-network.

2.2 The Properties of Boundary Current

When the current flows toward node **a** and flows away from node **b** in Fig.1, applying the current continuity equation, we have

$$\sum_{i=1}^{n+1} I_i = I, \quad \sum_{i=1}^{n+1} I'_i = I, \quad \sum_{i=1}^{n+1} I''_i = I \tag{43}$$

If we consider Eq. (43), summation of Eq. (42) ($k=1, 2, 3, \dots, n+1$) gives

$$(x_2 - \beta x_1) \frac{1 - \alpha^{n+1}}{1 - \alpha} - (x_2 - \alpha x_1) \frac{1 - \beta^{n+1}}{1 - \beta} = (\alpha - \beta)(1 + \sqrt{3} + 1)I \tag{44}$$

$$(y_2 - \delta y_1) \frac{1 - \gamma^{n+1}}{1 - \gamma} - (y_2 - \gamma y_1) \frac{1 - \delta^{n+1}}{1 - \delta} = (\gamma - \delta)(1 - \sqrt{3} + 1)I \tag{45}$$

$$(z_2 - \nu z_1) \frac{1 - \mu^{n+1}}{1 - \mu} - (z_2 - \mu z_1) \frac{1 - \nu^{n+1}}{1 - \nu} = (\mu - \nu)(1 + \sqrt{3} + 1)I \tag{46}$$

Up to now, we obtain differential equations model of current parameters under boundary conditions by analyzing 5×n-laddered resistance network. Based on Kirchhoff's current law and mesh analysis,¹¹ we also find the following formula from Fig. 3,

$$I_{a1} = I - I_1 \tag{47}$$

$$I_{b1} = I_1 - I'_1 \tag{48}$$

$$I_{c1} = I'_1 - I''_1 \tag{49}$$

Due to the symmetry, we have

$$I_{c1} = I_{d1} \tag{50}$$

Applying Kirchhoff's voltage law to the first loop produces

$$I_2 r + I_{a1} r - I_{b1} r - I_1 r = 0 \tag{51}$$

$$I'_2 r + I_{b1} r - I_{c1} r - I'_1 r = 0 \tag{52}$$

$$I''_2 r + I_{c1} r - I''_1 r + I_{d1} r = 0 \tag{53}$$

Substitute Eqs. (47), (48), (49), and (50) into Eqs. (51), (52), and (53), and then simplify them, we obtain

$$I_2 = 3I_1 - I - I_1', \quad I_2' = 3I_1' - I_1'' - I_1, \quad I_2'' = 3I_1'' - 2I_1' \quad (54)$$

Eq. (54) can be written in matrix form, consequently the differential equations model of $5 \times n$ -laddered resistance network under boundary conditions are obtained.

$$\begin{bmatrix} I_2 \\ I_2' \\ I_2'' \end{bmatrix} = \begin{bmatrix} 3 & -1 & 0 \\ -1 & 3 & -1 \\ 0 & -2 & 3 \end{bmatrix} \begin{bmatrix} I_1 \\ I_1' \\ I_1'' \end{bmatrix} - \begin{bmatrix} I \\ 0 \\ 0 \end{bmatrix} \quad (55)$$

For Eq. $x_2 = I_2 + \sqrt{3}I_2' + I_2''$, substitute Eq. (54) into it and simplify, we achieve

$$x_2 = (3 - \sqrt{3})(I_1'' + \sqrt{3}I_1' + I_1) - I \quad (56)$$

In the same manner for $x_1 = I_1 + \sqrt{3}I_1' + I_1''$, and $\alpha + \beta = 4 - \sqrt{3}$, Eq. (56) can be expressed as

$$x_2 = (\alpha + \beta - 1)x_1 - I \quad (57)$$

Similarly, we have

$$y_2 = (\gamma + \delta - 1)y_1 - I \quad (58)$$

$$z_2 = (\mu + \nu - 1)z_1 - I \quad (59)$$

Eqs. (57), (58), (59) can be written in matrix form

$$\begin{bmatrix} x_2 \\ y_2 \\ z_2 \end{bmatrix} = \begin{bmatrix} (\alpha + \beta - 1)x_1 - I \\ (\gamma + \delta - 1)y_1 - I \\ (\mu + \nu - 1)z_1 - I \end{bmatrix} \quad (60)$$

Substitute Eq. (60) into Eqs. (44), (45), (46), and simplify them, we get

$$\begin{bmatrix} x_1 \\ y_1 \\ z_1 \end{bmatrix} = \begin{bmatrix} (1 + \sqrt{3} + 1)\left(1 - \frac{\alpha^n - \beta^n}{\alpha^{n+1} - \beta^{n+1}}\right)I \\ (1 - \sqrt{3} + 1)\left(1 - \frac{\gamma^n - \delta^n}{\gamma^{n+1} - \delta^{n+1}}\right)I \\ (1 + \sqrt{3} + 1)\left(1 - \frac{\mu^n - \nu^n}{\mu^{n+1} - \nu^{n+1}}\right)I \end{bmatrix} \quad (61)$$

where $x_1 = I_1 + \sqrt{3}I_1' + I_1''$, $y_1 = I_1 - \sqrt{3}I_1' + I_1''$, $z_1 = I_1 + \sqrt{3}I_1' + I_1''$, therefore, these matrix equations give the current properties of $5 \times n$ -laddered resistance network under boundary conditions.

2.3 General Properties of the Equivalent Resistance

2.3.1 The equivalent resistance $R_{af}(n)$ in finite network

From the above discussion, we obtained

$$I_1 + \sqrt{3}I_1' + I_1'' = x_1, \quad I_1 - \sqrt{3}I_1' + I_1'' = y_1, \quad I_1 + \sqrt{3}I_1' + I_1'' = z_1$$

These formulas give the relationship of between $I_1, I_1',$ and I_1'' . Therefore we easily solve I_1, I_1', I_1'' with respect to $x_1, y_1,$ and z_1 .

$$I_1' = \frac{1}{2\sqrt{3}}(x_1 - y_1); \quad I_1 = \frac{1}{\sqrt{5} + 1}(x_1 + y_1); \quad I_1 + I_1'' = \frac{1}{2}(x_1 + y_1)$$

Substitute I_1', I_1 and $I_1 + I_1''$ into $(2I_1 + 2I_1' + I_1'')$ yields

$$\begin{aligned}
 &2I_1 + 2I_1' + I_1'' = \\
 &= \frac{3\sqrt{3} + \sqrt{15} + 2\sqrt{5} + 2}{2(\sqrt{15} + \sqrt{3})} (2 + \sqrt{3}) \left(1 - \frac{\alpha^n - \beta^n}{\alpha^{n+1} - \beta^{n+1}}\right)I + \frac{3\sqrt{3} + \sqrt{15} - 2\sqrt{5} - 2}{2(\sqrt{15} + \sqrt{3})} (2 - \sqrt{3}) \\
 &\left(1 - \frac{\gamma^n - \delta^n}{\gamma^{n+1} - \delta^{n+1}}\right)I \\
 &= \frac{8\sqrt{3} + 4\sqrt{15} + 7\sqrt{5} + 13}{2(\sqrt{15} + \sqrt{3})} \left(1 - \frac{\alpha^n - \beta^n}{\alpha^{n+1} - \beta^{n+1}}\right)I + \frac{8\sqrt{3} + 4\sqrt{15} - 7\sqrt{5} - 13}{2(\sqrt{15} + \sqrt{3})} \left(1 - \frac{\gamma^n - \delta^n}{\gamma^{n+1} - \delta^{n+1}}\right)I \quad (62)
 \end{aligned}$$

From Fig. 3, we have

$$U_{af} = (2I_1 + 2I_1' + I_1'')r$$

Applying Ohm's law yields

$$R_{af} = U_{af} / I = r(2I_1 + 2I_1' + I_1'') / I$$

Therefore, we find

$$\begin{aligned}
 \frac{R_{af}(n)}{r} &= \frac{8\sqrt{3} + 4\sqrt{15}}{\sqrt{15} + \sqrt{3}} - \frac{8\sqrt{3} + 4\sqrt{15} + 7\sqrt{5} + 13}{2(\sqrt{15} + \sqrt{3})} \left(\frac{\alpha^n - \beta^n}{\alpha^{n+1} - \beta^{n+1}}\right) - \frac{8\sqrt{3} + 4\sqrt{15} - 7\sqrt{5} - 13}{2(\sqrt{15} + \sqrt{3})} \\
 &\left(\frac{\gamma^n - \delta^n}{\gamma^{n+1} - \delta^{n+1}}\right) \quad (63)
 \end{aligned}$$

2.3.2 The equivalent resistance $R_{af}(\infty)$ in infinite network

As n tends to infinity, Fig. 1 becomes a $5 \times n$ -laddered resistance network. From Eqs. (29), (30), and (31), we easily obtain that

$$0 < \frac{\alpha}{\beta} = \frac{\frac{1}{2}(4 - \sqrt{3} + \sqrt{15 - 8\sqrt{3}})}{\frac{1}{2}(4 - \sqrt{3} + \sqrt{15 - 8\sqrt{3}})} < 1, \quad 0 < \frac{\gamma}{\delta} = \frac{\frac{1}{2}(4 + \sqrt{3} + \sqrt{15 + 8\sqrt{3}})}{\frac{1}{2}(4 + \sqrt{3} + \sqrt{15 + 8\sqrt{3}})} < 1,$$

Consequently, we have

$$\lim_{n \rightarrow \infty} \left(\frac{\alpha}{\beta}\right)^n = 0, \quad \lim_{n \rightarrow \infty} \left(\frac{\gamma}{\delta}\right)^n = 0 \quad (64)$$

Eq. (63) is taken limit, and then applying the formula (64) gives

$$\frac{R_{af}(\infty)}{r} = \frac{8\sqrt{3} + 4\sqrt{15}}{\sqrt{15} + \sqrt{3}} - \frac{8\sqrt{3} + 4\sqrt{15} + 7\sqrt{5} + 13}{2(\sqrt{15} + \sqrt{3})} \beta - \frac{8\sqrt{3} + 4\sqrt{15} - 7\sqrt{5} - 13}{2(\sqrt{15} + \sqrt{3})} \delta \quad (65)$$

where $\beta = \frac{1}{2}(4 - \sqrt{3} - \sqrt{15 - 8\sqrt{3}})$, $\delta = \frac{1}{2}(4 + \sqrt{3} - \sqrt{15 + 8\sqrt{3}})$.

Eq. (65) is a general expression which denotes the equivalent resistance R_{af} of $5 \times n$ -laddered resistance network between nodes a and f, and R_{af} has a limited value in this case.

2.3.3 Measurements of $R_{af}(n)$ by Simulation Experiments

The equivalent resistance R_{af} of $5 \times n$ -laddered resistance network is measured by NI Multisim 10 when n is a

series of positive integer. In the meantime, the equivalent resistance R_{af} of $5 \times n$ -laddered resistance network is calculated from Eq. (63). The relationship curves of the equivalent resistance R_{af} versus n are plotted in Fig. 4. It is found that agreement is achieved between the experimental values and the theoretical ones. These results indicate that the equivalent resistances of $n \times n$ -laddered resistance network were not only calculated by matrix transform and but also the calculated results are reliable.

4. Conclusion

General formula $\frac{R_{af}(\infty)}{r}$ and $\frac{R_{af}(n)}{r}$ for $5 \times n$ -laddered resistance network in infinite and finite networks are achieved by the matrix transform method to solve a set of differential equations. In addition, the equivalent resistance R_{af} of $5 \times n$ -laddered resistance network is calculated from Eq. (63). Moreover, the equivalent resistance R_{af} is measured by NI Multisim 10 when n is a series of positive integer. The result exhibits that the theoretical values are consistent with the experimental ones for the equivalent resistance R_{af} of $5 \times n$ -laddered resistance network. This study also reveals that the matrix transform method may be extended to calculate the equivalent resistances of $n \times n$ -step resistance network.

References

- Zhang, D. T. (2008). Effective cultivating migration ability of students. *Phys Teaching*, vol.30, pp.37-38, Feb. 2008.
- Cao, X. H., & Tan, Z. Z. (2008). A general study on equivalent resistance of $2 \times N$ -laddered network. *College Phys*, vol.27, pp.25-26, May 2008
- Tan, Z. Z., & Luo, D. F. (2004). The study on the Diagonal Equivalent Resistance of $2 \times N$ Ordered Network, *Guangxiwuli*, vol.25, pp. 43-46, May 2004.
- Li, Y. A. (2002). Net work analysis on equivalent resistance of a ladder-shaped network *College Phys*, vol. 21, pp.9-10, Dec. 2002;. Li, Y. A. (2003). Study on equivalent resistance of a ladder-shaped network. *College Phys*, vol. 22, pp.9-10, March 2003.
- YLi Y A . (2003). The restudy is on equivalent resistance of ladder-shaped network *College Phys*, vol. 22, pp.12-14, Oct. 2003.
- Tan, Z. Z. (2004). Study on the Equivalent resistance of $2 \times N$ -laddered network. *J. Hebei Normal University (Natural Science Edition)*, vol. 28, pp. 258-262, March 2004; Tan, Z. Z. (2004). Restudy on the Equivalent resistance of $2 \times N$ -laddered network. *J. Hebei Normal University (Natural Science Edition)*, vol.28, pp.480-482, May 2004.
- Carpentieri, E. (1996). Model characterizes transmission – line transformers. *Microwaves & RF*, vol.35, pp.73-80, Nov. 1996
- Lu, J. L., & Tan, Z. Z. (2001). A general study on equivalent resistance of ladder-shaped network. *College Phys*, vol.20, pp.26-28, Oct. 2001.
- Shao, J. X. (2006). The General Formula of the Equivalent Resistance of Ladder Type Network. *Phys and Eng.*, vol.16, 29-33, Apr. 2006
- Halliday, D, Resnick R., & Walker, J. (2001). *Fundamentals of Physics*, 6-th ed (John & Sons Inc.) pp.677-785.
- Nilsson, J. W., & Riedel, S. A. (2000). *Introduction to Pspice Manual—Electric circuits using or H CAD release 9.1*. The fourth edition (Prentice-Hill).

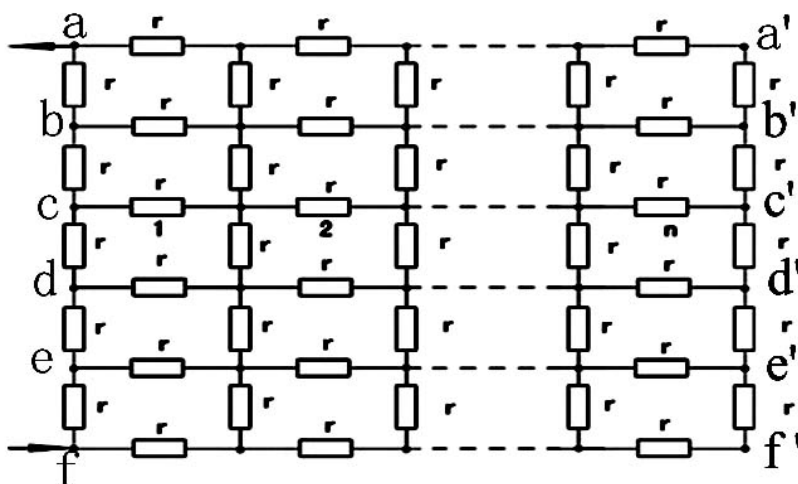


Figure 1. Schematic diagram of 5×n-laddered resistance network

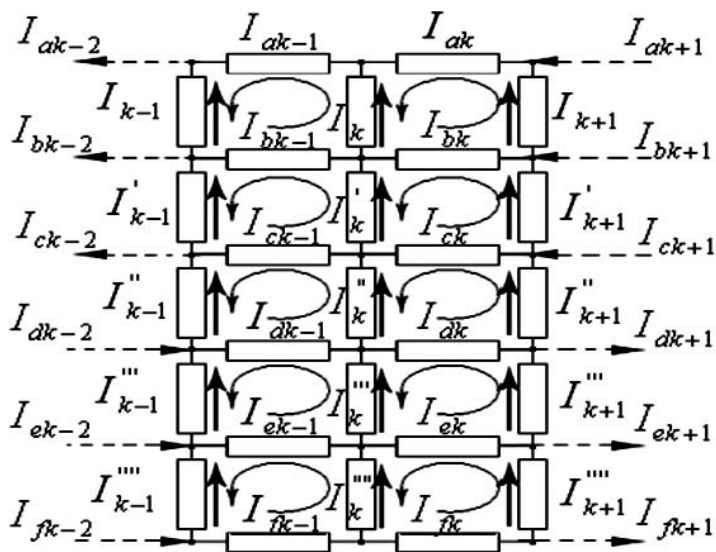


Figure 2. Schematic diagram of 5×n-laddered resistance sub-networks

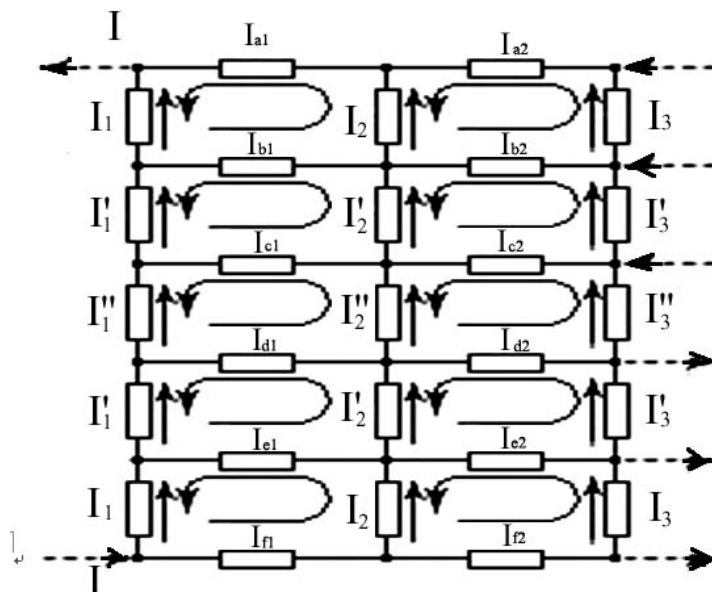


Figure 3. Current parameters of the network under boundary conditions

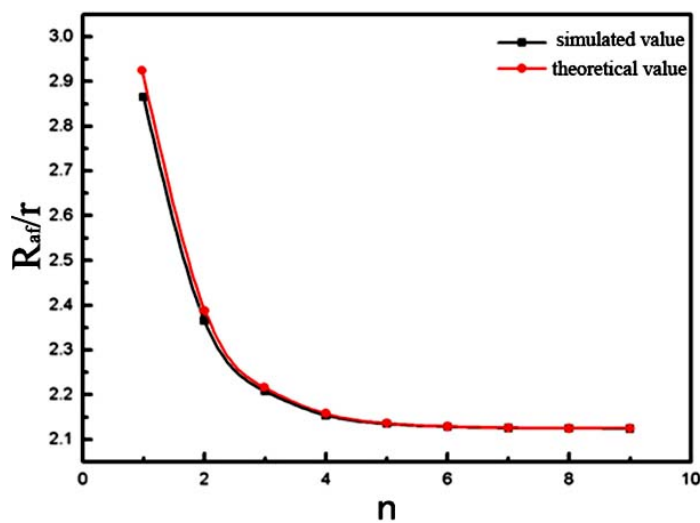


Figure 4. The relationship curves of the equivalent resistance R_{af} and n of $5 \times n$ -laddered resistance network

Analysis on Essence, Types and Characteristics of Leisure Sports

Jie Min & Houzhong Jin

School of sports economics and management, Central University of Finance and Economics

Beijing 100081, China

Funded by Beijin philosophical social science project (09BaZh126).

Abstract

Leisure Sports are freeform, voluntary and non-competitive activities, which aim to regulate the mental state of people. Leisure Sports are not a specific sport project but a kind of social existence form of sport. Leisure sports projects are all-inclusive, which are generally divided into four types: sports recreational activities, sports fitness activities, sports adventure activities and sports social activities. They are characterized by the diversity of sports forms, the epochal character of sports contents, the voluntary participation in sports groups and the complexity of sports levels.

Keywords: Leisure sports, Essence, Types, Characteristics, Analysis

Leisure sports are the production of modern society, which change with the change of society and develop with the development of economy. Especially, the advancement of modern scientific technology improves the social productive force significantly, which releases people from heavy work and short the time of people participating in the social necessary work, so people have more idle time. Meanwhile, the ways to spend spare time are more and more with the advancement of society and sports activities have been a choice to spend spare time for people, which is emphasized with the development of society. From the development of leisure sports of modern developed countries and China in these years, participating in the leisure sport activities has become one indispensable life style for the people in these countries.

1. The contents of leisure sports

1.1 The concept of leisure

When leisure sports are discussed, the concept of leisure should be defined clearly firstly. Leisure is from the English word, "leisure", whose concept is: living in a life of ease (<Longman English-Chinese dictionary>) and the meaning of the word leisure in <Dictionary of Modern Chinese> is: having a rest or living a life of vacancy. From the explanations of leisure in English and Chinese, we can find that leisure means living a life of easy, which should also be said that is one life type or one part of life type.

So, what are the understandings about leisure in the West and the East?

1.1.1 The understanding about leisure for Europe and America

In ancient Greece, Plato described leisure as an ideal and believed that the governing class was not annoyed by real life and all the time was spent on thinking deeply about the truth, the good and the beautiful to obtain happy results and make it more perfect. Aristotle held the opinion that leisure was the state of not needing to consider the problem of survival and only people in their leisure time are really happy and fully mature people. From the explanation about leisure of ancient western sages, we can see that in the ancient west leisure is the affaire of wealthy people, who needed not to consider survival and living problems, and the life of ease based on the abundant substances, which was the life style of very few people and dreamed of by the most poor.

In the modern west, an American scholar Jeffery Gobbi thinks that, "leisure is a life which is released from the outer pressure of civilization and substance environment and relatively free." (Jeffery, Gobbi. 2000). An French scholar De Grazia points that, "leisure should be an quality of feeling." (Hu, Xiaoming and Yu, Chonggan. 2004). Pieper points that, "leisure is an attitude of heart and spirit and not an result of outer factor." (Hu, Xiaoming and Yu, Chonggan. 2004) From the explanation about leisure of modern western scholars, it is found that leisure is a constituent part of human life and an important life style when people enter modern society, of course, which is arisen as an life style when the society develops to some extent.

We also can see that leisure is not negative rest, while it is the activity which can accomplish the human's psychological requirement and the psychological feelings of human beings is very important. From this point, we can see that, people have more leisure time, which shows that the country is richer. Leisure is the symbol of developed degree of country to some extent.

1.1.2 The Chinese understanding of leisure

Leisure is called easy in the ancient China. Leisure was an exalted life style promoted in the ancient Chinese culture and the easy life can cultivate human beings' minds. The ancient China canonized leisure very much, emphasized the relation between leisure and health, stressed the physical activities cultivating minds and emphasized quiet mode of exercise like Guiding, Taichi and so on, which having the distinguishing ethnic feature.

In modern times, with the continuous improvement of life quality, human beings have new understandings about leisure. Introducing the concept of leisure from the western civilization, which combines the consciousness of traditional Chinese leisure and the concept of western leisure, makes the modern Chinese have new understandings about leisure. Leisure is not only the pure cultivated mind but the life style and an important constituent part of their lives for one part of affluent demographics. The styles of leisure become more plentiful. Therefore, some scholars in China believe that leisure is "the self-entertainment activity undertaken with the comfortable mood in the freely dominant time." (Hu, Xiaoming and Yu, Chonggan. 2004) Others think that leisure is that "people engage some activity with pleasure in the optional state and mood in the relatively free environment and condition." (Lu, Feng. 2008)

These views are the combination of the consciousness of traditional Chinese leisure and the concept of western leisure, from which it is found that Chinese leisure is the activity engaged at their own will in their time. The above views not only emphasize "inertia" but also associate the activity and inertia and all kinds of sports activities are adopted as the modern Chinese leisure styles at large.

1.2 The concept of leisure sports

The formation of leisure life styles has a very close relationship with sports. The required time, space and money of leisure life styles are also the requirement of sports activities or sports consumption. A large part of leisure life styles are sports activities and different kinds of sports activities are the main contents of modern leisure lives.

The Chinese scholar Lu Feng believes that "leisure sport is the general term of sports activities which are selected and engaged voluntarily by people in the relatively free social environment and condition. It is one existing style of sports and one important style of social leisure activities." (Lu, Feng. 2008)

The French scholar Roger Su thinks "sports leisure is higher stage of physical activity, which needs stronger and longer physical effects, but it cannot be confused with in the true sense of sport. It is an intermediate stage between the simple relax of walk and in the traditional sense of sport and has some sport characteristics distinguished from strict sense, which neither pursues achievement through matches nor requires regular intense trainings, but to pursue physical relax and comfort through informal and voluntary sport activities.(Roger, Su. 1996)"

Japan's leisure sport development association makes presentations for leisure sports as follows: leisure sports don't refer in particular to sports programs but no matter what sports program, as long as it is taken as leisure sport which achieves the aims at delight, exultance, a light heart and fatigue elimination we call it leisure sport."(Liang, Limin. 2007)

According to the presentation above and domestic research of leisure sport, there has not been a very authoritative definition about leisure sport. Leisure sport is not a specific sport program but a kind of social existence state of sport. So I think leisure sports are non-competitive physical recreations which People make use of free time to participate in voluntarily in free form with relaxed feelings in relaxing environment. This kind of physical recreations is mainly to adjust psychology, cultivate temperament, relieves fatigue, restores energy, strengthen physical fitness, improve healthiness and enjoy the pleasure of life.

2. The types of leisure sports

According to my recognition to the connotation of leisure sports above, leisure sports should be coverall and it can be all kinds of different sports. But in order to analyze leisure sports better, we should classify it. Of course there are standards for classification but there have not been uniform standards for the classification of leisure sports until now. There are different types according to different standards. For example someone divided leisure sports into bare-handed, equipped, air, land, overwater, appreciative, static and dynamic sports. Lu Feng et.al scholars classified leisure sports to seven types including the activities of body shaping, recreation, competition, relaxation, social interactive activities, seek the extraordinary and stimulus."(Lu, Feng et al. 2006) I think according to the connotation of leisure sports, they should be classified on basis of motives and purposes people participate in leisure sports so the authors divided numerous leisure sports into physical recreation activities, physical fitness activities, physical exploration activities and social sports.

2.1 Physical recreation activities

There are very colorful recreations in society and physical activities are one of them. The basic composite of physical recreations is game. Game is the reflection of human imagination and creativity and the aim that people engage in games is recreation. Likewise the prime desire people engage in physical activities is also recreation.

Physical recreation activities mainly are the sports which people participate in voluntarily in form of physical activities and obtain pleasure physically and mentally, and the fundamental goal of people is to get psychological and physical relax and happiness from this kind of activities. When the participants take part in physical activities, they will become happy and pleasant. Regardless of the feelings is psychological or physical they will bring happiness and pleasure to people, which make people choose various physical activities such as all kinds of folk non-competitive activities, for example, people organize and participate football game, basketball game, badminton game et. al voluntarily, which stress the process and form of people's participation more than results. Essentially, this kind of competitions is a form of relax and recreation of each participant and a kind of active way with strong attraction which can meet human various physical and psychological needs.

In addition, such programs which are not very competitive and easy to grasp their technology comparatively as bowling, table tennis, billiards et. al are also physical recreation activities people often choose. Their competition is weak relatively, it is easy relatively to study their technology, there is strong comparatively entertainment in the process of sports and they may bring pleasure to people.

2.2 Physical fitness activities

Physical fitness activities is that people have sports in order to shape a well-built body, keep perfect physical function and prompt physical and psychological health. In essence people participate in this kind of sports for pursuing individual physical beauty absolutely and embodying the psychology that people' love of beauty. People make use of leisure time by way of participating in physical fitness activities to shape individual body, cultivate personal psychology, improve individual quality so as to become more confident of themselves. Such as running, excising, aerobics, yoga, shaping, sports dancing, Taichi and so on could play such roles.

In addition, we know that good psychology lies hidden in healthy body while well-built body is the material foundation of good psychology and spirits. From social development and progress we can see that the higher people's life is, the higher the need of pursuit for fit body and good spirits is. Therefore, physical fitness activities have become modern people's leisure activities to pursue perfect ego.

Currently people are keen on building up strong and handsome physical body with all kinds of sports, which is the reflection of the improvement of people's life standards and the pursuit for gracious spiritual life. People participate in various physical fitness activities so as to develop people's aesthetic concept and expand the types of leisure sports.

2.3 Physical exploration activities

Exploration is a psychological need of human beings. Technological progress brings great changes to people's life and work in modern society. Life becomes repetitive and dull and work is more formulized. People's life and work become more and more boring. For most of people life and work are activities on a regular routine without any new ideas and interest so the psychological need of exploration is often suppressed. But while the progress of modern society bring such suppression it also brings more leisure time, so people may make use of it to satisfy their psychological need of exploration so as to alleviate the repression that life and work brings to.

Physical exploration activities emerged in order to satisfy people's psychology of exploration. People participate in physical exploration activities in order to release the pressure brought by work and life and satisfy psychological need of seeking for stimulus and exploration. There are many exciting adventure sports in Physical exploration activities so as to meet people's psychological need in the nature, such as mountain climbing, rock climbing, skiing, drifting, outside traversing and so on. The exploration activities are far away from people's working and living environment and can make participants experience the psychology of exploring natural mysterious environment in the nature so as to make them obtain great psychological satisfaction.

2.4 Physical intercourse activities

Intercourse activities are necessary activities in human society. People interact with each other, communicate feelings and prompt social progress by intercourse activities. People's intercourse activities mostly happen in spare time besides working time. In other words, leisure provides best opportunity for people's intercourse activities.

“Leisure sports is not only the carrier of leisure recreation and health, but also lube of expand communication,

prompting affection communicates and making friends. Leisure sports have more changes to take direct part in to step into openness and freedom, satisfy people's needs, communicating people's feelings and strengthen the image, grade and cohesion of a city." (Xu, Jike. 2008) Physical activities are ways which people often choose to communicate with, such as chess, sports dancing, community sporting meeting, household sporting meeting and so on. People participate in these activities in order to make friends and expand social interaction with the help of open and pleasant form, and exchange feelings, dispel loneliness and enrich spiritual life through such free forms, and meanwhile also harmonize atmosphere of a family, increase feelings and prompt social stability.

3. The characteristics of leisure sports

The sports recreational modes are different from others, which is ultimately characterized by their own participation. Selecting the sports recreational mode is through participating in sports activities, which brings the pleasure of bodies by experiencing sports activities. Leisure sports are different from other entertainments and other sports and have their own characteristics. Chinese scholar of leisure sports Lu Feng concludes the characteristics of leisure sports in <Leisure Sports> as: participation, nature, fashion, time-spirits, the diversity of the levels and spontaneity. Reading these characteristics and referring to other references, I think that the characteristics of leisure sports can be analyzed in the two aspects of content and form of leisure sports and the characters of participating crowds: on the one hand, the modes of leisure sports activities are diversity and the contents are time-spirits; on the other hand, the crowds participating in leisure sports are voluntary and the levels of crowds are complexity. It is concluded that leisure sports are characterized by the diversity of sports forms, the epochal character of sports contents, the voluntary participation in sports groups and the complexity of sports levels.

3.1 The diversity of modes

Leisure sports are based on all kinds of sports activities and the modes of leisure sports are diversity. Leisure sports items nearly include all sports activities according to the above classifications. Leisure sports are generally divided into two kinds of sports modes including indoor and outdoor ones according to the sites of participated leisure sports activities. The indoor leisure sports activities, such as aerobics, yoga, Shaping, sports dancing and so on, are all processed in some stadiums. The outdoor leisure sports activities, such as mountain climbing, rock climbing, skiing, drifting and so on, are mainly processed in natural or artificial environments. Some scholars also divided the outdoor sports into the continental, water area, airspace forms in the references. "Continental area: mountaineering, rock climbing, orienteering, wilderness survival, exploration, hunting, riding, skiing, skating, playing balls in the wild of mountain forests; water area: boating, diving, surfing, swimming, diving, fishing, drifting, dragon-boating, boat race, playing in beach and so on; airspace: gliding, parachuting, fire balloon and so on."(Zhou, Bing et al. 2000) In addition, the forms of leisure sports activities may be with instruments or non-instruments in the view of weather making use of instruments. Therefore, from the above analysis we can see that, the types of leisure sports activities are diversity.

3.2 The time-spirit of contents

The contents of sports activities are enriched with the development of history and culture. Different sports activity items arise in different historical backgrounds and the contents accord to the development of sports activities. Looking back into history, sports activity is one type of the participated leisure activities whether in any times. Of course, leisure sports activities are also the manifestation of social civilization at that time and relate to the developing level of social sciences closely. That is to say, different contents of leisure sport activities arise in different historical times and different social civilizations and the contents evolve and develop with the development of history and the advancement of times.

Today, we can clearly see that, the contents of leisure sports activities in this beginning century have changed much compared with the last beginning century. Let us take outdoor activities as an example, the outdoor activities in the last beginning century mainly refer to athletics, however, now the outdoor activities mainly refer to wide extreme sports, from which it is found that the substances of activities having the same names change much. The contents of leisure sports activities reflect the psychological requirements of participated people at different times, which are the reflections of psychologies of people affected by the advantages of science and technology and social civilizations. Therefore, the contents of leisure sports activities often reflect the social civilization at that time and have the evidence time-spirits.

3.3 The voluntary of participation

From the analysis of the concept of leisure sports, they are the sports activities participated voluntarily and the social existing configuration of sports activities. Its basic feature is participatory, which is initiative and

voluntary but not passive. Without this initiative participatory, people can not get the expected psychological requirement when they participate in the leisure sports activities and the aims to eliminate tiredness, heal physical bodies, strength physique, promote health and enjoy the fun of lives can not been achieved.

Moreover, leisure sports are the sports activities processed by people in their leisure times, which are the spontaneity and voluntary appeals from any individual or group and do not contain any mandatory or passive components. People participate in the activities voluntarily and their own physical and psychological requirements are satisfied directly, and moreover, these good psychological experiences will promote the enthusiasm and durability of participating in the activities, which forms the virtuous circle of participating in the activities voluntarily. The virtuous circle brings the leisure sports activities into the lives of people in the modern society, which is a symbol of society progress.

3.4 The complexity of levels

The complexity of levels refers to the complexity of levels of groups participating in the leisure sports activities, which is reflected mainly in two aspects: one is the complexity of consumption levels; the other is the complexity of age levels.

Firstly, the consumption levels are complexity. We know that leisure is the life style of some rich and richer groups in the society and leisure sports are one of the important contents of leisure life styles. The groups who can participate in the leisure sports activities are rich and free and the stratum composing these groups are very complexity, whose income differs much and the consumption levels participating in leisure sports activities are also not same. In this group, there are people who play golf, go to the gym, or orienteering. Their consumption is different absolutely when they participate in different activities, which forms a huge and complex consumer group of leisure sports in modern society.

Then from the development of modern society we can see that, the consumption form of many leisure sports is a gradual process from luxury to popularization. A lot of leisure sports programs are activities which few people participate in at the beginning, but with social progress and its popularization, the consumer price which is used for take part in the program declines sharply so that the sport becomes popular gradually. For example, the development of the sport golf in China is a process of gradual popularization so that the consumption levels of the group who participate in leisure sports become more complex.

Secondly, the levels of age also have complexity. We know that leisure sports are non-competitive and voluntary activities. From this sense, people of different ages can participate. But people of different ages have different needs and they influence people's choices for different ways of sports leisure. The crowd of different ages will have their predilections while choosing leisure sports. Teenagers choose the activities which are their favorite and with challenges mainly such as football, basketball, skateboarding, roller skating, skiing and rock climbing et. al. The middle and old aged people choose activities which reflect status with taste, a certain grade and strong communications, such as golf, tennis, fishing, sports dancing and Taichi, et. al. Of course, in the reality that people participate in leisure sports, the levels of ages are very careful, which are up to participants' hobbies and income and also the result of leisure sports market option. Therefore, the levels of ages of the crowd who participate in leisure sports are multiple and complex relatively.

From the two aspects above it is not difficult for us to see that the levels of the crowd who participate in leisure sports are complex relatively.

References

- Hu, Xiaoming and Yu, Chonggan. (2004). *The theory and practice of sports and Recreation*. Beijing, Higher Education Press, 2004: 35, 36, 38.
- Jeffery, Gobbi. (2000). *Leisure and leisure services of 21st century*. Kunming, Yunnan Ren Min Press.
- Liang, Limin. (2007). Survey Certain Questions of Current Leisure Sports Research. *Journal of Chengdu Sport University*. 2007, (1): 36.
- Lu, Feng et al. (2006). Classification of Leisure sports activities. *Journal of Wuhan Institute of Physical Education*. 2006, (12): 60.
- Lu, Feng. (2008). *Leisure Sports*. Beijing, People's Sports Publishing House. 2008: 4, 99.
- Roger, Su. (1996). *Leisure*. The Commercial Press.
- Xu, Jike. (2008). Survey Certain Basic Questions of Leisure Sports. *Sports World Scholarly*. 2008, 6.
- Zhou, Bing et al. (2000). *Sports Leisure*. Guilin, Guangxi Normal University Press.

Adaptive Vibration Condition Monitoring Techniques for Local Tooth Damage in Gearbox

Kobra Heidarbeigi (Corresponding author)

Mechanical Engineering of Agricultural Machinery Department

School of Agricultural Engineering and Technology, University of Tehran, Karaj, Iran

E-mail: kobra.heidarbeigi@gmail.com

Hojat Ahmadi

Mechanical Engineering of Agricultural Machinery Department

School of Agricultural Engineering and Technology, University of Tehran, Karaj, Iran

M.Omid

Mechanical Engineering of Agricultural Machinery Department

School of Agricultural Engineering and Technology, University of Tehran, Karaj, Iran

Abstract

Vibration analysis that is the main conditions monitoring techniques for machinery maintenance and fault diagnosis, in rotating parts of tractor MF-285 for optimizing them is important. Practical experience has shown that this technique in a machine condition monitoring program provides useful reliable information, bringing significant cost benefits to industry. The objective of this study is to investigate the correlation between vibration analysis and fault diagnosis tractor gearbox. This was achieved by vibration analysis and investigating different operating conditions of tractor (M-F) gearbox. This gearbox coupled to the electromotor that was initially run under normal operating conditions and its speed was at two levels, 500 and 1000 RPM respectively. Even tooth in a gearbox is alternately meshing and detaching during its operation and the loading condition of the tooth is alternately changing. Hence, the gear conditions were considered to be normal gearbox and worn and broken-teeth gears faults with the aim of fault detection and identification. Vibration data was collected from the inspected gearbox and are used for compare with vibration spectra in normal condition of healthy machine, in order to quantify the effectiveness of the Vibration condition monitoring technique. The results from this study have given more understanding on the dependent roles of vibration analysis in predicting and diagnosing machine faults.

Keywords: Vibration condition monitoring, Gearbox, Fault diagnosis

1. Introduction

Tractor, as the most important agricultural machinery, has main share in planting, retaining and harvesting operations and then in mechanization sector. Hence, in order to reach sustainable agricultural and to increase mechanization level quality and manufacturing technology of this agricultural machinery and also its quantity must be reached to optimum level. Above statements show the importance of condition monitoring in gearbox of tractor MF-285 for optimizing them. In this regard, vibration condition monitoring in tooth gears of this tractor was studied. For years, condition monitoring of power transmission has been deemed imperative. Thus, gearboxes, the core of power transmission, have received considerable attention in the field of condition monitoring and fault diagnosis. In particular, gear localized defects have been extensively studied, since a large percent (60%) of gearbox damages are due to gear faults, which in turn are mostly initiated by localized defects. Vibrations externally measured on a gearbox have been used to monitor the operating condition of the gearbox and diagnose the fault, if there is any, without interfering with the normal operation. The most common method employed for examining mechanical vibration is spectral analysis. Condition monitoring and fault diagnostics is useful for ensuring the safe running of machines [Peng and Chu, 2004]. Vibrations signals are often used for fault signals diagnosis in mechanical systems since they often carry dynamic information from mechanical elements. These mechanical signals normally consist of a combination of the fundamental frequency with a narrowband frequency component and the harmonics. Most of these are related to the revolutions of the rotating system since the energy of vibration is increased when a mechanical element is damaged or worn. Some of the conventional techniques used for fault signals diagnosis include power spectra in time domain or frequency

domain, and they can provide an effective technique for machinery diagnosis provided that there is the assumption that the signals are stationary [Peng and Chu, 2004]. By measuring and analyzing the vibration of a machine, it is possible to determine both the nature and severity of the defect, and hence predict the machine's useful life or failure point. The main advances in vibration analysis in recent years are the development in signal processing techniques, for vibration diagnostics of gearing systems [Ebersbach et al, 2006]. Early work on the formalization of vibration diagnostics using spectral analysis [Blackman et al, 1958] progressed slowly through the 1960s, mainly due to the expense of analysis equipment. The development of the Fast Fourier Transform (FFT) in 1965 [Cooley and Tukey, 1965] allowed the development of commercial real-time spectral analyzers and, as the use of these analyzers become more widespread, a number of authors describe the vibration effects of various machine faults and how these could be diagnosed using spectral analysis [White, 1972, Braun, S, 1987, Minns and, 1972, Swansson, 1980, Randall, 1987]. In the mid 1970s, Stewart [Stewart, 1977] made a significant contribution to the use of vibration analysis as a diagnostic tool for machine faults, especially for gear faults. Further work by Randall [Randall, 1982] and McFadden [McFadden, 1985] in the underlying causes of gear vibration resulted in a better understanding of the correlation between Stewart's figures of merit and mechanical condition. McFadden [McFadden, 1988] showed the importance of phase modulation in the diagnosis of cracks and outlined a signal parameter sensitive to phase modulation. In this paper, investigate the correlation between vibration analysis and gearbox (Massey Ferguson-165) fault diagnosis. This was achieved by vibration analysis of a Massey Ferguson gearbox. A series of tests were conducted under the operating hours of gearbox. Vibration data was regularly collected. Overall vibration data produced by vibration analysis was compared with previous data. Numerical data produced by vibration analysis were compared with vibration spectra in standard of healthy gearbox, in order to quantify the effectiveness of the vibration condition monitoring technique. The results from this paper have given more understanding on the dependent roles of vibration condition monitoring in predicting and diagnosing of electromotor faults.

2. Experimental set-up

The test rig used for the experimentation was a gearbox. The experimental setup to collect dataset consists of Massey Ferguson gearbox, an electrical motor with two independent variable speeds that drive the system (details of electromotor are given in Table 1), a triaxial accelerometer (X-Viber, VMI is manufacturer) and four shock absorbers under the base of test-bed. Test-bed was designed to install gearbox, electric motor and four shock absorbers under bases to cancel out vibrations. This gearbox coupled to the electromotor that was initially run under normal operating conditions and its speed was at two levels, 500 and 1000 RPM respectively. All vibration signals were collected from the experimental testing of gearbox using the accelerometer which was mounted on the outer surface of the bearing case of input shaft of the gearbox. For each configuration different fault conditions were tested that were worn, broken teeth of gear and one faultless condition. The signals from the accelerometer were recorded in a portable condition monitoring signal analyzer.

2.1 Damaged Gear

The gear set was damaged by removing a portion of a tooth from the pinion gear. This damage was achieved by filing down a section of the tooth, such that the driven gear would impact the sharpened lip of the fault at the beginning and end of the gear meshing cycle.

Gear sets generate tones known as the *gear mesh frequency*. The gear mesh frequency is calculated via equation 1.

$$GMF = No.ofTeeth \times RPM \quad (1)$$

The corresponding spike at this frequency generally amplifies as gear damage increases [Andy et al, 2003].

3. Results and Discussion

The most basic form of vibration analysis is called an overall vibration measurement. This reading provides a single number that describes the total amount of vibration energy being emitted by a machine. The idea is that more vibration indicates a problem. Signal data was acquired for machine conditions, including: a normal gearbox, worn and broken-teeth gears of these machine conditions at operating speeds of 500 and 1000 rpm. Data analysis required comparing the plots obtained for each test condition to those expected for the specific machine faults simulated. Prominent frequency spikes determined from the time and frequency domain graphs were also compared to the theoretical vibration fault signatures. The gear damage tests successfully illustrated the theoretical predictions at a rotational speed of 500 and 1000 rpm. The results showed that the RMS values for healthy gearbox at 500 rpm (1000 rpm was the same) were on acceptable status (Figure 1). The results showed that the RMS values for the worn and broken gear at 500 rpm (at 1000 rpm) were on critical status (Figure 2 and

3). Measurement values and mean of them were higher than the RMS value of gearbox in healthy condition. Figure 4 (at 500 rpm) and figure 5 (at 1000 rpm) showed the overall vibrations of worn and broken gear condition. As can be seen in figures, the prominent frequency peak occurred with high accuracy near the predicted value of gear mesh frequency, as shown in Table 2.

Vibration analysis technique has been used to assess the condition of the gearbox and diagnose any problems of that. The results from vibration analysis of our experimental research indicate our defaults those made in our gearbox. Vibration analysis of gearbox discovered the worn and broken teeth in gears. The correlation between the vibration analysis and fault diagnosis was excellent as vibration technique was able to pick up on different issues, thus presenting a broader picture of the machine condition. Vibration analysis detected a continuing gear defect along with a possibility of mechanical faults of the outer casing from assembly. Vibration analysis technique was capable in covering a wider range of machine diagnostics and faults within the gearbox.

4. Conclusions

The results clearly indicate a significant variation in vibration trend as a function of operating conditions. The experimental results demonstrated that the vibration monitoring rig modeled various modes of machine failure was indeed capable of both independently and simultaneously generate common machine faults. In this research we have been made an experimental test system that we were able to perform practical tests on the constructed rig to confirm the expected theoretical frequencies that we needed. This research was offered complementary strengths in root cause analysis of machine failure, and natural allies in diagnosing machine condition. It reinforces indications correlation between vibration condition monitoring and fault diagnosis for gearbox. Both amplitude of the dominating peak and its location along the frequency axis changes in various conditions of gear. The data indicate that it is not possible to conclude that the cause of real world machinery malfunction is fault gear just by looking at a single vibration spectrum at an operating condition. A careful examination is essential to differentiate fault gear from other sources of vibration. The corresponding stress will depend upon the stiffness of the machine structure. The frequencies of peak vibration amplitude, set locations and directions were inconsistent even with speed and coupling held constant. Increased speed also caused increased peak vibration with frequency shifts that did not correlate with the speed. For predictive maintenance applications where the goal is machinery health monitoring, it is sufficient to realize that the problem is complex. One can routinely trend the vibration spectra until it becomes severe. But for root cause analysis, one must exercise caution and perform a detailed analysis. Obviously, the rules provided in training courses and wall charts are doubtful at best.

Acknowledgment

Acknowledgment is made to the University of Tehran for its concentration for this research.

References

- Andy C., C. Tan, L. Katie, McNickle and L. Daniel Timms. (2003). A Practical Approach to Learning Vibration Condition Monitoring, *World Transactions on Engineering and Technology Education*, 2 (2).
- Blackman, R.B and J.W. Tukey. (1958). The Measurement of Power Spectra. *Dover Publications*, New York.
- Braun, S. (1987). *Mechanical Signature Analysis*, Academic Press Inc, London.
- Ebersbach, S., Z. Peng, N.J. Kessissoglou. (2006). The investigation of the condition and faults of a spur gearbox using vibration and wear debris analysis techniques, *Wear* 260: 16–24. Available online at www.sciencedirect.com.
- Cooley, J.W and J.W. Tukey. (1965). An Algorithm for the Machine Calculation of Complex Fourier Series. *Mathematics of Computing*, 19: 297-301.
- McFadden, P.D. (1985). Analysis of the vibration of the input bevel pinion in RAN Wessex helicopter main rotor gearbox WAK143 prior to failure, *Aero Propulsion Report 169*, Department of Defence, Aeronautical Research Laboratory.
- McFadden, P.D. (1988). Determining the Location of a Fatigue Crack in a Gear from the Phase of the Change in the Meshing Vibration, *Mechanical Systems and Signal Processing*, 2(4): 403-409.
- Minns, H and R.M. Stewart. (1972). An Introduction to Condition Monitoring with Special Reference to Rotating Machinery. *Workshop in On-Condition Maintenance*, Section 8, Institute of Sound and Vibration Research, University of Southampton.
- Peng, Z.K., F.L. Chu. (2004). Application of the wavelet transform in machine condition monitoring and fault diagnostics. *Mechanical Systems and Signal Processing*, 18: 199–221.

Peng, Z.K., F.L. Chu. (2004). Extraction of Gearbox Fault Features from Vibration Signal Using Wavelet Transform. *J. Physics: Conference Series* 48: 490–494.

Randall, R.B. (1987). *Frequency Analysis*, Bruel and Kjaer, Copenhagen, 3rd edition.

Randall, R.B. (1982). A New Method of Modeling Gear Faults, *J. Mechanical Design*, 104: 259-267.

Stewart, R.M. (1977). *Some Useful Data Analysis Techniques for Gearbox Diagnostics*, University of Southampton Report MHM/10/77.

Swansson, N.S. (1980). *Application of Vibration Signal Analysis Techniques to Signal Monitoring*. Conference on Friction and Wear in Engineering, Institution of Engineers, Australia, 262-267.

White, C.J. (1972). *Detection of Gearbox Failure*. Workshop in On-Condition Maintenance, Section 7, Institute of Sound and Vibration Research, University of Southampton.

Tables:

Table 1. Detail of Electromotor.

Table 2. Fundamental Gear Damage Frequency.

Table 1. Detail of Electromotor.

Electromotor	Description
Electromotor capacity (kW)	1.5 (2 HP)
Motor driving speed (rpm)	Variable
Voltage	380 v
Phase	Three phase
Ambient air temperature (°C)	≈25
Non driven end bearing	FAG 6205
Driven end bearing	FAG 6205

Table 2. Fundamental Gear Damage Frequency.

Shaft Speed (rpm)	Theoretical Frequency (Hz)	Experimental Central Frequency(Hz)	
		Broken teeth	Worn
500	366.67	345.5	400
1000	733.33	701.5	795.5

Figures:

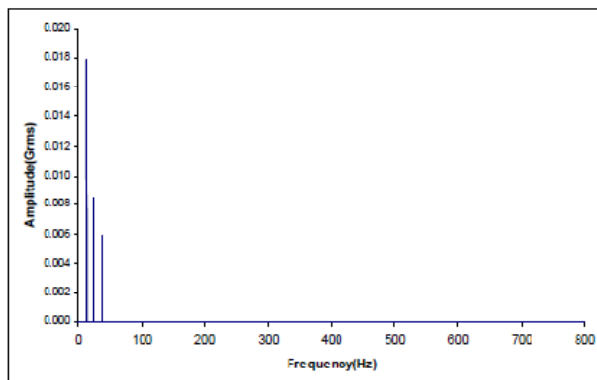
Figure 1. Frequency spectrum of the healthy gear at A) 500 rpm, B) 1000rpm.

Figure 2. Frequency spectrum of the worn gear at A) 500 rpm, B) 1000rpm.

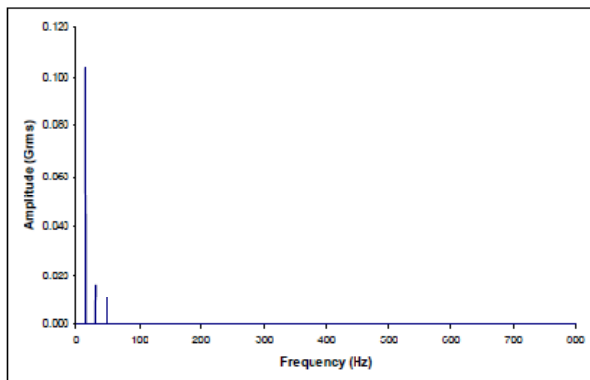
Figure 3. Frequency spectrum of the broken gear at A) 500rpm, B) 1000rpm.

Figure 4. Comparison of Overall vibrations of gear in healthy and won and broken conditions at 500 rpm. The graphs illustrate the effect of speed on the trend.

Figure 5. Comparison of Overall vibrations of gear in healthy and won and broken conditions at 1000 rpm. The graphs illustrate the effect of speed on the trend.

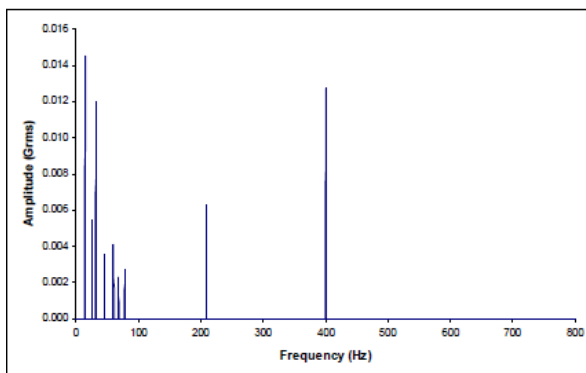


(A)

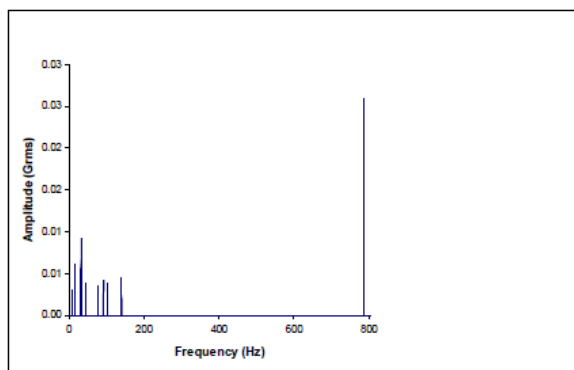


(B)

Figure 1. Frequency spectrum of the healthy gear at A) 500 rpm, B) 1000rpm.

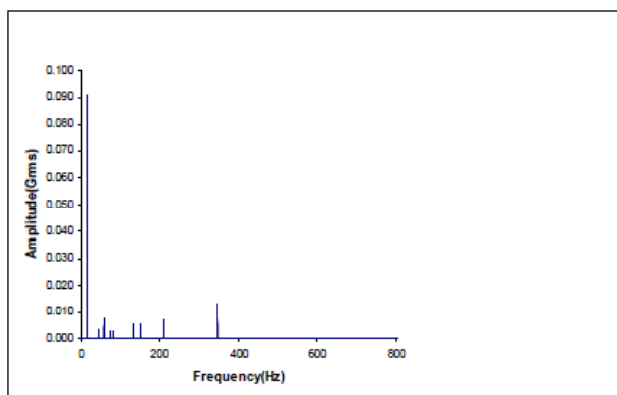


(A)

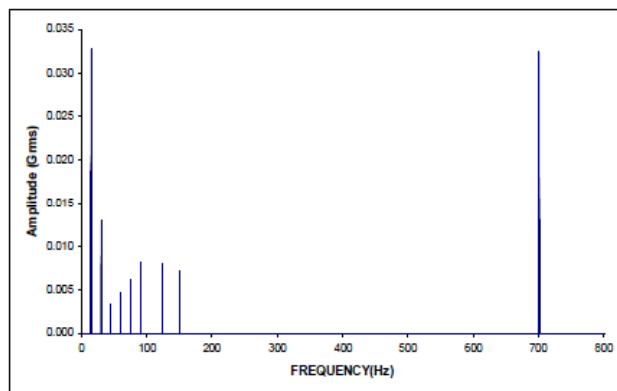


(B)

Figure 2. Frequency spectrum of the worn gear at A) 500 rpm, B) 1000rpm.



(A)



(B)

Figure 3. Frequency spectrum of the broken gear at A) 500rpm, B) 1000rpm.

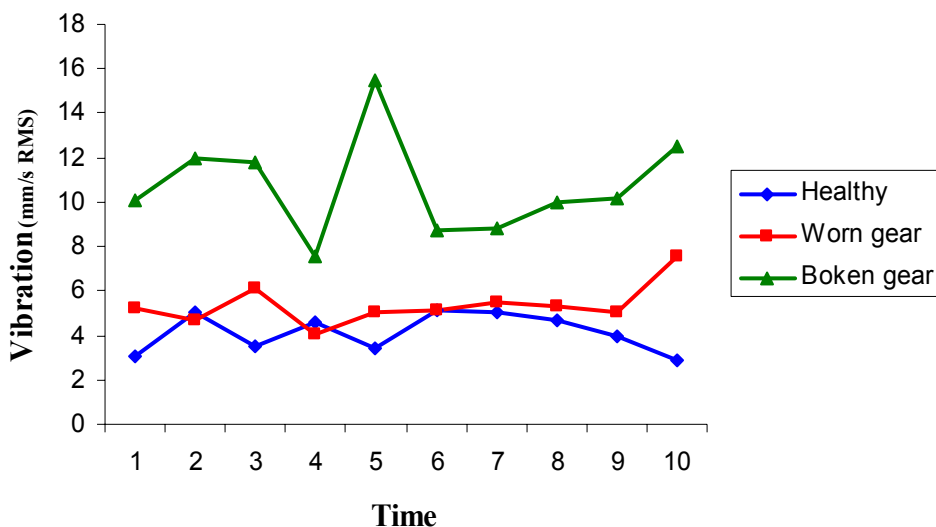


Figure 4. Comparison of Overall vibrations of gear in healthy and won and broken conditions at 500 rpm. The graphs illustrate the effect of speed on the trend.

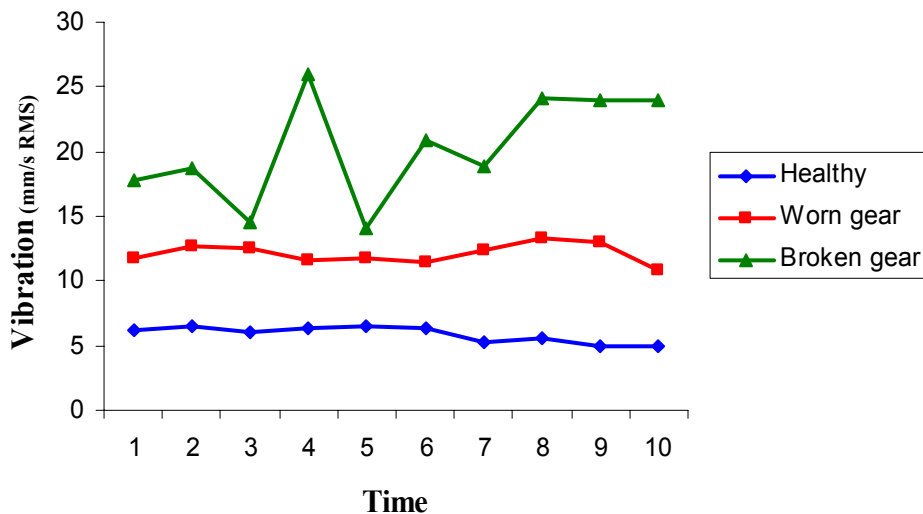


Figure 5. Comparison of Overall vibrations of gear in healthy and won and broken conditions at 1000 rpm. The graphs illustrate the effect of speed on the trend.